GEOLOGY AND OBSIDIAN SOURCES AROUND NAIVASHA AREA, KENYA

By

Enock Israel Owiti

A Thesis submitted in partial fulfillment for the degree of Master of Science

University of Nairobi.

1994

Go my sons, buy stout shoes, climb the mountains,
search the valleys, the deserts, the sea shores
and the deep recesses of the earth.
Mark well the various kinds of minerals,
note their properties and their mode of origin.

Petrus Severinus (1571)

DECLARATION

This thesis is my original work and has not been presented for a degree in any other University.

....
Enock Israel Owiti
University of Nairobi.

This thesis has been submitted for examination with our knowledge as University Supervisors.

....
Professor Isaac Nyambok
Department of Geology
University of Nairobi.

....
Mr. Benson Mboya
Department of Geology
University of Nairobi.

....
Mr. Antony M. Kinyua
Institute of Nuclear Science
University of Nairobi.

CONTENTS

Page

CHAPTER 4

CHAPTER 5

TABLES

PLATES

FIGURES

Abstract

The study examines in detail an area between Mount Longonot in the east through Lake Naivasha Basin to Mount Eburru in the west. The result is a model of major occurrences of obsidian quarry sources that may have been mined by prehistoric man as quarry sources of raw material for the production and/or making of his tools (artifacts). By combining this model, derived mainly from physical data in the field with that deduced essentially from chemical data in the laboratory, the obsidian outcrops have been categorized into major petrological groups. This enables questions about the origin, area of recharge and availability of magma to be discussed. The initial sections are concerned with the physical geology of the study area incorporating faulting and physiography as possible contributors to the formation of obsidian. The section on geochemistry deals with geochemical manifestations together with information on the temporal evolution of the crust that is considered to be the source of the obsidian in the Naivasha area. The approach thus discusses and reviews both the petrographic and geochemical features in order to establish magmatic trends and the possible transitional stages involved. Using relative concentrations of both major and trace elements determined by x - ray fluorescence analysis, the various sources are separated and assigned to individual petrographic groups within the study area.

Obsidian occurrences from several quarry sources within this general area are described including their geochemistry. Geochemical results suggest possibility of extreme interaction and assimilation with the crust in the 'secondary' volcanic feeder chambers. The associated rocks encountered, are limited to volcanic lava flows and pyroclastics of the central rift system. Faulting, a major structural feature in the area is described and later considered as a possible major contributor to the development and distribution of obsidian outcrops although some of the faults have been covered by late stage volcanic activity together with weathering.

To derive such information as distance and possible areas of mining during prehistoric times, an attempt is made to correlate artifacts from four widely separated Archeological Sites at Narosura in Kajiado and Gogo Falls in South Nyanza, Jawuoyo in Kisumu and Cartwright's site located on the Kinangop Escarpment. Merrick and Brown (1984a) have suggested that such studies can lead to an insight regarding authenticity, trade routes and trading connections and other features of historical and archeological interest.

Acknowledgment

This study was conducted to fulfill the requirements for a Master of Science degree at the University of Nairobi. Special thanks go to Dr. Mohamed Ishahakia, Director/Chief Executive, National Museums of Kenya and Ms. Jackie Davies, past Chairperson, Kenya Museum Society. Thanks are also due to my Supervisors, Professor Isaac Nyambok and Dr. Benson Mboya both of the Geology Department and Mr. Antony Muriithi Kinyua of the Institute of Nuclear Science, for their discussions and suggestions. The Late Mr. Wewa of the Geology Department helped with the thin section preparations. The Director's Office, National Museums of Kenya, Professor Hidemi Ishida, Kyoto University Japan and the Kenya Museum Society funded the fieldwork. The Department of Geology, University of Nairobi and the National Museums of Kenya provided Field facilities. Laboratory analyses were carried out at the Faculty of Science, Department of Geology and Faculty of Engineering, Institute of Nuclear Science.

Finally, special thanks are due to Plummy and Stacey for so much encouragement.

CHAPTER 1
INTRODUCTION

1.1 Purpose and locality of the project

The purpose of this study was to investigate the occurrence of obsidian rock in relation to the geology of the area around Lake Naivasha. The area sampled covers approximately 2,500 square kilometers in Central Rift Valley around Lake Naivasha, Kenya, bounded by latitudes 10 00' S and 10 27' S and longitudes 360 03' E and 360 30' E. The greater part of this area is covered by shrubs and scattered trees and is relatively flat while to the east and west, the Kinangop and Mau escarpments respectively rise to form the shoulders of the Rift Valley as shown in the locality map, Fig. 1.

Geological and geochemical data of the Rift Valley lavas, in particular those from central Kenya rift, have accumulated from different research initiatives over the years (see section 1.3). However, there is little comparable information on obsidian as a separate rock from within this area. The study thus aims at providing geological and geochemical information to be used as a database on the occurrences and distribution of obsidian quarry outcrops.

1.2 Method of Mapping

Data collection sites of obsidian quarry sources in the research area was initially plotted on series Y731 Topography Maps published by the Survey of Kenya at a scale of 1:50,000 (Sheet Numbers 129/1, 129/2, 129/3 and 129/4). The final geological map of the area including sampled sites has been compiled at a scale of 1:100,000 covering an area of approximately 2,500 km^2. The geological map at the end of the text shows the details of the areas covered.

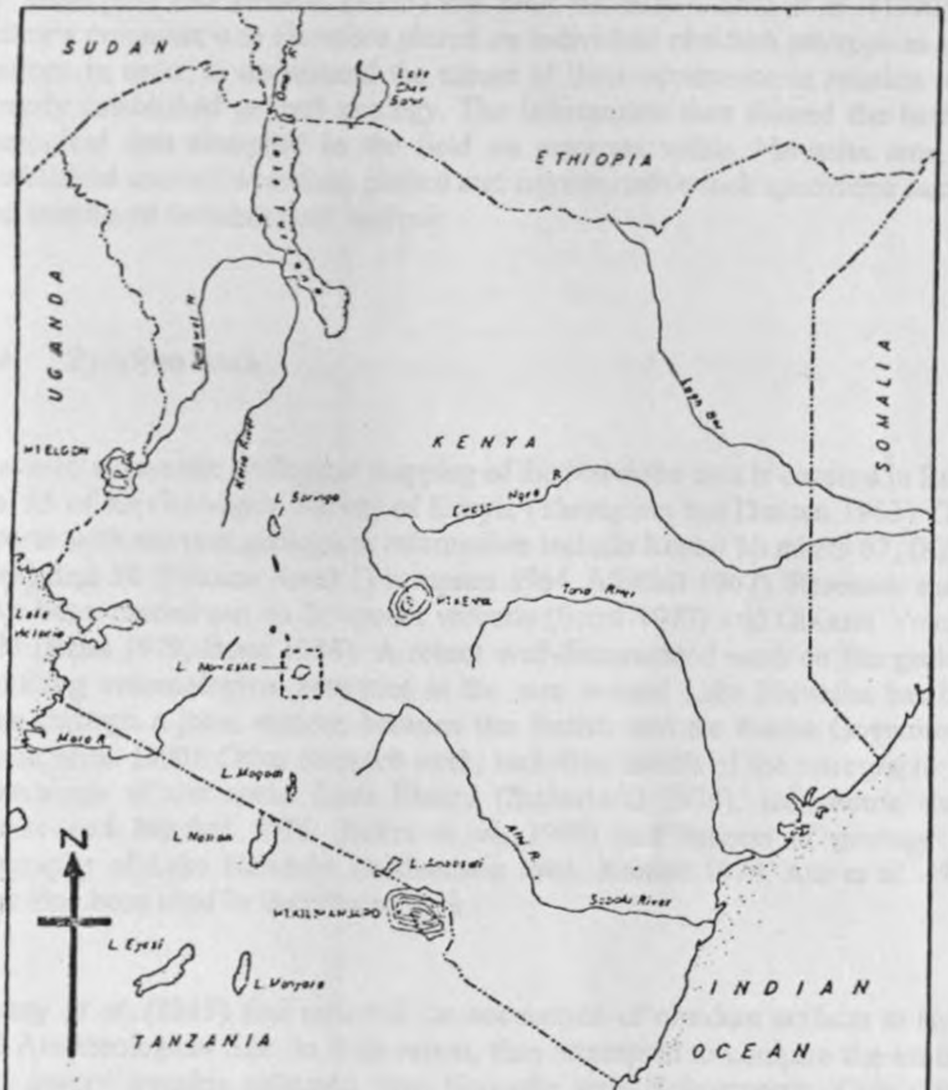

Figure 1 Map showing the location of the study area (modified from Merrick and Brown 1984a)

Since regional geological survey of the general area has been reasonably covered by Thompson and Dodson (1963) and more recently Clarke *et al.* (1990), the author's emphasis was therefore placed on individual obsidian outcrops as major sources in order to understand the nature of their occurrence in relation to the already established general geology. The information then formed the basis for geological data compiled in the field on outcrops within Naivasha area. The established sources were then plotted and representative rock specimens sampled and numbered for laboratory analysis.

1.3 Previous work

Previous systematic geological mapping of the Naivasha area is covered in Report No. 55 of the Geological Survey of Kenya, (Thompson and Dodson 1963). Other reports with relevant geological information include Report Numbers 67, (Kijabe Area) and 78 (Nakuru Area) (Thompson 1964, McCall 1967). Research studies have been carried out on Longonot volcano (Scott 1977) and OlKaria Volcanic field (Bliss 1979, Bone 1988). A recent well-documented work on the geology, including volcanological activities in the area around Lake Naivasha has been done through a joint venture between the British and the Kenya Governments (Clark *et al.* 1990). Other research work, including details of the petrography and mineralogy of the rocks from Eburru (Sutherland 1974), radiometric dating (Baker and Mitchel 1976, Baker *et al.* 1988) and aspects of geology and geography of Lake Naivasha (Richardson 1966, Kamau 1974, Ase *et al.* 1986) have also been sited in the present work.

Leakey *et al.* (1945) first reported the occurrence of obsidian artifacts at Hyrax Hill Archaeological Site. In their report, they attempted to compare the artifacts with quarry samples collected from Naivasha area. Subsequently, Cole (1954) described the obsidian occurrence at Njorowa Gorge area and considered them to be the only obsidian source in Kenya. Artifact studies continued and later, Cann and Refrew (1964) concluded that the Naivasha area could be the main source region for most artifacts found in archaeological sites. Walsh and Pawsys (1970), sharing the same view, carried out relative index and density studies to show that obsidian artifacts collected from Kisima Farm in Laikipia also originated from the Naivasha area.

A similar approach using petrological analysis on a quarry sample from Mount Eburru and artifacts collected from the surrounding areas was attempted by Omi and Agata (1977). Michels *et al.* (1983) reported chemical analyses on obsidians from Kenya but failed to give details of specific localities from where they had obtained their samples.

More recently, Merrick and Brown (1984a) have carried out preliminary sample studies on source utilization in Kenya and Northern Tanzania. Detailed source studies on obsidian including utilization have, however, been carried out in other parts of the world notably in Central and North America, the Mediterranean region and in New Zealand (Bowman *et al.* 1973, Nelson *et al.* 1975, Nelson *et al.* 1977, Duerden *et al.* 1980, Joron *et al.* 1990).

1.4 Physiography

The area around Naivasha is part of the central Kenya rift that underwent intense faulting during the last stages of rift formation. The physiographic expression consists of numerous subparallel fault ridges and troughs trending approximately NNW. The valley floor slopes southwards with a gradient of approximately one to one hundred from Lake Naivasha to Lake Magadi and the surface of the fault blocks dip similarly gently southwards (Clarke *et al.* 1990). To the west, the Mau escarpment rises to some 3,000 m, while the Nyandarwa - Kikuyu Escarpment to the east has a maximum elevation of about 4,000 m. The physiographic map of the area is shown in Fig. 2.

Further fault scarps on either side, notably the Mau (2,400 to 2,670 m) to the west and the Kinangop plateau (2,100 m) in the east bounds the region with Lake Naivasha (1880 m above sea level), forming the central part. To the SSE, Mount Longonot rises to some 2,780 m while directly south of Lake Naivasha, the OlKaria geothermal field with its spectacular recent lava flows and the Ol - Njorowa Gorge, form the main feature. Physiographically, the area can thus be divided into five units, namely: -

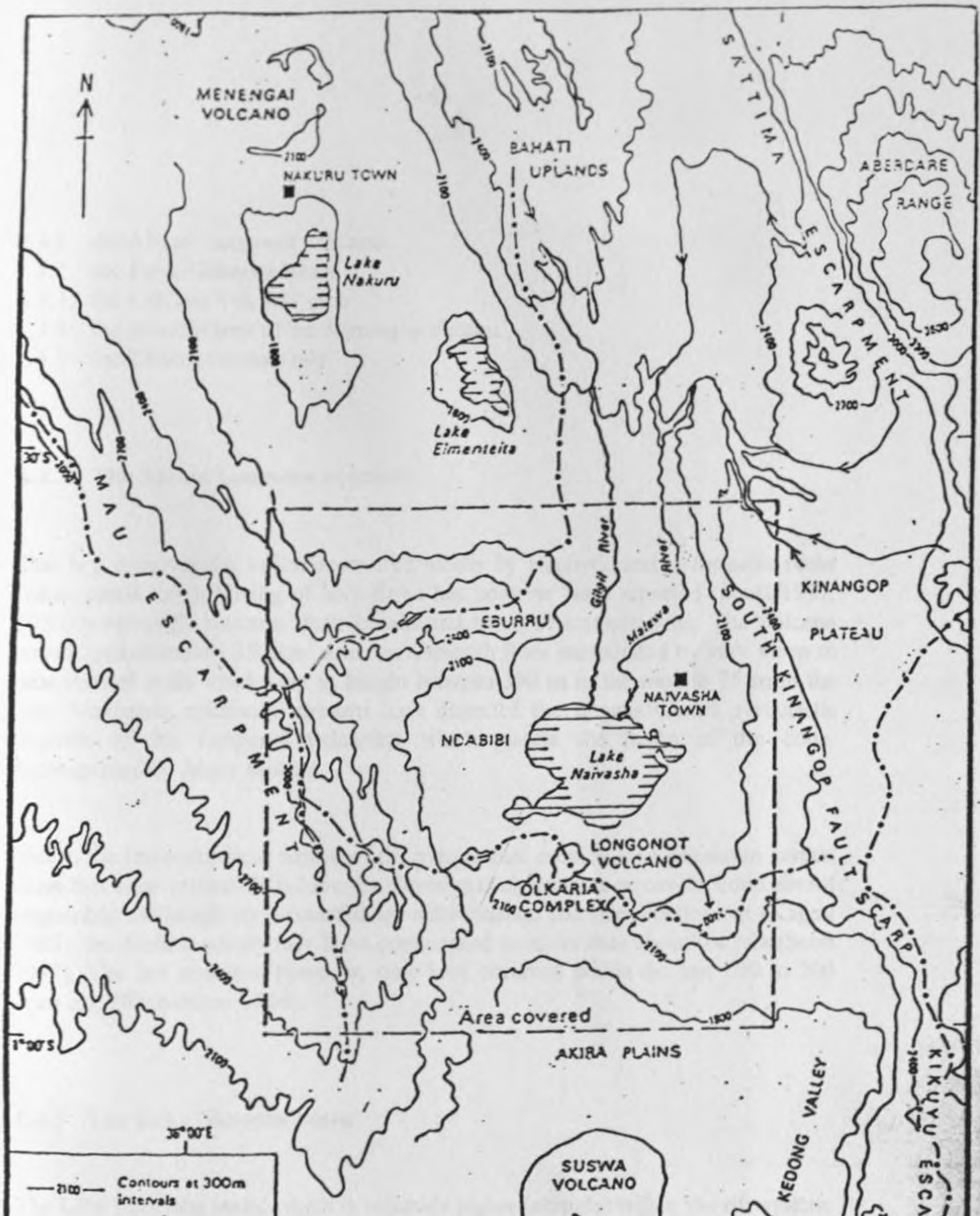

Figure 2 Physiographic map of the Naivasha area.
(modified from Clarke *et al.* 1990)

1.4.1 the Mount Longonot volcano
1.4.2 the Lake Naivasha Basin
1.4.3 the OlKaria Volcanic area
1.4.4 the western limit of the Kinangop Plateau
1.4.5 the Eburru volcanic pile

1.4.1 The Mount Longonot volcano

This is a near-circular volcano covered mostly by trachytic and pyroclastic rocks (often paralkaline). Mixing of lava flows has however been reported (Scott 1977, 1980) particularly between alkali basalts and trachytic compositions. The volcano covers approximately 350 km^2 and has a smooth floor surrounded by very steep to near vertical walls which vary in height between 350 m in the west to 75 m in the east. Numerous ephemeral streams have dissected the unconsolidated pyroclastic deposits of the Longonot volcanics, which mantle the flanks of the cone, accompanied by heavy erosion.

Due to the unconsolidated nature of the pyroclastics, erosion is so intense in certain cases that near vertical cliffs have developed making traverse across the cone almost impossible. Although no successful age determination has been carried out (Kagasi 1983), the earliest activity may have commenced no more than about 0.4 Ma (Scott 1977). The last eruption, however, may have occurred within the last 100 to 200 years ago (Richardson 1966).

1.4.2 The Lake Naivasha basin

The Lake Naivasha basin, which is relatively higher (altitude) within the rift system, occupies the lowest part in the whole area investigated and contains Lake Naivasha whose area is about 200 km^2. Faulting together with accumulation of recent volcanic material has resulted in a localized drainage basin development, creating a potential gradient to the south.

Plate 1 The Ol - Karia recent lava flows associated with geothermal resources

Plate 2 Fischer's Tower showing comenditic volcanism associated with characteristic columnar jointing

The lake whose level in 1983 stood at an elevation of 1,889.3 m (Ase *et al.* 1986) has a smooth floor and a mean depth of 4.7 m. Much of the shore of the main lake is however covered mainly by papyrus and salvina. Lack of surface outlet has led to the believe that there must be an underground outlet to the lake although borehole records indicate that the piezometric surface generally follows the surface contour (Clarke *et al.* 1990) with a steeper fall to the south. It is therefore not surprising that many geologists have considered this underground outlet of the lake as a possible source of some of the aquifers exploited at OlKaria Geothermal Station.

1.4.3 The OlKaria volcanic formation

The OlKaria Volcanic area lies to the south of Lake Naivasha and forms the geothermal field covering some 240 km^2. The dominant exposed rock is commendite or peralkaline rhyolite occurring as domes. A thick obsidian flow extends to over 2 km with a north - west trend within the volcanic field. The lava flow, also referred to as the Ol - Olbutot Lava, is the youngest flow within the area and its surface is still blocky with only light to no vegetation. Plate 1 shows the Ol - Olbutot lava flow in the background. Around Hell's Gate National Park comenditic volcanism is prominent within a varied but relatively thick cover of pyroclastics possibly originating from the nearby Mount Longonot. Plate 2 shows Fischer's Tower at the entrance of Hell's Gate with the associated comenditic volcanism and characteristic columnar jointing.

1.4.4 The western limit of the Kinangop Plateau

To the northwest of Naivasha Town, a steep fault line marking the edge of the western limit of the Kinangop Plateau marks the physiography. Plate 3 shows the edge of the fault scarp along Naivasha - Kinangop road. It is characterized by north - northwest trending fault scarps with very steep edges resulting from faulting. The combined width of these fault - scarps ranges between 2.5 to 5 km (Thompson and Dodson 1963) and exposes both volcanics and palaeosols most of which occur in layers of varied thickness.

Plate 3 Western limit of the Kinangop Plateau with the edge of the fault scarp north of Naivasha Town

Plate 4 Pyroclastic obsidian formation exposed along the Kinangop Road north of Naivasha Town

1.4.5 The Eburru volcanic pile

The Eburru volcanic pile is on the western limit of the study area where a maximum elevation of upto 3,080 m is attained to the west of Ndabibi Estate (Fig. 2). Relative to the rift floor, the Eburru volcanic pile rises to about 1,100 m and the top is dotted with very recent volcanic activities (including fumaroles). It has become the second area of interest after OlKaria in terms of geothermal resource exploration.

1.5 Description of methodology

Initially, freshly broken pieces of obsidian were thoroughly scrubbed in distilled water with a toothbrush and dried. Powdered samples were prepared by first crushing in a pressure crusher to sand sized grains, followed by pulverization with an agate pestle and mortar to sieve size 40 mm. Phenocrysts were easily avoided during the analysis by choosing fresh samples from field and breaking such samples until non-phenocryst portions were separated. Another advantage for this kind of analysis over other volcanic rocks is its obvious glassy occurrence that makes it easy to distinguish in the field. The procedure for transparent solid sample preparation for x-ray fluorescence analysis was followed as given by Kinyua (1982). Similarly, the same mathematical procedures were followed in calculating concentrations for each of the observed elements in the pellets.

The main advantage of x-ray fluorescence analysis is its multi-element nature of analysis (data for all the elements are collected simultaneously) as illustrated by the spectra in Fig. 4. Such spectra form very good basis for archaeological comparisons particularly where only qualitative analysis is carried out with no quantitative determinations. This is usually the case for artifacts (which should not be ground to powder form or destroyed) since they are protected by an Act of Parliament (The Antiquities and Monuments Act 1983, (Cap. 215 repealed) of the Laws of Kenya). Kinyua *et al.* (1992) have used this technique to study provenance of Kanjera fossils. Table 1a. gives the average energies and assignments for the peaks shown in Fig. 4. Individual flows of obsidian are quite homogenous in the amounts and kinds of major and trace elements present. Consequently, separate flows of obsidian can be distinguished from one another by relative concentrations of certain elements (Gordus and Wright 1968, Griffin *et al.* 1969, Bowman *et al.* 1973). Apart from this, chemical alteration in obsidian is usually minimal for even exposed rocks.

Basically, obsidian is composed of SiO_2 (72-76%), Al_2O_3 (10-15%), Na_2O (3-5%) and K_2O (1-7%) with many other elements in much smaller amounts (Michels and Carl 1971). It is the ability of the x-ray fluorescence to 'fingerprint' the obsidian by determining which major and/or trace elements are present and how much, that makes it useful in differentiating the various sources.

1.5.1 Instrument sensitivity

In order to determine the overall instrument sensitivity for the results obtained, (i.e. the instrument response per unit charge in concentration) standard reference materials are normally used. When using such standards, it is always assumed that nothing changes between the measurement of the standard and the unknown sample(s).

The most common method of verifying results is to analyze a series of certified standard samples and compare the results obtained against element concentration values given in a standard certificate. A reasonable fit of the data is then used to confirm the sensitivity of the instrument as shown in Tables 1b. and 1c. The columns of figures listed under chemical concentration are the values of the standards. The data listed as calculated concentration are those obtained from the analyses of the standards. The last column gives the range within which calculated concentration values is expected to fall. The results obtained shows no major deviation from the standard values. Provided nothing changes between the measurement of the standard and a given unknown specimen, it can be assumed that the only difference in the sensitivity of the spectrometer for the two measurements is that due to matrix effect.

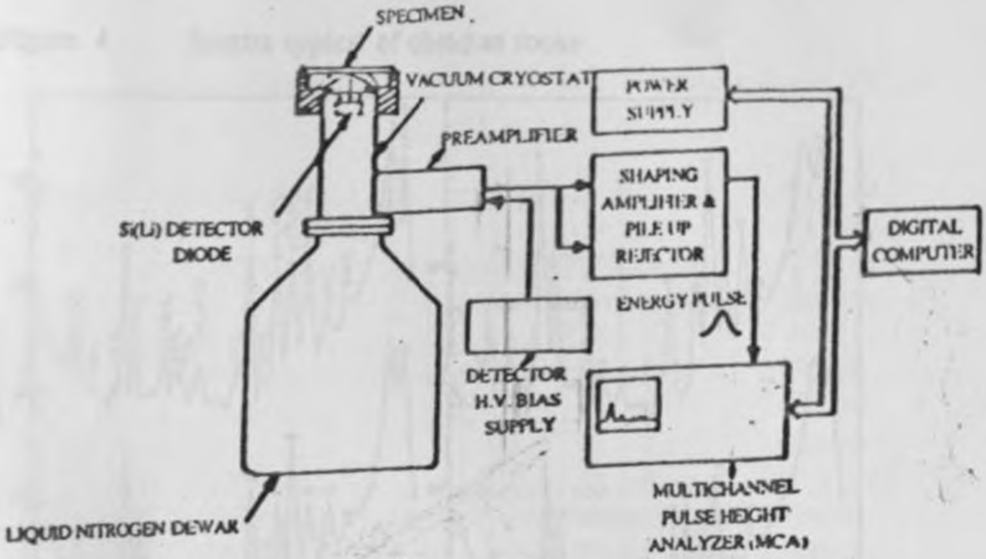

Figure 3 Schematic diagram of the XRF analysis equipment (modified from Jenkins *et al.* 1981)

1.6 Sample preparation and analysis

Major and trace element analyses shown in Table 3 were carried out on pressed powder pellets using XRF at Nairobi University. In all, a total of 12 elements ranging from Potassium, Calcium, Titanium, Magnesium, Iron, Zinc, Copper, Rubidium, Yttrium, Zirconium, Thorium to Niobium were selected in an analysis time of 500 seconds per sample. The selection of the elements was based on their being able to discriminate potentially the different quarry sources.

Relative determination of element concentrations in the obsidian was made by photon - excited energy dispersive x - ray fluorescence analysis. This method involves the excitation of the sample atoms with a beam of x - rays and the analysis of the characteristic fluorescent x -ray by semi-conductor detector e.g. Si(Li) and other electronic devices. A description of this analytical technique is given by Jenkins *et al.* (1981). Figure 3 shows a schematic diagram of the equipment used in this study. The beam of photons that excite the sample consists essentially of monochromatic (K_α and K_β) characteristic x-ray radiation from a chosen radioisotope. In this work ^{55}Fe and ^{109}Cd radioisotopes were used. The characteristic x-rays emitted by the atoms in the sample are detected using a Si(Li) spectrometer. Pulses from this detector are processed and accumulated in channel groups (memory location in a multichannel analyzer). The data is then transferred to a computer and peak energies and intensities extracted by spectrum - stripping and fitting.

Figure 4 Spectra typical of obsidian rocks

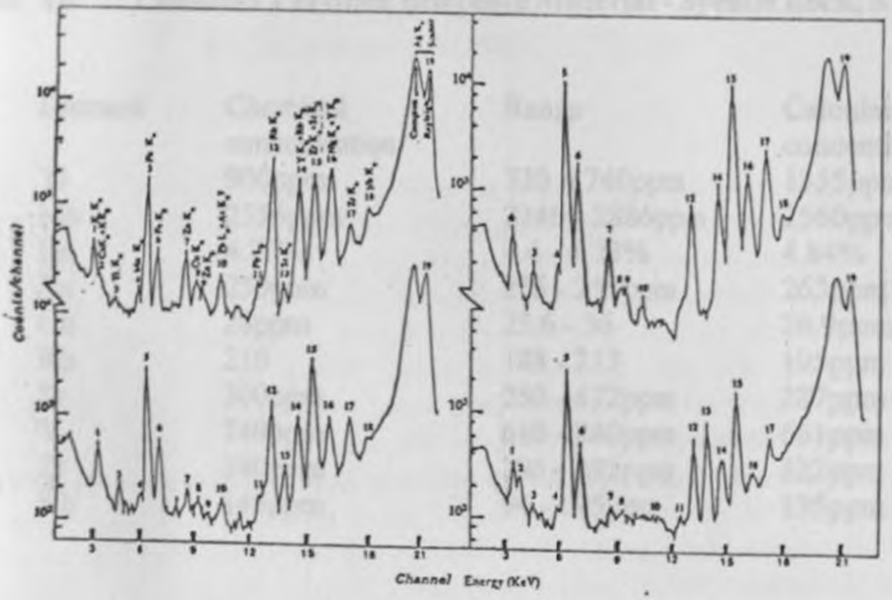

Table 1a **Average energies and assignments for the peaks in obsidian spectra**

Peak No.	Average Energy (KeV)	Elemental Assignment	Peak No.	Average Energy (KeV)	Elemental Assignment
1	3.31	K K_α	11	12.74	Pb L_α (+Fe K_β)
2	3.65	Ca K_α (+K K_β)	12	13.40	Rb K_α
3	4.54	Ti K_α	13	14.16	Sr K_α
4	5.89	Mn K_α	14	14.96	Y K_α (+Rb K_β)
5	6.40	Fe K_α (+Mn K_β)	15	15.76	Zr K_α (+Sr K_β)
6	7.06	Fe K_β	16	16.61	Nb K (+Y K_β)
7	8.64	Zn K_α	17	17.68	Zr K_β
8	9.25	Cu K_α	18	18.67	Nb K_β
9	9.59	Zn K_β	19	22.17	Rayleigh scatter of AgK_α
10	10.55	Pb L_α (+As K_α?)			

Table 1b **Canadian Certified Reference Material - Syenite Rock, SY - 3**

Element	Chemical concentration	Range	Calculated concentration
Ti	900ppm	720 -1740ppm	1355ppm
Mn	2556ppm	2246 - 2886ppm	2560ppm
Fe	4.70%	4.4 - 4.73%	4.84%
Zn	250ppm	256 - 259ppm	263ppm
Ga	28ppm	25.6 - 36	26.9ppm
Rb	210	188 - 213	195ppm
Sr	300ppm	250 - 472ppm	287ppm
Y	740ppm	610 - 880ppm	681ppm
Zr	340ppm	295 - 392ppm	322ppm
Nb	145ppm	94 - 195ppm	135ppm

Table 1c **Canadian Certified Reference Material, KIA - OG1**

Element	Chemical concentration	Range	Calculated concentration
Zn	20.37%	N/A	19.85%
Pb	6.98%	N/A	4.4%
Cu	0.11%	N/A	0.98%

CHAPTER II
REGIONAL GEOLOGIC SETTING

The Kenyan Rift Valley is part of a worldwide system of sublinear belt of active seismicity, volcanicity and heat flux defining the edge of a lithospheric plate. Of the commonly known plate margins, the Kenyan Rift System appears to conform to a divergent plate margin situation dividing the country almost into two. The break up process is however incomplete as evidenced from geophysical data (Wendland and Morgan 1982) which has shown that the lithosphere is anomalously thin. Rift bottoms have also been shown to represent seismic discontinuity zones made up of less dense, partially melted mantle forming areas of low velocity (Windley, 1984). Additional research carried out by the KRISP Working Group (1987) using Deep Seismic Refraction method have further confirmed that the flanks of the Kenyan Rift Valley have relatively normal crustal thickness which reduces to about 20 km thick within the rift particularly around Lake Turkana.

As a result of intense faulting and volcanic activities within the surrounding areas of Longonot, OlKaria and Eburru, rocks within the Naivasha area are relatively young in age (Clarke *et al.* 1990). Plio-pleistocene trachytic lavas and ignimbrites occupy nearly all the floor of the central rift and occur in places on the marginal plateux. The lower part of this group consists mainly of trachytic tuff with prominent Ignimbrite units which are best exposed on the Kinangop Escarpment, to the east of the study area (Thompson and Dodson 1963).

Extensive pyroclastics and rhyolitic lavas associated with alkaline trachyte cover much of the area between Lake Naivasha and Mount Longonot volcano. Similarly, towards mount Eburru, thick pyroclastics and trachytes cover most of the area and only the OlKaria seems to be dominated by commenditic lavas. The subaqueous pyroclastics on the Kinangop scarp and within the Hell's Gate National Park (Ol - Njorowa Gorge) are mainly of Lower Middle Pleistocene (Thompson and Dodson 1963). Around Lake Naivasha, however, widespread lacustrine sediments that cover the rift floor were deposited towards the end of Pleistocene (Thompson and Dodson 1963).

2.1 Formation of the Kenya Rift System

Many theories have been suggested in an attempt to explain the present structure of the Kenya Rift System. The most supported theory is an origin from a domal or shield structure as summarized by the author in Fig. 3. Scattered occurrences of Miocene sediments have further been used as additional evidence to support the theory of structural doming leading to the concept of pre-Miocene erosion surface (Shackleton 1951, Pulfrey 1960). King and Chapman (1972) have also discussed the concept of a broad structural dome and believes that there was a gentle basement arch under the Kenyan Rift zone but that it developed earlier as a continental watershed consequent to the breakup of Gondwanaland. However, Williams (1978), in his argument believes that much of the pre - Miocene topography near the rift consisted of basement high ground.

The oldest rocks though unexposed in the Naivasha basin consists of Precambrian metamorphosed basement rocks. These rocks were rift faulted since the Miocene in central Kenya and were later covered by volcanic lava (Baker and Mitchel 1976). In the course of the rift development, small grabens formed on the rift floor and this is registered by volcano - sedimentary sequences which were deposited in these basins particularly away from the center of the domes (Fig. 5) in the Turkana and Magadi - Natron basins. The major faulting events were associated with volcanic eruptions at every stage and therefore tectonic activities can be said to have had a significant influence on the early development of weaker zones along which lava escaped through to the earth's surface.

2.2 Structural evolution of the Naivasha area

Section 2.1 above reviews faulting as a major contributor to many of the tectonic and magmatic features observed in present Kenya. From about 4 - 1.7 Ma an inner narrower trough developed within the central region of the rift and it is within this trough that eruptions of the recent salic volcanoes (Baker *et al.* 1988) associated with obsidian formations occurred at 0.4 - 0 Ma. Middle and upper Pleistocene grid faulting within the graben floor has further resulted in step fault platform which are sub - parallel to the main Rift faults (Fitton and Upton 1987).

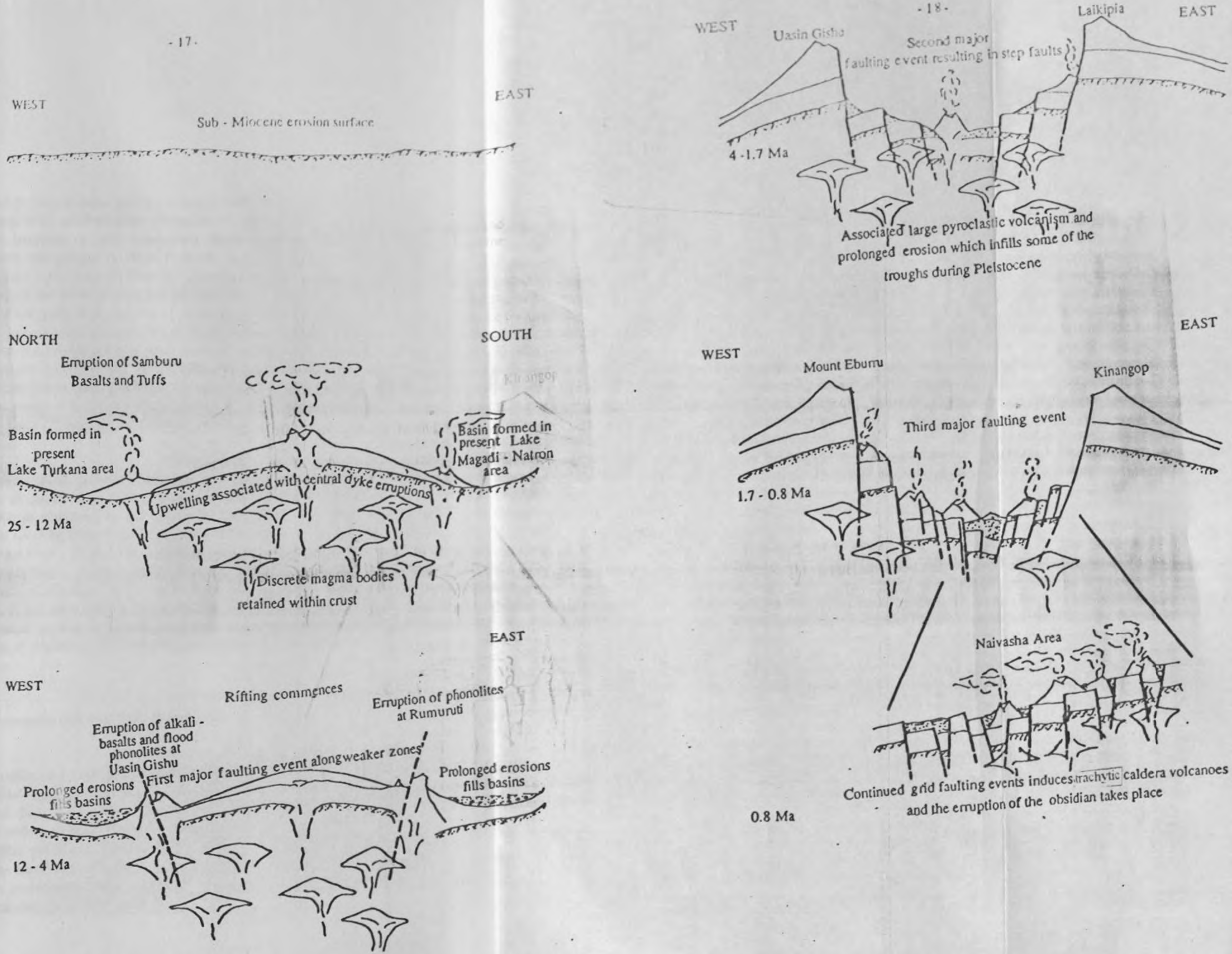

Figure 5 Successive stages in the development of the rift system and the associated obsidian formation. (modified from McCall 1967)

Three distinct periods of minor faulting occurred from about 4 to 0.4 Ma. Between 3 - 2 Ma. step faults resulted in the formation of narrow grabens and these were followed by eruptions of early Quaternary flood trachytes. Renewed faulting affecting mostly the margins occurred from about 1.7 Ma and is associated with Quaternary flood lavas of the rift floor of 1.65 - 0.9 Ma. The last stage of extensive minor faulting of the rift floor occurred between 0.8 - 0.4 Ma. Post 0.4 Ma faults are associated with parts of the Eburru - OlKaria major volcanic alignments (Clarke *et al.* 1990), and are conspicuous on the northern flanks of eastern Eburru volcanic pile. There has been reactivation of some of the rift margin faults and it is possible that these are post 0.4 Ma in age. Most of the rift floor faults are, however, locally obscured by late Quaternary pyroclastic volcanic piles derived from the younger rift floor volcanoes such as Longonot and the lower to middle Pleistocene sediments in the Naivasha basin (Thompson and Dodson 1963).

Based on seismic results and the distribution of volcanic areas (Longonot, OlKaria and Eburru), the present high relief (topography), with highlands rising to between 3,000 - 4,000 m traversed by the rift faults, is however a result of immense accumulation resulting from volcanic eruptions from within these centers (KRISP Working Group 1987). From Table 2 which gives a summary of the main stages of rift development, together with evidence gathered in the field concerning the nature and occurrence of obsidian, there seems to be a relationship between obsidian formations and the latest and youngest of these volcanoes. Figure 5 and Table 2 can thus be used together to summarize possible lines of events that finally led to the formation of obsidian in the Naivasha area as discussed in Chapter 5.

2.3 Environment and evolution of obsidian

Although obsidian rocks have not attracted much attention because of their present non-economical value, they are on the other hand of importance in understanding the mode of their occurrence. This section therefore attempts to relate field observations with the already described tectonic activities in an attempt to establish the stratigraphic position of the obsidian formation. The stratigraphic position in relation to the associated rocks is necessary in order to fully understand the origin and possible evolutionary lines. A generalized sequence commonly associated to obsidian occurrence is summarized below.

Table 1. Main stages of rift development in central Kenya Rift
(modified from Clarke *et al.* 1990)

STAGE	PRE - RIFT DEPRESSION	HALF GRABEN	FULL GRABEN	INNER TROUGH
AGE	25 -12 Ma BP	12 - 4 Ma BP	4 - 1.7 Ma BP	1.7 - 0 Ma BP
TECTONIC STYLE	Broad shallow decompression and warping marking the beginning of rift formation	Faulting in northern Kenya spreading southwards by 7 Ma BP	Grid faulting in Central Rift including the Naivasha area	Extensional tectonics in narrow zones
VOLCANISM	Basalts and basanites erupted over wide areas in Kenya accompanied by carbonatite volcanism on the flanks of the Kenya Dome.	Alkali basalts and flood phonolites followed by transitional basalts/trachytes	Basalt trachyte volcanism in central region associated with large pyroclastic eruptions	Eruption of flood trachytes followed by grid faulting at less than 0.8 Ma. Trachytic caldera volcanoes with rhyolite and obsidian (comendites) prominent in the Naivasha area

There is usually a progressive upward increase in silica content as one moves from the Miocene rocks to the more Recent types (King and Chapman 1972, Baker *et al.* 1988):

(1.) Obsidian usually occurs as the latest and therefore on top of the sequence although usually there is a cover of pyroclastic rock or in association with comendite of very young age.

(2.) In association with and/or close to the obsidian is usually a succession of rhyolite to pumiceous volcanic material of possible similar age or slightly older than the obsidian.

(3.) Where comenditic exposures are absent, there is usually trachyte forming the next younger rocks. Around Kongoni as well as along the road near Obsidian Ridge, sporadic exposures of basalt may be observed. The trachytes are usually of about Pleistocene age (Thompson and Dodson 1963).

(4.) Phonolite of Pleistocene age with a reduced degree of trachyte - basalt occurrence is then exposed (King and Chapman 1972).

(5.) Underlying the younger volcanic sequences are the flood plain basalts, which were erupted in most parts of Kenya during the Miocene (King and Chapman 1972).

(6.) Below the whole sequence, though unexposed within the Naivasha area, are the basement rocks of Precambrian age (Baker *et al.* 1988).

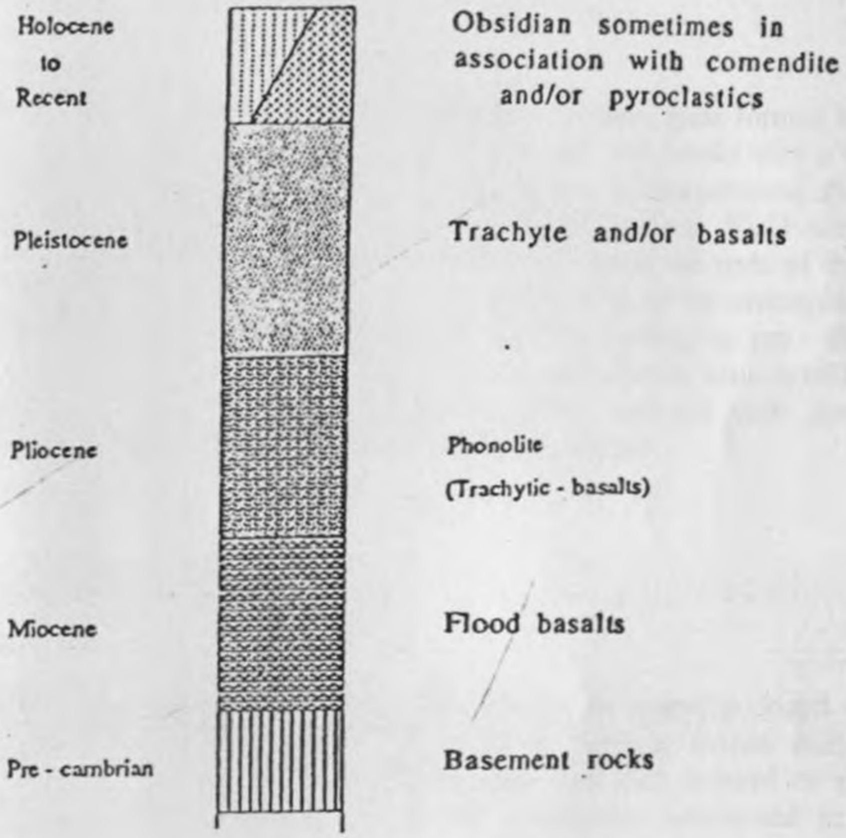

Figure 6 Summary of observed stratigraphic position of obsidian in relation to other rocks in Naivasha area.

CHAPTER III
OBSIDIAN FORMATION

Obsidian is a dark greenish to nearly black shiny volcanic glass formed basically by super cooling of magma. Typically, it is very brittle and breaks with a conchoidal fracture. Flaked chips have extremely sharp edges, a characteristic that made it useful to pre - historic man for the manufacture of artifacts. Field occurrence of obsidian, however, varies considerably influencing both the style of exposure as well as the chemistry of the rock. One of the objectives of the investigation was to establish obsidian quarry sources that could have been mined by pre - historic man for tool manufacture. Sampling tended to be concentrated on sources with adequate quality for stone working i.e., the highly glassy material with good flaking properties, avoiding the dull, almost crystalline 'pitchstone'.

3.1 Obsidian Occurrence

The highest concentration of obsidian occurrences in Kenya is found within the Naivasha area. The exposures occur both as massive frozen skin covering comendite flows, as well as separate flows of vesicular, layered or pyroclastic obsidian. The four identifiable models of occurrences established in the field include:-

3.1.1. Pyroclastic obsidian
3.1.2. Layered obsidian
3.1.3. Massive obsidian
3.1.4. Vesicular obsidian

3.1.1 Pyroclastic Obsidian

These usually occur as blocks of variable sizes embedded within trachytic lava flows as seen at Kinangop Plateau and at the edge of Crater Lake quarry sources. Obsidian occurring in this form is usually older than the associated rocks and is likely to have been formed and then later blown up together with the pyroclastic or volcanic ash. This is further supported from the fact that their contact is very sharp exhibiting no gradation with the associated rocks. The obsidian also contains no inclusion of the associated rock. In most cases therefore, obsidian rock has been to some extent displaced from its source area. The cooling of the pyroclastic obsidian is therefore expected to have taken place prior to their transportation and final deposition (judging from their shattered nature and the sharp contact together with exclusion of the host rock).

3.1.2 Layered Obsidian

Obsidian flows were also found to exhibit layering. A possible cause of layering observed in some of the obsidian outcrops can be said to have resulted from flotation of lighter materials. Micro - rhythmic layering on the other hand can be attributed either to multiple injection or an alteration of stagnant and convecting conditions. Other possibilities include the fact that layering could have been controlled by the relative rates of chemical and thermal diffusion in the melt during cooling. This has a direct bearing on density and viscosity of the melt, which in turn affects the degree of super cooling. Typical examples of small scale layering were observed on an exposure at Cedar Hill quarry source where some of the outcrops exhibited layering up to a few centimeters thick with well defined bases - the lower parts possibly rich in heavy dark colored minerals grading into an upper part with less darker and therefore lighter colored minerals.

3.1.3 Massive Obsidian

This is the most common mode of occurrence for obsidian in the area. In most cases, their sources can be assumed to be relatively nearer to/or actually below the sites where they are exposed. Usually, they are found to be associated with weathered plugs or along faulted blocks. The obsidian under this category possibly formed through chilling induced by contact with a different medium (host rock) on exposure. At certain sampled quarry sources, they exhibited gradation with the country or associated rocks, as seen at a quarry source on the road near Elsamere Conservation Centre. At this locality, obsidian shows good gradation into rhyolite and then to pumiceous rock. A typical quarry source of massive obsidian is exposed at the foot of Fischer's Tower within Hell's Gate National Park.

3.1.4 Vesicular Obsidian

Some obsidian exposures were found to contain vesicles. Obsidian melts containing variable amounts of dissolved volatile constituents at the time of eruption, of which the most abundant are H_2O and CO_2, can solidify to form vesicular type of obsidian. Under pressure, these volatiles will remain in solution, but with pressure reduction on exposure, or an increase of their concentration in the liquid as volatile free phases, they may evolve to form bubbles. Bubbles trapped during solidification of the melt are preserved as vesicles. A typical exposure was sampled along the the Giraffe Circuit within Hell's Gate National Park.

3.2 Systematic Summary of Sampled Quarry Sources

A total of 48 quarry sources were sampled during the field survey. Of these, only 20 representative quarry sources are summarized here in detail as the rest exhibited little or no variations in terms of field occurrence from those that are described. The included geological map at the end of the thesis shows the distribution of sampled quarry sources in relation to the general geology of the area.

Also considered is the possible recovery of obsidian from the site as a product for tool making operations by pre - historic man. The obsidian formations are described together with the geology and quarry potential.

3.2.1 Kinangop Quarry Source No. K-1

This is a quarry source on the western margin of the Kinangop Plateau situated at an elevation of about 2,400 m. The Kinangop Plateau is separated from the floor of the rift by a series of down - faulted platforms. The obsidian formation exposure which is near the road has been cut by a north - north - west trending South Kinangop fault scarp exhibiting steep to near vertical rock faces. Plate 4 shows a road cutting exposing the Kinangop Formation overlain by trachyte which appears to be pyroclastic and within which obsidian occurs. To the extreme south, the scarp has been buried by younger pyroclastic rocks. At the sampled site, a succession of the Kinangop Tuff Formation dated at 3.4 - 4.5 Ma (Baker *et al.* 1988) consists mostly of welded tuffs, palaeosols and weathered zones and measures about 150 m thick, underlying pyroclastic obsidian formation.

Mode of formation

These pyroclastic obsidians were possibly formed by emplacement of widespread trachytic flows from a centre or centres unknown but possibly within the area of the rift floor now covered by younger volcanics (Thompson and Dodson 1963). Further trachytic flows containing no obsidian overlies this flow. The quality of obsidian found here is good and considering the strategic position of the site at the edge of the scarp together with the moderately high quality of obsidian found, this site could possibly have been quarried for tool making. The presence of obsidian mined from this region has been noted at the nearby Cartwright's Archaeological Site (details of artifact - source comparisons are given in Section 4.3.1).

3.2.2 Obsidian Ridge Quarry Source No. OBR-1

This is a ridge trending in a north - south direction and is lithologically composed of tuffs and lapilli - tuffs with a layer of welded scoriaceous blocks and volcanic bombs. Lithic blocks of trachyte, welded tuff and porphyritic basalts are also exposed. In contact with trachyte is a phonolitic lava flow exhibiting water - laid structures as shown in Plate 5. Obsidian is exposed at the top of the ridge from which the name is derived. This formation is classified under massive type of occurrence.

Mode of formation

The presence of water - lain (shattered) structures together with volcanic bombs suggests that a possible volcanic eruption of extreme violence (phreatic), usually resulting from the conversion of ground water into steam, was involved. Such phreatic explosions are known also to have low temperatures and the resulting water could have caused the chilling of obsidian. The scoriaceous veneers however, are probably of late stage magmatic eruptions, possibly emanating from the nearby Mount Longonot volcano (Clarke *et al.* 1990). Good quality obsidian is exposed here and could have formed a good mining site considering its proximity to the major archaeological sites in the region. Large concentrations of broken pieces, typical in areas of mining were observed at the foot of the ridge as well as on the flat ground between the ridge and Lake Naivasha.

3.2.3 Fischer's Tower Quarry Source No. HG-1

Fischer's Tower is a pinnacle to the south of the main entrance to Hell's Gate National Park. It is a volcanic plug which has been left standing after the erosion of the surrounding pyroclastic rocks. The comendite forming the main tower is variably porphyritic exhibiting columnar jointing. Massive obsidian is exposed at the foot of this tower. Plate 2 shows the Fischer's Tower pinnacle at the entrance to Hell's Gate National Park.

Mode of formation

A massive occurrence of obsidian formed possibly through chilling by contact with the surrounding country rocks forming the main pinnacle. Subsequent erosion, within the surrounding area, has since exposed the plug forming the pinnacle. Columnar jointing affecting the commendite has further reduced the pinnacle exposing obsidian at its base. It is possible that large chunks have been quarried from this source (Merrick and Brown 1984a). This is supported by the amount of debris scattered at the foot of the pinnacle. In Section 4.3.1 where inter - quarry artifact comparison is discussed, obsidian mined from sites around this area (Hell's Gate region) seem to have dominated in most of the known Archaeological Sites in Kenya.

3.2.4 Hell's Gate Quarry Source No. HG - 2

The locality is on the circular road (Giraffe Circuit) within the Hell's Gate National Park and in association with layered sediments. The distribution of these sediments is widespread including the farm areas of Oserian and Sulmac (Thompson and Dodson 1963). They are lithologically pumiceous being composed mostly of granules including pebbles, gravels, coarse sand, silts and clays. Thicknesses of up to 15 metres have been measured in sections. The obsidian formation here occurs as thin vesicular bands or layers intercalated with the sediments.

Mode of formation

These were probably formed by reworking in shallow water environments (hence the presence of water laid deposits) and obsidian here was formed from possible chilling. The vesicles could therefore be as a result of included volatile fluids that escaped during cooling. Although the quality of obsidian exposed is good, the fact that they are vesicular also means that for quarrying purposes, a lot of material had to be mined in order to obtain "vesicle free" samples for artifact manufacture.

This would probably seem to be an unlikely case to have happened in an area with numerous exposures of better quality obsidian. Possibilities of mining are further reduced by the limited occurrence of this type of obsidian which appears to be patchily distributed. Best exposures occur mostly where erosion has been intense.

3.2.5 Ol - Karia Quarry Source No. HG-5

Minor displacements within the Ol - Karia geothermal field area have exposed several obsidian bands. Only one such typical quarry source is described here as a representative case. These obsidian formations are exposed as good quality massive varieties within the widespread pyroclastic formations in the area. It is, however, difficult here to comment on the possible usage of these sources for tool making activities because they appear to be confined to relatively small bands and the nature of the topography is such that most of them are covered by late Pleistocene to Recent tephras.

Mode of formation

These are usually exposed lenses or bands associated with widespread volcanism in the general area. The pyroclastic veneer within which they occur are similar to those covering the nearby Hell's Gate area and can be tentatively said to have originated from the nearby Mount Longonot (Clarke *et al.* 1990).

3.2.6 Ol - Njorowa Gorge Quarry Source No. HG-6

The Ol - Njorowa Gorge starts near Central Tower within the Hell's Gate National Park and extends southwards down to the entrance to Akira Plains. It is characterized by narrow and deeply incised cliffs. Obsidian is exposed on the sides of these cliffs at several localities where they occur as chilled zones or dykes.

The quality of obsidian exposed at these localities is moderately good and it is possible to associate them with other quarry sources of good quality which were mined for tool making (Merrick and Brown 1984a).

Mode of formation

Subsequent faulting and erosion within the gorge has greatly contributed to exposing these obsidian quarries. Their compact and massive occurrence in addition to their dyke - like structures suggest that they are lava tubes which were chilled on exposure by the surrounding country rock.

3.2.7 Ol - Njorowa Gorge South Quarry Source No. HG - 9

This is an obsidian source located at the southern end of the gorge just before it opens into the Akira Plains. It is exposed on a cliff near the steam jets with good quality obsidian.

Mode of formation

This is a massive occurrence of obsidian that chilled to form a dyke but has subsequently been exposed by faulting and erosion along the gorge. The high amount of erosion at the foot of the cliff along the gorge limits the possibility of finding any remaining broken chips to associate it with mining activities. The exploitation of most of the Ol - Njorowa Gorge quarry sources for tool making is doubtful and must depend on the age of faulting and erosion that exposed obsidian seen in this area.

3.2.8 Ol - Olbutot Quarry Source No. OL - 3

The largest obsidian exposure is located within the Ol - Olbutot commendite member whose most striking expression is a very thick and young flow within the OlKaria geothermal area. The associated lavas consist of subaerially erupted rhyolitic, trachytic and basaltic pyroclastic rocks associated with the obsidian. Quite a good amount of rolling and churning seems to have taken place at the time of deposition of this lava flow as evidenced from field occurrence. The quality of obsidian within this flow varies considerably from the crystalline looking pitchstone to the high quality glassy obsidian typical of those used in tool manufacture.

Mode of formation

The lava flow forming the Ol - Olbutot is part of a fissure eruption overlying the original surface. Carbonized tree branches from a pumice flow associated with this lava flow has been dated as 180±50 BP. (Clarke *et al.* 1990). It has been classified under massive type of obsidian. The quality of the lava flow is good but the age of the flow, which is estimated to have erupted within the last one hundred years or so, puts some limits on the possibility of the flow having been exhaustively mined for tool making.

3.2.9 Elsamere Conservation Centre Quarry Source No. KB - 1

Pumice grading into rhyolitic commendite containing obsidian was observed in a road cutting quarry site near Elsamere Conservation Centre. The pumice is trachytic to agglomeratic and the occurrence is obsidian banded with rhyolite into which it easily grades. The whole sequence is mantled by pyroclastic rocks typical in the general area.

Mode of formation

Banding and layering in an active volcanic region like the Naivasha area sometimes is suggestive of welded pyroclastic rocks rather than lava flows. Since some undoubted pyroclastic rocks composed of pumice, lithic lapilli and blocks also occur in association, it is possible to associate this occurrence with pyroclastic eruption.

3.2.10 Kibikoni Quarry Source No. KB-3

Several obsidian lava flows were encountered at the southern end of Lake Naivasha along the South Lake Road near Kibikoni Farm. The flows have a north - south trend and are heavily covered in pyroclastic rock. The quality of obsidian is good and these flows could easily have been mined for stone tool working. They are classified under massive variety.

Mode of formation

These are lava flows which were possibly erupted from within the Ol - Karia area and were chilled as they flowed towards the lake. Subsequent eruptions in the area resulted in the thick pyroclastic cover which has now partly buried the flows. The exposures appear not to be large enough to have attracted extensive mining since most units are covered by subsequent pyroclastic material. The style of field occurrence, i.e. gradation, could also have limited their chances of being mined taking into account the fact that there are other sources nearby which do not grade with the country rock and could have been easier to exploit.

3.2.11 Kongoni Police Station Quarry Source No. KN-1

This quarry is located within a comendite formation zone. The associated comendite is variably vesicular and occasionally pumiceous. It is porphyritic crystalline with feldspar and associated obsidian occurring in devitrified bands. Locally, the obsidian is highly spherulitic, although good quality obsidian also occurs.

Mode of formation

Possibly a result of extrusion of comendite as dome/ridge together with obsidian occurring as a lava flow. Good quality obsidian is found here and its strategic locality, being at the top of a ridge, makes it an ideal site for mining and possibly even tool manufacturing. This conclusion is drawn from the fact that there is a large concentration of broken pieces together with moderately good shaped pieces left at the site.

3.2.12 Green Crater Lake Quarry Source No. GCL-1

At the Green Crater Lake or Sonanchi, obsidian is exposed as pebble conglomerates (tephra) as well as embedded material within the trachytic exposures at the rim of the crater, hence the classification as pyroclastic type. The quality of obsidian exposed is moderately good and has been classified under the pyroclastic variety. It is therefore probable to associate the source with those that were mined for manufacture of artifact. Details of a possible utilization of this quarry source by pre - historic man for tool making is discussed further under Section 4.3.1

Mode of formation

These occurrences were definitely associated with the formation of the crater itself and it is possible the lava flow incorporated obsidian on its way to the surface. Obsidian is likely to have been extruded at the time of formation of the crater itself. This is further supported both by the blocky nature of obsidian as well as the shattered nature in which it is seen to occur. Sonanchi obsidian was quarried for tool making as presented by the large amount of obsidian scatter found within the vicinity of the crater lake as well as its strategic position together with the general proximity to major archaeological sites in the area.

3.2.13 Hippo Point Quarry Source No. HPF - 1

An occurrence within a pantellarite formation lithologically consisting of obsidian with devitrified bands and visible phenocrysts of feldspar and quartz. The quality of obsidian here varies greatly from pitchstone to the characteristic good quality glassy variety associated with the manufacture of tools. This exposure is classified under massive occurrence.

Mode of formation

This is an extrusion of obsidian flow with no evidence of any associated pyroclastics. An ideal site for mining with very good quality obsidian association. No concentration of debris material was however observed on/or near the site sampled.

3.2.14 Lake Road Quarry Source No. BX - 1

This is a roadside quarry source before the junction to Mount Eburru. The obsidian here is nodular, occurring as a seam along a chilled zone within a soft pyroclastic deposit. The nodules vary in size from small pebble sizes, which easily disintegrate, to large boulder sizes. Plate 6 shows a section of the seam, which appears also to have experienced some minor displacement (faulting) subsequent to intrusion. Although of fairly good quality, the sizes of the pebbles could have restricted exploitation of this type of obsidian since only microliths could have been curved. The distribution of debris typical of mined quarries, however, is widespread around this area.

Mode of formation

This appears to be a chilled zone of an obsidian flow that cooled and was covered by the overlying rhyolitic pyroclastic rocks from subsequent flows. It is massive in occurrence and does not exhibit any inclusions from the associated rock with which it forms a very distinctive contact.

3.2.15 Maasai Gorge Quarry Source No. MG - 1

Pebbly to nodular obsidian also occurs along Maasai Gorge. At least two quarry sites were identified in the gorge with similar geochemical signatures and only one of them is described here in detail. Merrick and Brown (1984b) have established that there are archaeological sites in Kenya whose artifacts were made from obsidian quarried from Maasai Gorge area.

Plate 5 Water laid structures associated with the lava flow at Obsidian Ridge Quarry source

Plate 6 Lake road quarry source showing intrusive seam - like obsidian occurrence

Mode of formation

The obsidian occurrence at the Maasai Gorge is massive and is associated with the typical comenditic exposures found in many parts of the area. Moderately good quality obsidian is found to occur here although very fragile varieties were also encountered.

3.2.16 Ridge Quarry Source No. MG-2

This quarry source is located on a ridge formed from volcanic rocks with several prominent fault scarps to the north - western end of Lake Naivasha near the Gilgil river bridge. The high quality obsidian found here together with large concentrations of scattered debris suggests that the quarry could possibly have been mined for stone tool making.

Mode of formation

This occurrence is in association with commendite and thick pyroclastic cover. Widespread erosion associated with faulting has exposed some of the obsidian outcrops. This is a massive occurrence of obsidian where chilling was probably caused by direct exposure of the flows most likely in association with intense rifting.

3.2.17 Cedar Hill Quarry Source No. CH - 3

Several exposures were sampled around this region but after laboratory analysis, it was found that most of them showed similar geochemical signatures. Only one such representative quarry source is described. The obsidian lava flow is massive, sometimes vesicular with sparse to high feldspar porphyries. Some associated thick flows consist of crystalline lava with obsidian at the surface. High concentrations of debris attest to several mining localities.

Mode of formation

Possibly formed by volcanism dominated by lava extrusion in the youngest flow accompanied/preceded by eruption of pumice blocks and lapilli dispersed westwards towards the nearby Lion Hill.

3.2.18 Mount Eburru Quarry Source No. E - 1

This is a quarry source on Mount Eburru where the down faulted platform separate the Mau escarpment from the rift floor. Characteristic associated rock types include trachytes (peralkaline, rhyolites and trachytes). The general lithology is made up of unwelded pyroclastics composed of pale yellowish - gray pumice lapilli, blocks and obsidian lithics. Obsidian also occurs as a layer on top of unwelded pyroclastics.

Mode of formation

The comparable lack of weathering and vegetation cover indicates that the youngest activity must be similar in age to those at Longonot and/or OlKaria, i.e., recent times, and probably only hundreds of years (Clarke *et al.* 1990).

The distributions of the majority of fumarolic activity coinciding with many of the summit craters further indicate more recent activities. Unwelded pyroclastics possibly represent proximal fall deposits. The obsidian formation is a welded deposit composed of pyroclastics.

3.2.19 Eburru Station Quarry Source No. ET - 1

To the south of Cedar Hill, near the abandoned Eburru Railway Station, is a huge obsidian lava flow of very good quality. The lava flow, which has a north - south trend extends towards Mount Eburru where it disappears under the thick but young pyroclastic cover of deposits. The quarry source shows extensive mining at different sites associated with high concentrations of left over debris.

Mode of formation

This is a massive obsidian lava flow associated possibly to earlier eruption from the nearby Mount Eburru volcano. The flows were possibly chilled as they flowed down the sides of the mountain. Subsequent eruptions from the mountain have since covered the upper reaches with thick pyroclastic deposits.

3.2.20 Eburru Road Tunnel Quarry Source No. ET - 2

This is located along the abandoned Railway Line and to the west of Eburru Station. Several localities were sampled but laboratory analyses have shown that they have similar geochemical signatures. Although it was not possible to pin - point any specific quarrying site within these flows, the high quality obsidian exposed is characteristic of the type used in pre - historic tool industries. The quarry is classified under massive type of occurrence.

Mode of formation

This, similarly, is a lava that cooled as it flowed and with its proximity to Eburru, it is difficult not to associate the source of the flow to Mount Eburru. Subsequent volcanism within the region has covered portions of the flow.

CHAPTER IV
LABORATORY ANALYSIS

In addition to the physical data obtained during fieldwork, samples from each obsidian flow in the area under study were subjected to detailed laboratory analyses in order to assess the homogeneity and distinctive characteristics of elemental composition. This involved obtaining petrographical and geochemical data. Part of these data has been used to supplement in the identification of other possible differences as well as to correct and improve the physical model established in the field. The rest of the results are used in Chapter 5 to discuss possible nature, temperature, maturity and mixing processes of the lava flows at the time of formation of the obsidian.

Under perfect equilibrium conditions, magma should complete crystallization by the time it cools to its solidus temperature. It should then consist of an assemblage of minerals whose crystallization sequence can easily be predicted from equilibrium phase relationships. Actually, crystallization does not take place so readily. Some volcanic rocks like obsidian cool right down to atmospheric temperatures without crystallizing at all, and many more have at least a glassy groundmass. Obsidian is a rock of volcanic origin which consists principally of massive imperfect glass sometimes containing bubbles and a variety of phenocrysts or micro - phenocrysts enclosed within the glassy matrix. The composition of its liquid phase can be estimated from the composition of this glassy groundmass.

Many techniques have been applied in trying to understand the composition of obsidian ranging from macroscopic and microscopic petrographic descriptions (Game 1945), to analyses of magmatic properties (McDougall *et al.* 1983) together with various chemical study utilizing either major and/or trace elements for characterization. In this study, an initial attempt was made to differentiate the various obsidian formations using petrological descriptions.

It was however realized that petrographic differences observed in obsidian using the microscope are not distinctive enough to separate the various flows from one another. Further analysis, using the x - ray fluorescence (XRF) technique, was therefore applied as the main method of distinguishing between the different flows as described under Section 4.2.

4.1 Petrography

The fact that obsidian rock has a groundmass of glass has an important petrogenetic consequence for it demonstrates the presence, at least at the time of formation, of a super heated fluid (magma above its liquidus temperature) in the near surface environment. Generally, the presence of phenocrysts (porphyritic texture) is attributed to a period of rapid cooling when the groundmass is formed. Based on the assumption that determination of similarities in obsidian groundmass could help in differentiating the various flows forming the obsidian outcrops (Shotton 1959), initial analytical work was therefore concerned with petrographic aspects of the rock capable of giving information on direct petrographic origin. However, in the case of obsidian, certain constrains on the amount of heat available for assimilation processes or thermal conditions necessary for crystal - liquid fractionation, appear to be lacking making it impossible to rely on petrographic differences alone.

4.1.1 Thin section study

Thin sections were prepared out of selected samples for study under the microscope. The slides were examined with a view to using petrographical differences in the identification and separation of the various obsidian formations. In the majority of samples observed in thin sections, it was noted however that obsidian, apart from being glassy, contains phenocrysts of anorthoclase, green clinopyroxenes, fayalites, quarts and a variety of ferromagnesian minerals. The rock is however uncolored and transparent, featureless except perhaps for some of the above crystallites which do not help in diagnostic study.

Plates 7 and 8 show photomicrographs of two obsidian samples collected from two widely placed quarry sources (Kinangop quarry source No. KN-1 and Fischer's Tower quarry source No. HG-1). It is however important to note that, although geochemical analyses carried out on these samples later (under Section 4.2) was able to separate them, the photomicrographs do not seem to show any major distinguishing features.

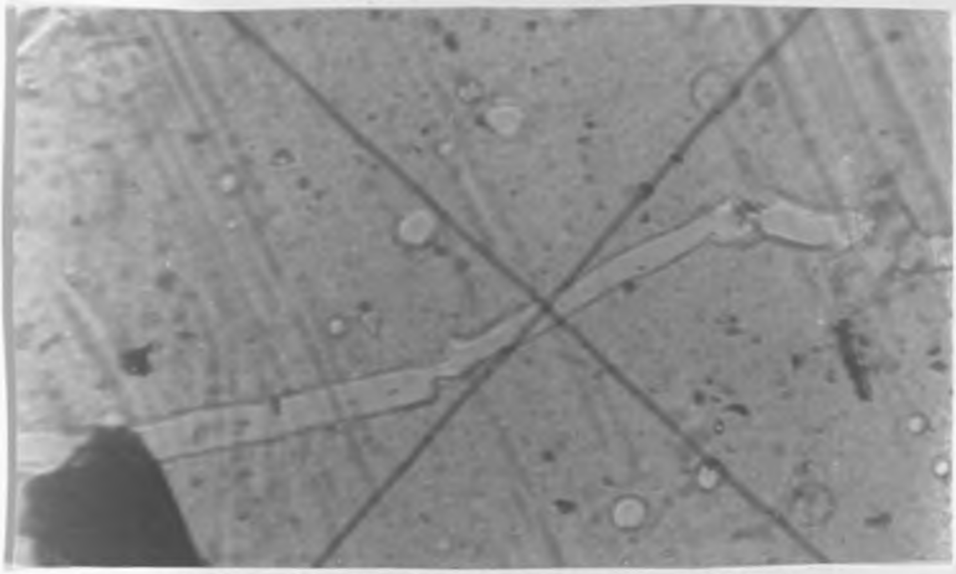

Plate 7 Photomicrograph of obsidian from Kinangop Escarpment with X-nicols at Mag. X 100

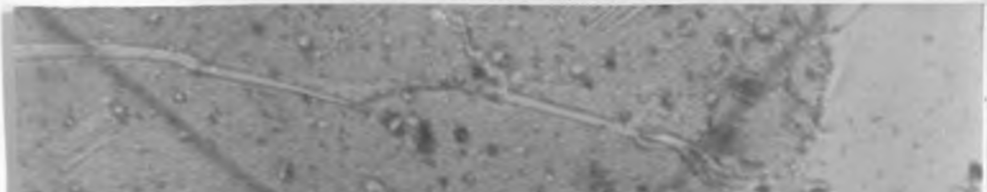

Plate 8 Photomicrograph of obsidian from Fischer's Tower with X-nicols at Mag. X 100

Omi and Agata (1977) have used some of the limited variations in chemical composition to study obsidian under the microscope (relative proportions of alkaline to alkali - earth elements and the range of silica content), but such variations are known to express themselves in very narrow ranges in terms of densities and refractive indices. The result is a broad spectrum of classes incapable of separating obsidian in an area where outcrops are relatively close to one another like the Naivasha area.

4.2 X - Ray Fluorescence Analysis

Characterization of obsidian sources is best done by analyzing the elemental composition (Cann and Renfrew 1964. Griffin *et al.* 1969. Bowman *et al.* 1973). It is then possible to distinguish different sources of obsidian using the variation of element proportions. Source discrimination analysis is usually based on the assumption that the elemental composition within a given flow of obsidian is uniform and that the source to source variations in the concentrations of the elements detected are sufficient to differentiate the various obsidian outcrops or flows.

The precise composition of any rock depends on the temperature and pressure at which it formed, the composition of the host rock and in some cases, the rate at which it formed. Compositional study can therefore provide useful information on the type of melt from which a rock has been derived as well as the geological environment.

Where a rock shows no textural evidence of differences and/or where petrography alone cannot be sufficiently definitive to identify the fabric of the source, then geochemical analysis can be applied for precise determination. The application of XRF technique should therefore be viewed as an extension of, or supplement to, the standard petrological approach.

4.2.1 Analytical Results

Analytical data obtained from the present study give major and trace element composition of obsidian from several geologic quarry sources around Naivasha area. These data are given in Table 3 and can be treated as average values obtained from 5 analyses (measurements of the same sample). Quarry source localities in relation to the general geology of the area are included in the geological map at the end of the thesis. From these results, it has been possible to distinguish 13 Petrographic Groups of obsidian on the basis of both major and trace element abundance from the different quarry sources. These groups shown on the map in Fig. 7 appear to reflect discrete outcrops assigned to each obsidian flow. These analyses also demonstrate that there are marked differences between many of these obsidian groups in terms of the major and trace elements observed (MacDonald 1974, Baker and Henage 1977). The distinction between these various sources have been obtained by considering both the stronger and the weaker peaks in the elemental analysis.

Table 4 summarizes the average elemental values for the major Petrographic Group areas. Note the obvious distinct difference shown by Fe in Kinangop area - 4.53%, Njorowa Gorge area -2.45% and the Mount Eburru - 7.0%. The Fe value for example is at its lowest at Ndabibi - 1.30% and Green Crater Lake - 1.43%, then rises to 7.0% in the nearby Mount Eburru! From the geochemistry of some of the major and trace elements of obsidian given in Table 3, certain elements such as Nb, Zr and Rb, show distinct differences in chemical compositions and hence illustrating the advantages of using more than one group of elements in differentiating the obsidian quarry sources from one another.

Data obtained from the analyzed obsidian sources varies consistently with the major domes within the Naivasha area. The clustering of these ratios particularly between the elements Rb, Zr and Nb have been used in identifying and establishing petrographic groups. A plot of niobium and zirconium variation (Fig. 8a) between mount Eburru and Hell's Gate area shows an obvious difference in trend between the two domes. Data for samples collected from Kinangop Escarpment and Obsidian Ridge quarry sources do not fall in either of the two established trends. This confirms further the possibility that these two formations belong to completely separate and distinct domes. It also supports the field observations on occurrence and possible mode of formation as summarized under Section 3.2.1 and 3.2.2.

Table 3. Whole Rock Geochemistry for Obsidians, Naivasha Area

Qry. No.	Ti	Fe*	Mn	Ca	K	Cr	Cu	Zn	Ga
HG - 1	0.06	2.80	0.04	0.29	2.16	14	19	289	-
HG - 2	0.06	2.41	0.03	0.28	1.92	7	22	270	-
HG - 3	0.06	2.14	0.03	0.28	1.93	-	9	282	-
HG - 4	0.05	2.30	0.03	0.37	2.20	17	8	268	-
OLB- 1	0.07	3.31	0.04	0.40	2.41	31	9	392	-
HG- 5	0.07	2.96	0.04	0.36	2.56	15	14	401	29
OLB- 2	0.06	2.40	0.03	0.27	2.00	-	8	273	25
OLB- 3	0.07	2.86	0.04	0.41	2.44	22	9	347	25
KIB - 1	0.07	1.93	0.03	0.23	2.28	-	26	231	20
KIB - 2	0.06	2.46	0.03	0.39	2.48	5	14	332	-
KIB - 3	0.05	2.27	0.03	0.26	2.26	6	17	317	-
KIB - 4	0.07	2.52	0.03	0.47	2.37	11	14	323	-
KIB - 5	0.07	2.04	0.03	0.29	2.39	10	14	283	-
KIB - 6	0.07	2.27	0.03	0.36	2.54	14	16	317	-
OSE - 1	0.02	1.09	0.03	0.10	0.84	7	3	144	-
KN - 1	0.07	5.74	0.05	0.18	0.86	8	-	46	-
OBR- 1	0.37	4.41	0.15	0.88	2.42	33	8	115	-
OLF - 1	0.12	3.20	0.08	0.46	2.69	32	8	244	-
OLF - 2	0.15	3.88	0.09	0.42	2.26	-	8	281	-
HPF - 1	0.03	1.29	0.02	0.35	1.73	13	8	79	-
GCL- 1	0.03	1.41	0.02	0.41	2.56	-	13	158	-
GCL- 2	0.03	1.40	0.03	0.46	2.53	-	18	234	-
NB - 1	0.03	1.06	0.05	0.27	1.78	-	8	117	-
NB - 2	0.03	1.30	0.03	0.43	2.14	-	10	100	-
LD - 1	0.16	6.47	0.19	0.53	2.46	18	10	447	-
LD - 2	0.12	5.56	0.16	0.47	2.41	-	7	552	30
BX - 1	0.15	5.37	0.17	0.43	2.15	25	11	552	14
BX - 2	0.15	5.85	0.16	0.47	2.52	32	8	596	27
CH - 1	0.30	6.92	0.21	0.63	2.45	19	6	358	1
CH - 2	0.16	6.48	0.20	0.50	2.62	13	-	441	27
EB - 1	0.13	5.53	0.15	0.50	2.53	27	6	440	10
EB - 2	0.12	5.23	0.14	0.40	2.37	21	9	389	25
HG - 7	0.07	2.60	0.04	0.40	3.00	6	18	295	26
HG - 8	0.08	2.70	0.05	0.42	2.59	7	12	293	17
MG - 2	0.11	5.07	0.14	0.51	2.71	36	12	477	19
MG - 1	0.13	5.27	0.16	0.52	2.87	-	12	546	30
LEB - 1	0.31	7.09	0.21	0.75	2.90	18	2	363	15
LEB - 2	0.31	6.87	0.23	1.03	2.79	31	12	258	19
CH - 3	0.17	6.16	0.19	0.63	3.01	40	10	436	36
EBS - 1	0.15	6.03	0.18	0.52	2.51	35	11	446	13
EBS - 2	0.12	6.76	0.21	0.55	2.53	32	10	502	14
K - 1	0.13	4.53	0.13	0.48	2.60	25	8	335	22
HG - 6	0.07	2.77	0.04	0.47	2.43	5	18	303	21
BX - 3	0.15	5.00	0.15	0.36	2.45	45	12	520	27
X - ?	0.10	3.26	0.10	0.35	2.29	7	5	249	28
Y - HG	0.06	2.79	0.04	0.33	2.40	-	16	394	35
HG - 9	0.09	3.32	0.04	0.45	2.35	10	12	298	21
MD - 1	0.06	1.34	0.03	0.42	2.25	20	7	107	10

Geochemistry of some major and trace elements by XRF

Fe* as Total Fe_2O_3 + FeO

Major oxides in wt % and trace elements in ppm

Key to Source Names:

K - Kinangop Escarpment, OBR - Obsidian Ridge, HG - Hell's Gate, OLB - Olobutot

KIB - Kibikoni, KN - Kongoni Road Junction, GCL - Green Crater Lake, OLF - Oleral Farm

NB - Ndabibi, LD - Loldia, MG - Masai Gorge, LEB - Lower Eburru, EB - Eburru Mountain

Table 3. Cont: Whole Rock Geochemistry for Obsidians, Naivasha Area

Qry. No.	Br	Rb	Sr	Y	Zr	Nb	Th	U	Pet. Grp.
HG - 1	3	482	1	205	1660	360	69	-	III
HG - 2	2	443	2	178	1565	331	52	-	III
HG - 3	1	416	1	183	1705	314	64	-	III
HG - 4	3	422	5	162	1645	339	60	-	III
OLB- 1	2	587	3	266	2460	440	78	3	IV
HG - 5	2	771	2	306	2790	637	49	18	III
OLB- 2	1	444	-	197	1830	323	64	18	IV
OLB- 3	1	471	-	210	2015	359	67	-	IV
KIB - 1	3	470	1	175	1815	278	48	-	V
KIB - 2	3	469	1	222	2250	326	43	-	V
KIB - 3	3	465	3	233	2155	311	64	-	V
KIB - 4	10	468	-	224	2255	338	56	-	V
KIB - 5	1	464	2	194	1960	291	51	-	V
KIB - 6	3	481	3	216	2050	319	63	-	V
OSE - 1	1	225	78	102	974	153	22	-	V
KN - 1	2	135	2	39	208	77	34	-	VI
OBR- 1	2	59	2	11	252	40	7	-	II
OLF - 1	2	251	3	151	1490	227	20	-	VIII
OLF - 2	3	258	1	154	1550	270	30	-	VIII
HPF - 1	2	283	2	1	459	172	9	-	IX
GCL- 1	3	297	5	85	493	191	34	-	VII
GCL- 2	1	324	7	90	2	194	36	-	VII
NB - 1	2	308	2	72	429	155	27	-	IX
NB - 2	2	295	5	86	468	174	18	-	IX
LD - 1	3	296	3	202	1535	307	21	-	X
LD - 2	3	488	2	344	3345	441	70	-	X
BX - 1	9	526	-	368	3790	531	73	42	XI
BX - 2	6	494	-	383	3855	540	74	-	XI
CH - 1	-	159	1	144	1080	200	13	-	XIII
CH - 2	3	230	7	203	1775	341	18	-	XIII
EB - 1	7	283	2	294	2335	397	20	-	XIII
EB - 2	7	223	1	265	1950	325	28	-	XIII
HG - 7	3	333	1	199	1830	371	60	-	III
HG - 8	4	490	2	208	1900	393	81	-	III
MG - 2	2	442	2	322	3290	488	68	-	XI
MG - 1	4	518	4	405	4070	594	83	3	XI
LEB - 1	2	165	1	191	1335	244	11	3	XII
LEB - 2	3	108	3	119	777	149	3	-	XII
CH - 3	2	275	3	268	212	398	13	-	XIII
EBS - 1	3	258	3	278	2030	365	23	-	XIII
EBS - 2	4	243	4	265	1850	349	14	-	XIII
K - 1	2	270	7	167	1735	254	22	-	I
HG - 6	4	465	2	193	1790	347	78	-	III
BX - 3	5	460	-	373	3385	506	69	-	XI
X - ?	-	265	1	139	932	257	19	-	?
Y - HG	6	492	-	211	2055	283	56	-	III
HG - 9	1	480	2	203	1825	364	61	-	III
MD - 1	1	295	-	82	471	168	32	-	IX

Geochemistry of some major and trace elements by XRF

Fe* as Total $Fe_2O_3 + FeO$

Major oxides in wt % and trace elements in ppm

Key to Source Names:

K - Kinangop Escarpment, OBR - Obsidian Ridge, HG - Hell's Gate, OLB - Olobutot
KIB - Kibikoni, KN - Kongoni Road Junction, GCL - Green Crater Lake, OLF - Oleral Farm
NB - Ndabibi, LD - Loldia, MG - Masai Gorge, LEB - Lower Eburru, EB - Eburru Mountain

Using the same elements (niobium versus zirconium), further attempt was made to identify possible variations within Hell's Gate and Mount Eburru. The trend established for obsidian sampled at Ol - Olbutot lava flow within the OlKaria geothermal field (Fig. 8b) is comparable to those sampled at the main entrance to Hell's Gate National Park. This variation in trend is also consistent with field observation - the Ol - Olbutot lava flow being relatively young.

At mount Eburru, a similar plot of niobium versus zirconium was incapable of distinguishing clearly any variation in trend between obsidian sampled at the summit near the steam jets and those collected from the flanks of the mountain close to the abandoned Eburru Railway Station. However, samples collected at the nearby Cedar Hill dome seem to show a significant difference in trend as depicted in Fig. 8c. From these figures, it is possible to suggest that the younger and therefore more recent flows seem to have a less steeper slope compared to those shown by the earlier and therefore older erupted flows. Such trends shown particularly by zirconium have been proposed to represent highly fractionated compositions in lava flows (Clarke *et al.* 1990), the less steeper trends representing more evolved varieties.

Variation plot of thorium versus zirconium was made for Hell's Gate area and Mount Eburru. Such plots can be used for understanding the thermal level in a volcanic area (Joron *et al.* 1990). Figure 11 shows the trend established for the two areas. The Mount Eburru trend is less steeper compared to the Hell's Gate trend. The high level of radioactive thorium established for the Hell's gate area has been suggested by Clarke *et al.* (1990) to represent an area of particularly thermally anomalous crust. It is also possible to argue that the high levels indicate the presence of a highly fractionated melt within the area.

The intercomparison table on normalized ratios given at the end in Appendix 1 acts as a spectrum analysis for the Naivasha area. Normalized ratios using element concentrations provide a simple method for testing the similarity of pairs of samples. From Table 4, it is evident that despite the very restricted major element variations between the various obsidian formations, the trace element data from the study area on obsidian samples e.g. Nb/Zr ratios seems to vary quite considerably.

Table 4. Average elemental values for the major petrographic groups, Naivasha area

Qry. No.	Ti	Fe*	Mn	Ca	K	Zn	Cu	Rb	Y	Zr	Nb	Th	*Pet. Gr.*
K	0.13	4.53	0.13	0.48	2.60	330	8	270	170	1700	250	22	*I*
OBR	0.37	4.41	0.15	0.88	2.42	110	8	59	11	250	40	7	*II*
HG	0.06	2.45	0.03	0.28	2.05	280	9	440	180	1600	330	61	*III*
OLB	0.07	2.86	0.04	0.40	2.42	370	9	460	240	2200	400	73	*IV*
KIB	0.05	2.49	0.03	0.43	2.42	330	14	470	220	2200	330	50	*V*
KN	0.07	5.74	0.05	0.18	0.86	46	-	140	40	210	77	34	*VI*
GCL	0.03	1.40	0.02	0.43	2.55	200	16	310	88	490	190	35	*VII*
OLF	0.13	3.54	0.08	0.44	2.47	260	8	250	150	1500	250	25	*VIII*
NB	0.03	1.30	0.03	0.38	1.80	110	9	300	80	460	170	22	*IX*
LD	0.14	6.50	0.18	0.50	2.44	500	8	480	340	3300	440	70	*X*
MG	0.15	5.50	0.16	0.52	2.87	550	12	500	400	4000	550	80	*XI*
LEB	0.31	7.00	0.22	0.90	2.90	300	100	150	150	1300	200	10	*XII*
EB	0.15	6.50	0.20	0.55	2.55	450	10	250	270	2000	350	20	*XIII*

Geochemistry of some major and trace elements by XRF
Fe* as Total $Fe_2O_3 + FeO$
Major oxides in wt % and trace elements in ppm

Key to Source Names:
K - Kinangop Escarpment, OBR - Obsidian Ridge, HG - Hell's Gate, OLB - Olobutot
KIB - Kibikoni, KN - Kongoni Road Junction, GCL - Green Crater Lake, OLF - Olerai Farm
NB - Ndabibi, LD - Loldia, MG - Masai Gorge, LEB - Lower Eburru, EB - Eburru Mountain

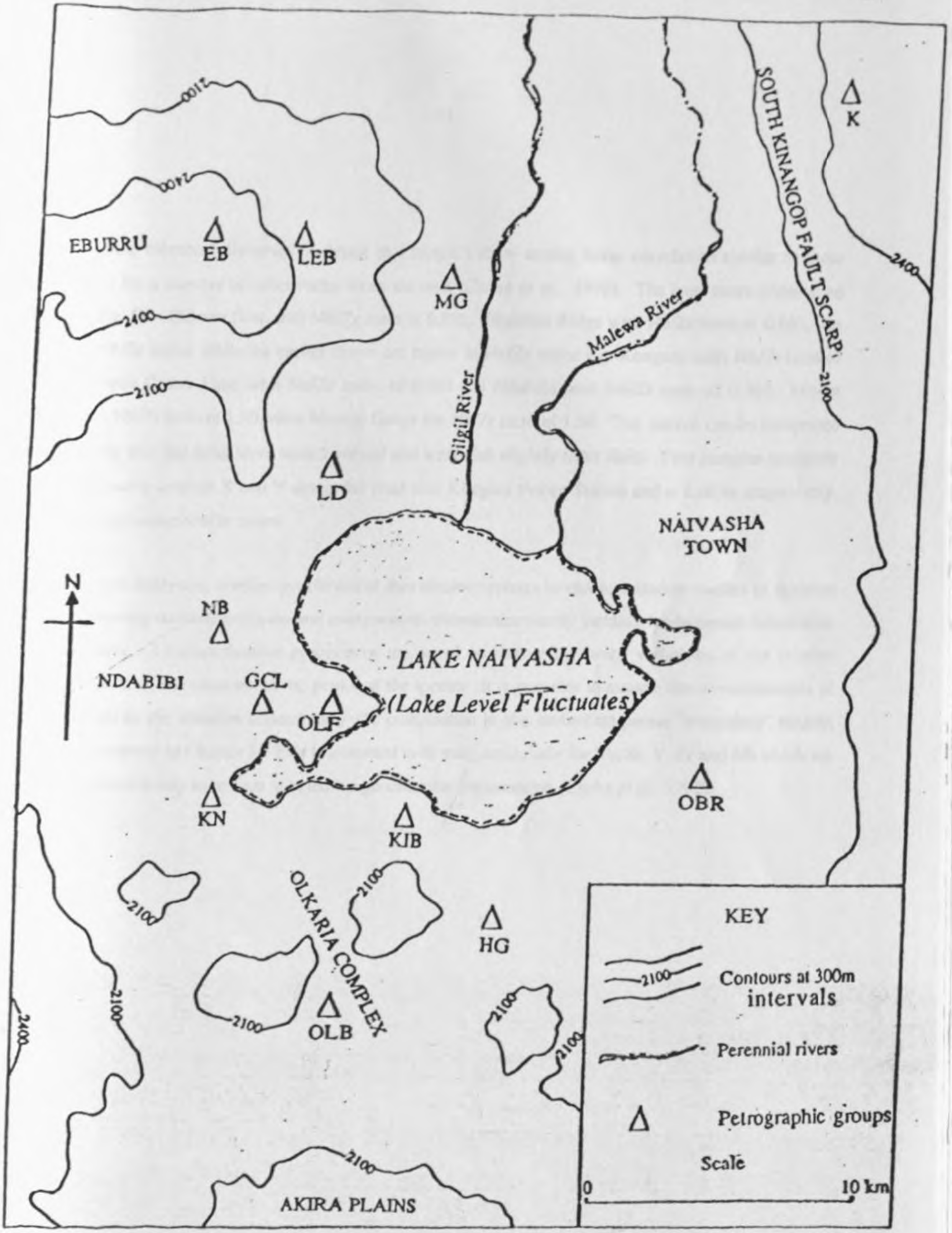

Figure 7 Locality map of quarries and the established petrographic groups

Pairs of these elements discussed in detail in Chapter 5 show strong linear correlation similar to those established for a number of other rocks from the area (Clarke *et al.* 1990). The later more widespread obsidian e.g. Ol - Olbutot flow with Nb/Zr ratio of 0.181, Obsidian Ridge with Nb/Zr ratio of 0.160, are lower in Nb/Zr ratios while the earlier flows are higher in Nb/Zr ratios e.g. Kongoni with Nb/Zr ratio of 0.366, Green Crater Lake with Nb/Zr ratio of 0.387 and Ndabibi with Nb/Zr ratio of 0.366. Mount Eburru has Nb/Zr ratio of 1.50 while Maasai Gorge has Nb/Zr ratio of 1.30. This pattern can be interpreted as indicating that the latter were more evolved and were also slightly more fluid. Two samples randomly picked at quarry sources X and Y along the road near Kongoni Police Station and at Loldia respectively, were assigned using similar ratios.

In the present analyses, average geochemical data obtained relates to characterization studies of obsidian sources allowing for differentiation and comparisons without necessarily yielding fundamental information on the source. Characterization procedures are based on source to source variations of the relative concentrations of the elements in the peaks of the spectra. It is possible to assume that concentrations of the elements in the obsidian reflects only the composition in the immediate parent "secondary" magma pools as discussed in Chapter 5. This is assumed to be true particularly for Rb, Sr, Y, Zr and Nb which are known geochemically to be least affected by geochemical fractionation (Clarke *et al.* 1990).

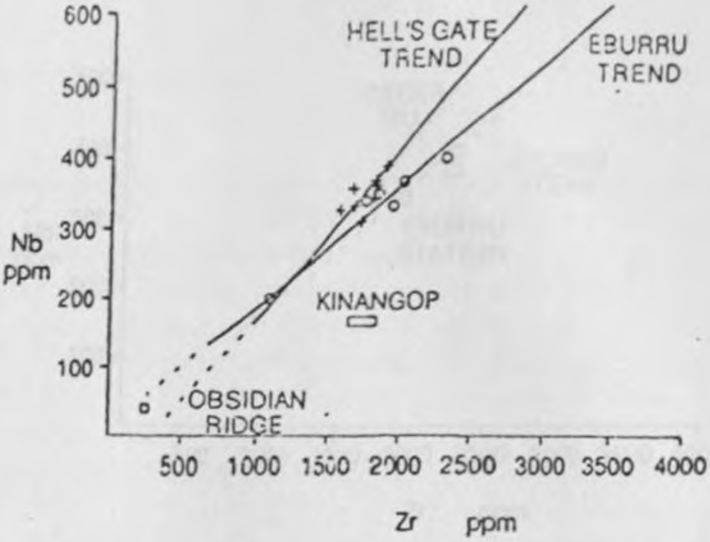

Figure 8:a Niobium and zirconium variation between Eburru and Hell's Gate

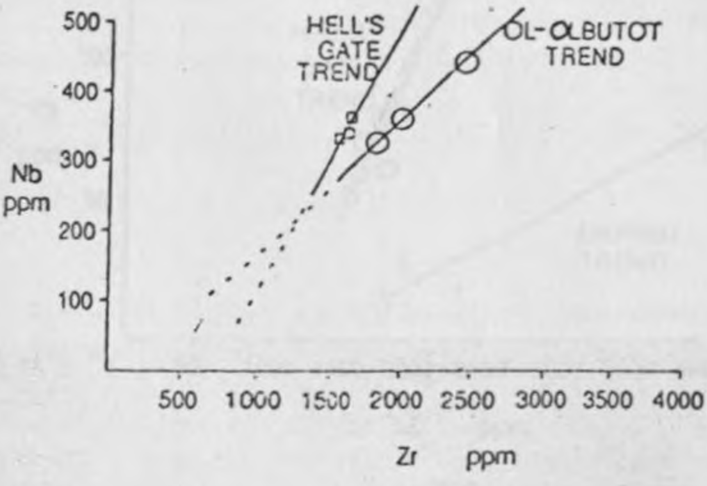

Figure 8:b Niobium and zirconium variation within Hell's Gate area.

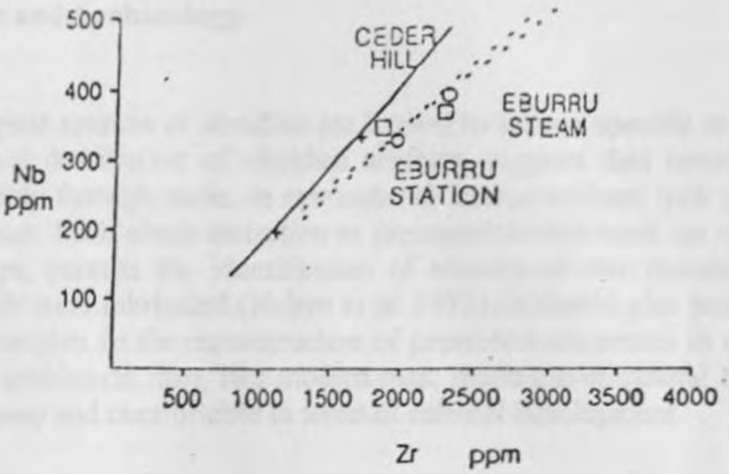

Figure 8:c Niobium and zirconium variation within Mount Eburru area.

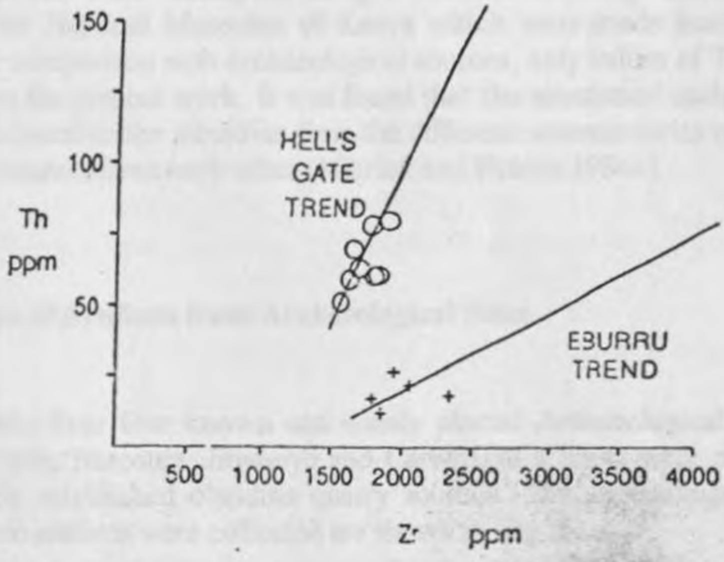

Figure 9 Thorium and zirconium variation between Hell's Gate and Mount Eburru

4.3 Obsidian and Archaeology

Since the geological sources of obsidian are limited to certain specific areas, the wide geographical distribution of obsidian artifacts suggests that considerable movement, possibly through trade, in raw material and/or artifacts took place in the prehistoric past. Such characterization as presented in this work on obsidian flows or outcrops, permits the identification of sources of raw material from which the artifacts were fabricated (Nelson *et al.* 1975). It should also prove very useful to archaeologists in the reconstruction of possible trade routes in order to understand how prehistoric man, like modern man, made use of natural material to make his life easy and comfortable in terms of cultural development.

4.3.1 Inter Quarry – Artifact Comparison

Source comparisons were attempted using a number of scrap artifacts from collections at the National Museums of Kenya which were made available for correlation. For comparison with archaeological sources, only values of Ti, Fe and Ca are shown in the present work. It was found that the amount of each of these elements that is found in the obsidian from the different sources varies enough to distinguish the sources from each other (Merrick and Brown 1984a).

4.3.2 Analyses of Artifacts from Archaeological Sites

Obsidian artifacts from four known and widely placed Archaeological Sites in Kenya (Gogo Falls, Narosura, Jawuoyo and Cartwright's Sites) were correlated with the already established obsidian quarry sources. The archaeological sites from which these artifacts were collected are shown in Fig. 10.

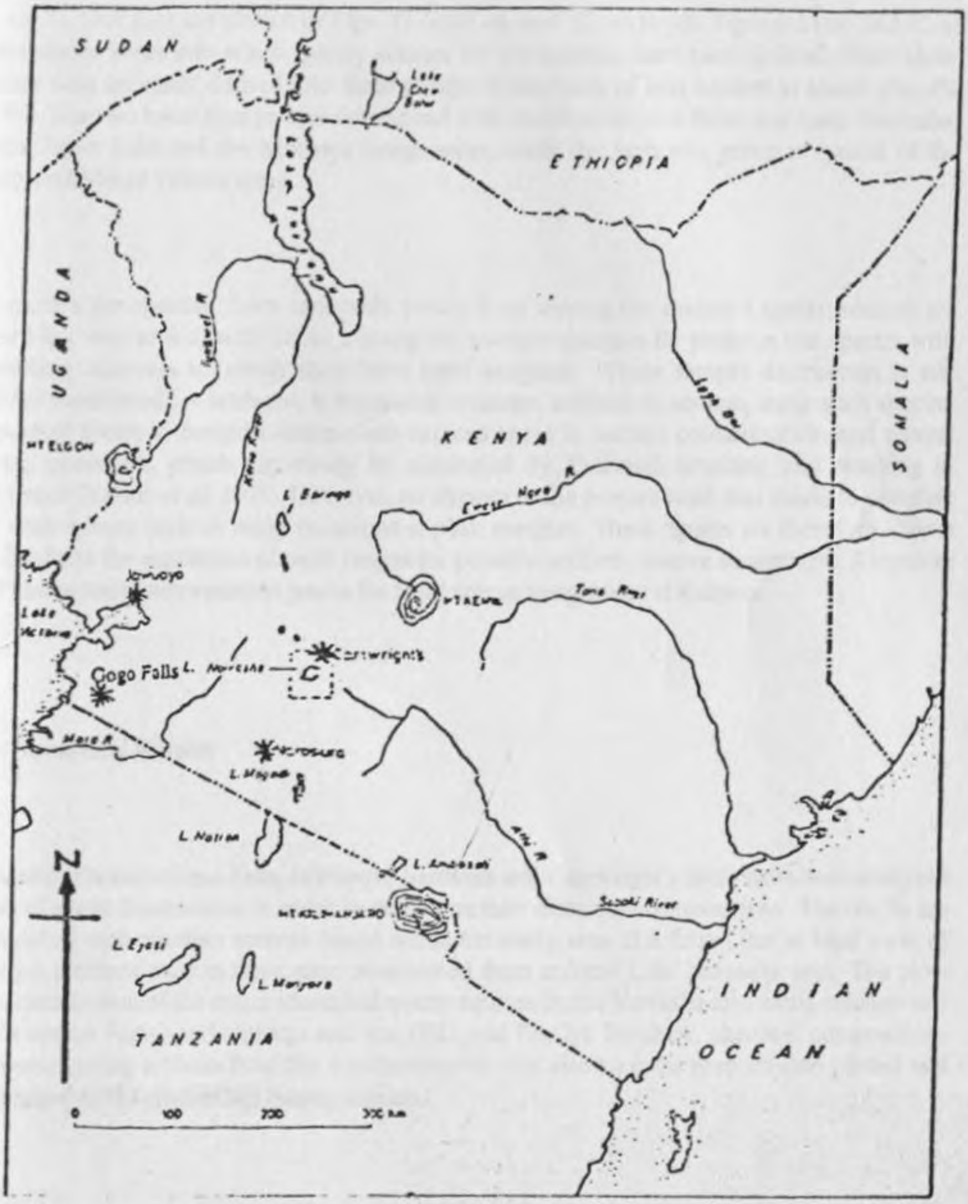

Figure 10 Locality map showing archaeological sites whose artifacts are analyzed for comparison with some of the established obsidian sources (*archaeological sites)

(modified from Merrick and Brown 1984a)

Data from the four sites are plotted in Figs. 11 (a) to (d) and 12 (a) to (d). Figures 11(a) and 12(a) shows the major zones into which quarry sources for comparison have been defined. They show that artifact data are easily derived into three groups on the basis of Iron content at about 2%, 4% and >6.5%. The two lower iron groups correspond with obsidian sources from near Lake Naivasha, the Green Crater Lake and the Njorowa Gorge areas, while the high iron group is typical of the Kinangop and Mount Eburru areas.

Typical spectra for obsidian flows randomly picked from among the analyzed quarry sources are shown in Figs. 6(a) to 6(d) with Table 2 listing the average energies for peaks in the spectra with corresponding elements to which they have been assigned. Where sample destruction is not possible (as mentioned for artifacts), it is possible to assign artifacts to sources using such spectra. The important factor to consider under such circumstances is surface contamination and natural weathering processes, which can easily be eliminated by thorough brushing and washing in distilled water (Nelson *et al.* 1975). However, no attempt in the present work was made to correlate artifacts with quarry sources using variations in peak energies. These figures are therefore shown only to illustrate the usefulness of peak ranges for possible artifact - source assignment. Kinyua *et al.* (1992) have used such variation peaks for fossil source assignment at Kanjera.

4.3.3 Analytical Results

Obsidian artifacts from Gogo Falls, Jawuoyo, Narosura and Cartwright's Sites have been analyzed by means of x-ray fluorescence in order to determine their elemental compositions. The results are then correlated with obsidian sources found within the study area. It is found that at least most of the obsidian artifacts used in these sites were mined from around Lake Naivasha area. The plots show the distribution of the major identified quarry sources in the Naivasha area using calcium and iron (CaO versus Fe_2O_3) and titanium and iron (TiO_2 and Fe_2O_3). Similarly, chemical compositions of the corresponding artifacts from the 4 archaeological sites shown in the map are also plotted and easily assigned to the established quarry sources.

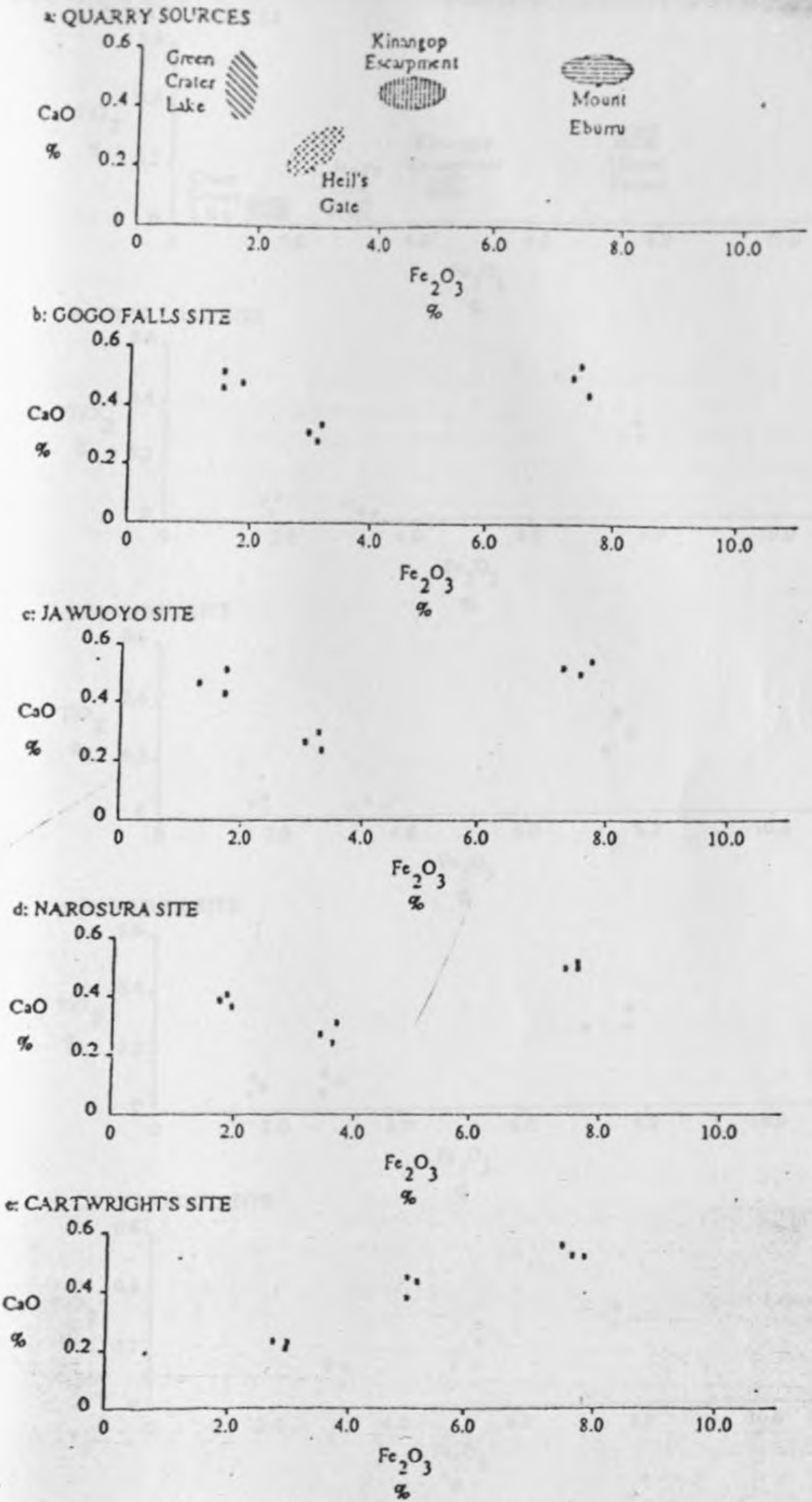

Figure 11 Plots of XRF values for CaO versus Fe_2O_3 for some of the established obsidian quarry sources compared with obsidian artifacts from archaeological sites at Gogo Falls, Jawuoyo, Narosura and Cartwrights (modified from Merrick and Brown 1984a)
]

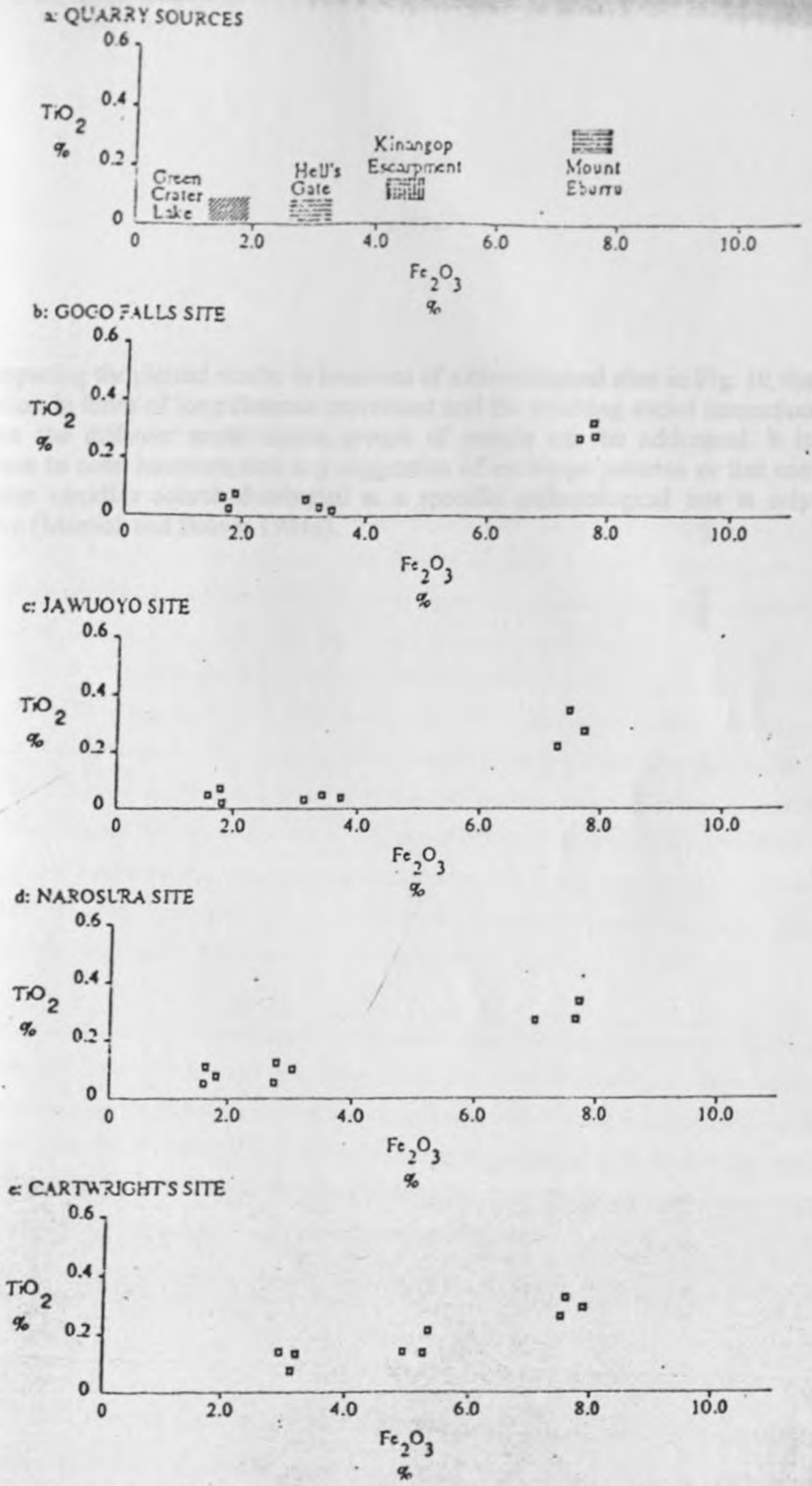

Figure 12 Plots of XRF values for TiO_2 versus Fe_2O_3 for some of the established obsidian quarry sources compared with obsidian artifacts from archaeological sites at Gogo Falls, Jawuoyo, Narosura and Cartwright's (modified from Merrick and Brown 1984a)

By comparing the plotted results to locations of archaeological sites in Fig. 10, the separation in terms of long distance movement and the resulting social interaction between the different areas and/or groups of people can be addressed. It is important to note, however, that any suggestion of exchange patterns or that one particular obsidian source dominated at a specific archaeological site is only tentative (Merrick and Brown 1984a).

CHAPTER V
DISCUSSION AND CONCLUSION

As mentioned earlier in Chapter 4, the absence of phenocrysts in obsidian has an important petrogenetic consequence which demonstrates the presence of superheated magma in the near - surface environment before quenching took place (Cox *et al.* 1987). It is this genetic interpretation of the texture which is of immediate interest because in the case of obsidian, it is clear that the quenching stage coincides with the eruption of the lava onto the surface. The formation of glass (obsidian) is commonly ascribed to extreme quenching of liquids (magma) caused by very rapid temperature fall. Although it is known that extremes of quenching prevents crystallization, the composition and structure of the magma are also important factors in determining whether or not a glass will form. Should the last liquid to form be enriched in silica (and potassium), the consequent increase in its viscosity will impede diffusion to possible crystal nuclei and the formation of glass by super cooling will be favoured (Cox *et al.* 1987). On the other hand, sodium is known to reduce the viscosity of silica bearing melts and its presence in some quantity may favour crystallization, with the formation of sodium bearing feldspathoids or zeolites.

In order to understand the way in which different outcrops of obsidian could have formed and how an initial melt, or magma could become compositionally differentiated to give rise to a variety of compositionally different obsidian rock types as ultimate products, an attempt has been made to extract any information the obsidian rock may give about processes at depth and what may be thought of as an applied stage in the project. In general, geochemical data derived from obsidian is applied to interpret igneous processes, evolution and nature of the source materials from which obsidians are formed.

5.1 Magma Generation

Except for the outer core, the earth consists of solid material and any magma must originate by the partial melting of this pre - existing solid rock. Melting can be induced by local increases in temperature, decompression or influx of mobile constituents such as volatiles.

The composition of a partial melt produced in the mantle is thus dependent upon the composition of the source rock and the degree of melting. The degree of melting is in turn dependent upon the temperature, pressure and water content of the source. For silicates, the melting point increases with load pressure and any decrease in pressure caused perhaps by faulting or upwelling (as was the case in the formation of the Kenyan Rift Valley), could reduce the effective melting temperature at a given depth resulting in melting (Bailey 1970).

Magma generation is usually found to be common along plate boundaries and in areas of tectonic stresses; mostly within the crust and/or the upper mantle. In general, melting of the source rock is rarely complete and most melts coalesce to form magma bodies, which then migrate, away from their source regions (Cox *et al.* 1987). This involves separation from the residual matrix and possible migration upwards where re-equilibrium *en route* with rocks at a higher level may take place. When and/or if the upward flow of a melt is arrested, a magma chamber may form. This can lead to cooling and possible commencement of crystallization if the liquidus temperatures are reached. These and subsequent changes, may have an effect on the eventual chemical composition of the magma prior to eruption at the surface of the earth.

5.2 Theory of Melt Segregation

The processes by which melts are extracted from partially molten source regions at depth and erupted at the earth's surface are known collectively as melt segregation (McKenzie 1984). These are usually simultaneous processes that depend on temperature, pressure and chemical composition. A volume of mantle can become partially molten by up welling (Bailey 1970) so that it is above solidus conditions due to a decrease in pressure (King and Chapman 1972). Frank (1968 in Ribe 1987) who regarded a molten region to be made up of saturated porous medium first proposed a usable theory for melt segregation. He also considered the migration of melt relative to matrix to be driven by pressure gradients brought about by the buoyancy of the melt or the deformation of the matrix and in the case of the Kenyan Rift situation, by up welling.

Once a partial melt has been produced, it must separate from the residual matrix and collect at a higher level to form a magma chamber. The path it ascends along has a negative P-T gradient in space because thermal energy is converted by the process of decompression. As the melt ascends, it transports heat toward the surface and releases gravitational potential energy, allowing further melting and chemical equilibration of the melt. If for example at this higher level, the new matrix has the same mineralogical composition as the melt, then there will be little or no effect on the element composition of the magma. But if the new matrix with which the melt comes into contact has not already been depleted, then it may become enriched in incompatible trace elements depending on the distribution coefficient for a given element (Norry *et a*l. 1980). Apart from these factors, the melt is also affected by several fractionation processes, which may cause some, or all of the chemical variation observed in most igneous rocks. It is therefore necessary to fully understand the effects of fractionation processes on an initial melt and the changes they can cause before eventual formation of a rock at the surface of the earth as a final product is considered.

5.3 Magma Evolution

One of the striking laboratory results observed about obsidian outcrops is that they are variable in chemical composition, leading automatically to evolutionary considerations and hence fractionation. If an initial single parental material is considered as the source material from which a variety of obsidian rocks of varied chemical compositions are formed, then the separation of a melt from this source constitutes a fractionation process.

In order to understand the petrogenesis of obsidian and the reasons for their compositional variations, it is therefore important to assess the relative role(s), if any, of different possible fractionation processes (MacDonald 1974). Diffusion, partial melting, crystal liquid separation and liquid separation and liquid immiscibility are among the possible fractionation processes that may/may not dominate in a melt to produce the kind(s) of varied compositions observed in obsidian rock.

Diffusion is a mechanism that can operate in a liquid system when elements migrate through the liquid body at different rates producing variations in the resulting bodies. The main causes of diffusion include major thermal and/or pressure gradients as well as compositional gradients. But differential elemental migration brought about by compositional gradient is unlikely in the case of obsidian since the changes are chemically variable from one source to another. Also, in a near surface environment (from where obsidian melts are believed to have originated), both temperature and pressure gradients are known to be low (Cox *et al.* 1987) and the effects of diffusion are accordingly negligible to cause the kind(s) of compositional ranges observed in obsidian.

In contrast, a drop in temperature and pressure may cause immiscibility in a migrating melt resulting in phase separation and migration. Liquid immiscibility is the separation of an originally homogenous magma into two or more coexisting fractions. However, Cox *et al.* (1987) investigating silicate systems have identified very limited extent of liquid immiscibility between one type of silicate melt and another. Obviously, the role of liquid immiscibility will be limited by very rapid increase in viscosity of melts which are super cooled and this could prevent the unmixed liquids from separating on a large scale to form discrete obsidian flows (outcrops) typical in the Naivasha area. Furthermore, as Bowen (1928 in Opiyo 1988) points out, petrographic evidence of liquid immiscibility in silicate melts is rare.

Differentiation processes involving crystal – liquid fractionation systems are known to be capable also of effecting gross compositional changes when magma is first formed or during the migration of magma when it is in contact with a variety of wall rocks. The only rocks that are closely associated with obsidian in the Naivasha area are the trachytes (Davies and MacDonald 1987). However, the absence of gross similarities in chemical composition between these rocks and the obsidians limits the role of direct crystal – liquid fractionation as dominating to produce the varied observed chemical differences in obsidian outcrops. The mechanisms of crystal – liquid fractionation are largely controlled by physical conditions such as the densities of magmas and the presence of crystals (Cox *et al.* 1987). Field samples of obsidians lack traces of any earlier formed crystals. Whatever the tendency of crystal – liquid fractionation, its possibility of occurring on a large scale is much greater in magmas of low viscosity than of high. Magmas of different compositions are known to vary in viscosity by several orders of magnitude (McKenzie 1984).

Also important is the rate of magma flow. Magmas that are viscous enough to carry large solid xenoliths can hardly be depositing small crystals at the same time. It is therefore difficult to visualize deposition of any earlier formed crystals in a crystal – fluid separation situation before the lava reached the surface to form different obsidian outcrops.

A partially molten magma is known to solidify over a wide temperature range during which there is a possibility of progressive compositional change and the material may be tapped off to erupt from time to time as varying series of lava (Cox *et al.* 1987). A typical melt from a single source material may also theoretically produce both basic and acidic magma (Yoder 1973) but the existence of mineralogical solid solution series in natural systems is likely to produce a compositionally continuous sequences of silicate melts not typical in obsidian outcrops under consideration. The formation of multiple outcrops of obsidian by direct ascent of partial melts along points of weaknesses is an unlikely case although it has been demonstrated experimentally to be possible in the production of a varied number of magmas depending on the temperature and depth from which such magmas are produced (Takahasi *et al.* 1985 in Opiyo 1988). Close assessment of a partial melting model is also not possible because of the difficulty in identifying the chemical composition and mineralogies of likely source materials. Higher vapour pressures are also known to accompany partial melting but some of the obsidian outcrops encountered contained vesicles that are only known to form under very low vapour pressures. In addition, linear correlation between the elements Nb and Zr (Fig. 8) are not considered to be indicative of partial melting products (Ferrara and Treuil 1974).

Thus, although it is common to interpret various lava units in sub – volcanic centers as sequences of magma pulses related to some fractionation processes, in the Naivasha area it is suspected that the obsidian are not simply direct ascent of residual systems (Samson 1990). The variations in modes of occurrences and/or compositions are as a result of crustal – residual fluid interactions rather than crystal – fluid reactions.

There is an inevitable involvement of at least some fluid phase of variable origin during the evolutionary history of obsidian bodies and consequently some modification of mineralogy and chemistry. There is therefore a tendency for a chemical and/or temporal continuum between magmatic processes and fluid rock interaction in general which makes it difficult to distinguish these two stages clearly from the limited chemical data available in the present study.

However, it is important to realize that the enrichment of certain elements like rubidium and potential mobility of others like uranium and thorium in the obsidian indicate that fluid rock interaction was probably responsible for some, albeit not a great deal, of chemical changes (Clarke *et al.* 1990). The strongest objection to the hypothesis of simple fractionation processes alone as the major petrogenetic mechanism in the formation of obsidian is the difficulty of extracting fractionated liquids in sufficient quantities to account for the varied chemical compositions and the inadequacy of the known fractionation mechanisms. In order for highly fractionated lavas to be extruded, a differentiating body of magma would have to be tapped (Weaver 1976), but this in turn would prevent the development of the extreme liquid compositions found in obsidian.

5.4 Major and Trace Element Analysis

Major and trace element analyses were also carried out to assist in indicating constraints on the nature and composition of the mineral assemblages with which the melts may have previously equilibrated. This is from the fact that there are certain characteristic compositional associations that can be produced by certain fractionation models particularly in major element trends (Timothy *et al.* 1982). Likewise, their analyses can be used to show variations that are inconsistent with certain fractionation origins.

Within the Naivasha area, the obsidians exhibit extremely low levels of Sr anomaly as shown in Table 3 of geochemistry of some major and trace elements, whereas in older volcanic rocks, the Zr values are usually low while the Sr values are higher (Weaver 1976). It is not possible, however, to generalize that these low values are due to depletion as a result of extended differentiation or alternatively that albitization has caused liberation of the elements as albite does not incorporate Sr (Imeokparia, 1992). In the northern Kenya for example, Weaver (1976) has shown that SiO_2 and MgO concentrations show negative and positive relationships respectively in older volcanic rocks. Davies and MacDonald (1987) on the other hand have confirmed otherwise in the Naivasha area where major element concentrations particularly between SiO_2 and MgO show positive and negative relationships respectively.

Consideration of several trace element ratios shown in Table 4 demonstrate further that the trace element relationships are not a result of simple mixing involving different suites (Ferrara and Treuil 1974). This can be argued from the fact that the variations in ratios are not consistent particularly in the closely placed outcrops. Detailed assimilation fractionation processes carried out by Davies and MacDonald (1987) in an attempt to establish the extent of interaction and its responsibility for the "between group variations" has further confirmed that the highly silicate rocks of the Naivasha area had low liquidus temperatures. It is therefore unlikely that the rocks could have existed within the crust at temperatures above 800^0 C. At such temperatures, it would be difficult or almost impossible to account for any assimilation processes.

5.5 Incompatible Element Variations

Certain elements can provide a means of investigating heterogeneity within the sources of lavas. These are elements which under given compositional conditions are excluded or largely excluded from the lattices of the minerals crystallizing and therefore becomes concentrated in the liquid in a manner simply related to the amount of the original material crystallized. However, any incompatible element sooner or later becomes compatible as its concentration in the liquid increases and new phases appear (Cox *et al.* 1987).

Norry *et al.* (1980) has observed that the abundance of incompatible elements decrease in most Kenyan lavas from the Miocene to Pleistocene times. Of interest to the present study is the fact that the decrease found in incompatible elements through time also parallels the increase in silica under saturation (Weaver 1976). One way of producing increased undersaturation in lavas is through melting at increasing depths or at higher CO_2 pressures (Opiyo 1988). If the degree of silica saturation is controlled by the amount of dissolved CO_2, then a relationship may be expected between the amount of SiO_2 and the concentration of certain trace elements that also are affected by the degree of partial melting. In the case of the Naivasha area, subsequent melting probably took place at comparatively low pressures and/or depths. Melting of material poor in CO_2, or reduced flux of CO_2 into the mantle at the time of melting could result in a higher SiO_2 and in lower incompatible element content as seen in the lavas erupted more recently in central rift region. This argument can be used to support the origin of high silica saturation as opposed to partial melting alone as a major contributing factor to increased silica saturation.

Further, the large Rb/Sr ratios in the range of upto 500 where available in the present study cannot be accounted for by partial melting alone (Norry *et al.* 1980). The fractionation observed between other pairs of incompatible elements would also seem unlikely to be caused by partial melting. This therefore makes it difficult to explain the variations in abundance and ratios observed in different quarry sources only by variable degree of melting. The effects of fluid phase transport of incompatible elements during partial melting would result in lavas grossly getting enriched in incompatible elements (Dostasl *et al.* 1985), which is not the case with the obsidian in the Naivasha area. A derivation from distinct sources is therefore implied. The presence of several incompatible elements such as K, Rb and Th together with certain light rare earth elements (LREE) (MacDonald 1974) can be used to further support the fact that a lava flow has been derived from a distinct, incompatible element enriched source.

Davies and MacDonald (1987) studying comendites associated with the obsidian in the Naivasha area have observed that fractional crystallization dominated processes cannot account for the chemical compositions of the comendites. Further processes must be involved to produce heavy rare earth elements HREE (Heavy Rare Earth Element) and HFSE (High Field Strength Element) together with the low Sr, Eu and Ba contents. Experimental evidence elsewhere have also confirmed that rare earth elements, particularly the HREE are preferentially partitioned into halogen – rich media (Flyn and Burnham 1978 and Bilal *et al.* 1979). This is of significance since HFSE such as Zr may also form stable fluoro-complexes like ZrF_{2-6} (Alderton *et al.* 1980). Halogens and other minor phases such as zircon can play an important role in the genesis of a volcanic suite (Watson and Harrison 1983). In the Naivasha area, a possible important consequence of the halogen – rich nature was that the obsidian flows were of very low viscosity enabling relatively small volumes of melt (<5%)(Davies and MacDonald 1987) to escape from their source and resulting in marked trace element enrichment.

The foregoing argument does not support the petrogenesis of the obsidian by a simple assimilation crystallization fractionation process from the associated rhyolitic and trachytic rocks with which they share an almost horizontal array on a Sr – Nd isotope diagram (Davies and MacDonald 1987) or other direct mantle derived magmas.

The alternative source for the obsidian is suspected to be the crust. The continental crust is known to have very high $^{87}Sr/^{86}Sr$ and low $^{143}Nd/^{144}Nd$ ratios and generally very low Nb/Zr and Nb/Y ratios as shown in Appendix 1 of normalized element ratios, relative to directly derived mantle magmas (Opiyo 1988). Within the Naivasha area, Davies and MacDonald (1987) have also concluded that the variable but relatively radiogenic $^{87}Sr/^{86}Sr$ ratios of the comendites associated with the obsidians, upto 0.7116 also suggests that a large proportion of their Sr could be of crustal origin. The relatively low Zr/Nb ratios ranging from 2 to 7 obtained (See Appendix 1 on normalized elemental ratios) are also compatible with a derivation from a relatively young, Pan – African continental crust (1.0 Ga) which is found in large areas of Kenya (Cahen and Snelling 1984). If this is combined with seismic data obtained by KRISP Working Group (1987), then a derivation close to the basement cover interface at 6 km depth is likely.

5.6 Conclusions

The Naivasha area obsidians show a range of variations in most of the major and trace elements. Such patterns can be employed to differentiate between the various obsidian outcrops (flows). This work does illustrate that there is variation in chemical composition characteristic of the various obsidian formations within the Naivasha area.

The nature of magmatism leading to established variations in chemical composition can be summarized by involving melting at shallow levels of a felsic crust (Davies and MacDonald 1987). Initial magma generation was caused by decompression of the mantle below (McKenzie 1984) and the ensuing partial melts then rose and coalesced to form basaltic magma bodies at relatively high levels. Extensive tectonism consequent to the rifting processes separated or sliced bodies of this basic magma into small and discrete source regions where they assimilated large volumes of the crust before solidification. At the same time the intrusive raised the local geothermal gradient inducing further melting (Bailey 1970). At such near surface levels, coupled with the raised geothermal gradients, the late grid faulting events (dated at 0.8 Ma) caused eruption of the already assimilated felsic melts onto the surface. Because of the relatively low temperatures and pressures, these melts were quenched and had no time to crystallize hence super cooling to form obsidian.

Finally, one of the elements which was not analyzed in the present study due to the inability of the set up of the x - ray fluorescence analysis system used is europium (Eu). Eu value is known to reflect the prevailing oxygen fugacity, melt composition and structure at the time of an eruption. At the same time, chemical coherence usually shown between Eu and Sr can be used to infer whether Sr may have been strongly stabilized during melt extraction, an important aspect in isotopic study which is recommended for any future work in the Naivasha area in relation to obsidian rock.

REFERENCES

ALDERTON, D. H. M., J. A. Pearce and P. J. Potts, 1980.
Rare earth element mobility during granite alteration: evidence
from southwest England.
Earth Planet. Sci. Lett. 49, 149 – 165.

ASE, L. E., K. Sembo and S. Per, 1986.
Studies of Lake Naivasha, Kenya, and its drainage area.
Stockholms Universitet Naturgeografiska Institutionen 106 91
Stockholm.

BAILEY, D. K., 1970.
Volatile flux, Heat focusing and the generation of magma.
In: Newall and N. Rast (Editors), Mechanism of Igneous Intrusion.
Geol. Journ., No. 2, 177 -186.

BAKER, B. H. and L. F. Henage, 1977.
Compositional Changes during crystallization of some peralkaline
silicic lavas of the Kenya Rift Valley.
J. Volcan. Geotherm. Res. 2: 17-28.

BAKER, B. H. and J. H. Mitchell, 1976.
Volcanic Stratigraphy and geochronology of the Kedong-Olorgesaile area
and the evolution of the south Kenya Rift valley.
J. Geol. Soc. London, Vol. 132, 467 - 484.

BAKER, B. H., J. H. Mitchell and L. A. J. Williams, 1988.

Stratigraphy, geochronology and volcano-tectonic evolution of the Kedong - Naivasha - Kinangop region, Gregory Rift Valley, Kenya.

J. Geol. Soc. London, Vol. **145**, 107-116.

BILAL, B. A., F. Herrmann and W. Fleischer, 1979.

Complex formations of trace elements in geochemical systems – 1.

J. Inorg. Nucl. Chem. **41**, 347 –350.

BLISS, C. M., 1979.

Geology and Petrochemistry of the Naivasha area, Kenya Rift Valley.

Ph. D. Thesis, University of Lancaster.

BONE, B. O., 1988.

The geological evolution of the SW-Naivasha Volcanic Complex, Kenya.

Ph. D. Thesis, University of Reading.

BOWMAN, H. R., F. Asaro and I. Perlman, 1973.

Composition variations in obsidian sources and the archaeological implications. *In Achaeometry*, **15(1)**, 123 - 127

CAHEN, L. and N. J. Snelling, 1984.

The Geochronology and Evolution of Africa.

Oxford University Press, 512p.

CANN, J. R. and C. Renfrew, 1964.

The characterization of obsidian and its application to the Mediterranean region. *In Proceedings of the Prehistoric Society*, **30**, 111-133.

CLARKE, M. C. G., D. G. Woodall, D. Allen and G. Darling, 1990
with contributions by J. K. Kinyariro, F. M. Mwagongo, J. P. Ndogo, W. Burgess, K. Ball, S. Scott, N. J. Fortey, B. Beddoe-Stephens, A. Milodowski, P. H. A. Nancarrow and L. A. J. Williams
Geological Volcanological and Hydrological controls on the occurrences of geothermal activity in the area surrounding Lake Naivasha, Kenya. *Britsh Geological Survey and Ministry of Energy, Kenya.* 1-138.

COLE, S., 1954.
The prehistory of East Africa. Middlesex: Penguin Books, 301p.

COX, K. G., J. D. Bell and R. J. Pankhurst, 1987.
The interpretation of igneous rocks. George Allen and Unwin. London, 450p.

DAVIES, G. R. and R. MacDonald, 1987.
Crustal influence in the petrogenesis of the Naivasha basalt-comendite complex: combined trace element and Sr - Nd - Pb isotope constraints. *Journ. of Petrol. Vol.* **28.** Part 6, 1009 - 1031.

DOSTASL, J., C. Dupuy and J. L. Poidevin, 1985.
Geochemistry of Precambrian basaltic rocks from the Central African Republic (Equatorial Africa).
Cont. J. Earth Sci., **22**: 653-662.

DUERDEN, P., J. R. Bird, M. D. Scott, E. Clayton and L. H. Russel, 1980.
PIXIE-PIGME studies of artefacts.
In Nucl. Instrum. Methods, **168.** p. 447-452.

FERRARA, G. and M. Treuil. 1974.

Petrological implications of Trace - element and Sr Isotope

Distributions in Pantellerite Series.

In Bull. Volcanol.. 38: p. 548-744

FITTON, I. and B. G. J. Upton, 1987.

Alkaline Igneous Rocks.

Special Publication of the Geological Society of London. **No. 30.**

FLYN, R. T. and C. W. Burnham, 1978.

An experimental determination of rare earth partition coefficients

between chloride containing vapour phase and silicate melts.

In Geochim. Cosmochim. Acta. **42.** p. 685-701.

GAME, P. M., 1945.

Note on the interrelationships of various obsidians collected by

Mrs. Leakey in Kenya Colony, in Report on the excavations at

Hyrax Hill, Nakuru, Kenya Colony.

In Trans. R. Soc. Afr. **30.** p. 271-409.

GORDUS, A. A. and G. A. Wright, 1968.

Obsidian sources characterized by neutron activation analysis.

In Science, **161.** p. 382-384.

GRIFFIN, J. B., A. A. Gordus and G. A. Wright, 1969.

Annual Review of Nuclear Science.

In Amer. Antiquity, **34(1).** p. 23, 45.

IMEOKPARIA, E. G., 1992.

Geochemical and Isotopic evidence for crystal melt and fluid phase equilibria and late stage fluid rock interaction in granitic rocks.

Afri. Journ. Sci. Tech. Series B. Vol. 6. No.1.

JENKINS, R., R. W. Gould and D. Gedeke, 1981.

Quantitative x-ray spectrometry.

Marcel Dekker, Inc., New York and Basel.

JONES, W. B., 1973

Chemical effects of deuteric alteration in some Kenyan trachyte lavas.

In Mineralogical Magazine, 44: 279 - 285.

JORON, J. L., A. Demant and V. Darras, 1990.

Détermination de l'origine d'obsidiennes archéologiques du Michoacán nordoccidental (Mexique), parl la géochimie des éléments en traces.

Geochimie. C. R. Acad. Sci. Paris, t. 311, Série II, p. 513-1520.

KAGASI, 1983

The volcanic petrology and geological structures of Mt. Margaret - Kijabe Hill area, Kenya Rift Valley. Unpublished M Sc thesis, University of Nairobi.

KAMAU, C., 1974.

The Lake Naivasha Basin.

Report. Geography Department, University of Nairobi.

KING, B. C. and G. R. Chapman, 1972.

Volcanism of the Kenya Rift Valley.

Phil. Trans. R. Soc. Lond. A. **271,** 185 - 208

KING. B. C., 1978

Structural and Volcanic Evolution of the Gregory Rift Valley.

Geological Background to Fossil Man ed. by W.W. Bishop, Scottish Academic Press, 29 - 54

KINYUA, A. M., T. Plumer, N. Shimizu, W. Nelson and R. Potts, 1992.

Provenance of Kanjera fossils by x-ray fluorescence and iron microprobe analysis.

Advances in x-ray analysis, Vol., **35**, pp. 1165-1173.

Edited by C. S. Barret *et al.* Plenum Press, New York.

KINYUA, A. M., 1982.

Multi-element analysis of solid and liquid samples by x-ray fluorescence (X. R. F. A.). M. Sc. Thesis, University of Nairobi.

KRISP Working Group 1987.

Structure of Kenya Rift from seismic refraction.

Nature. **325**: pp. 239-242

LEAKEY, M. D., L. S. B. Leakey and P. M. Game, 1945.

Reports on the excavations at Hyrax Hill Nakuru,

Kenya Colony, 1837-1938.

In Trans. R. Soc. South Africa, **30**, p. 271-409.

MACDONALD, R., 1974.

Nomenclature and Petrochemistry of the peralkaline oversaturated extrusive rocks.

Bull. Volcanol., Vol. **38**: 498 - 516.

McCALL, G. J. H., 1967.

Geology of the Nakuru-Thompson's Falls-Lake Hannington area.

Rept. Geol. Surv. Kenya, No.78, 122p.

MACDONALD, R., 1974

Nomenclature and petrochemistry of the peralkaline oversaturated extrusive rocks. *Bull. Volcanology*, Vol.38, p.498 - 516.

McDOUGALL, J. M., D. H. Tarling and S.E. Warren, 1983.

The magnetic sourcing of obsidian samples from Mediterranian and near eastern sources. *In J. Archaeol. Sci.*, **10**. pp. 441-452.

McKENZIE, D. P., 1984.

The generation and compaction of partially molten rock. *J. Petrol.*, **25**: 713-765.

MERRICK, H. V. and F. H. Brown, 1984a.

Obsidian source and Patterns of source utilization in Kenya and Northern Tanzania: some initial findings. *In Afri. Arch. Rev.*, **2**, p. 129-152.

MERRICK, H. V. and F. H. Brown, 1984b.

Rapid chemical characterization of Obsidian artifacts by Electron Microprobe Analysis. *Archaeometry*: **26**, 2(1984), 230 - 236

MICHELS, J. W. and A. B. Carl, 1971.

Obsidian hydration dating. *In Dating techniques for the Archaeologist*, p. 164-221.

MICHELS, J. W., I. S. T. Tsong and C. M. Nelson, 1983.

Obsidian dating and East African dating. *In Science*, **219**, p. 361-366.

NELSON, D. E., J. M. D'Aura and R. B. Bennett, 1975.

Characterization of Pacific Northwest coast obsidian by X-ray fluorescence analysis.

In Archaeometry, 17, p. 85-97.

NELSON, F. W., K. K. Nielson, N. F. Mangelson, M. W.Hill and R. T. Matheny, 1977.

Preliminary studies of the trace element composition of obsidian artefacts from Northern Compeche, Mexico.

In Amer. Antiquity, **42(2)**, p. 209-225.

NORRY, M. J., P. H. Truckle, S. J. Lippard, C. J. Hawkesworth, S. D. Weaver and G. F. Marriner, 1980.

Isotopic and trace element evidence from lavas, bearing on mantle heterogeneity beneath Kenya.

Phil. Trans. R. Soc. London., **A. 297**, pp 259-271.

OMI, G. and T. Agata, 1977.

Petrological notes on the obsidian mines in Kenya.

In Third Preliminary Report of African Studies:Archaeology, **1**, p. 18-20.

OPIYO-Akech, N., 1988.

Geology and Geochemistry of the late Archaean Greenstone Associations, Maseno Area, Kenya.

Ph. D. Thesis, University of Leicester.

PRITZ, M., G. Harlow and J. Peters, 1978

Simon and Schuster's guide to rocks and minerals.

Edited by M.Pritz, G. Harlow and J. Peters. New York, Simon and Schuster, 607p.

PULFREY, W., 1960.

Shape of the submiocene erosion bevel in Kenya.

Bull. Geol. Surv. Kenya, No. **3.**

RICHARDSON, J. L., 1966.

Changes in the level of Lake Naivasha, Kenya, during postglacial times.

Nature, London, Vol. 209, **No. 5020,** 290-291.

RIBE, N. M., 1987.

Theory of Melt segregation-A review.

J. Vol. Geoth. Res., **33:** 241-253.

SAMSON, I. M., 1990.

Fluid evolution and mineralization in sub-volcanic stock.

Econ. Geology, **85,** p. 145-163.

SCOTT, S. C., 1977.

The volcanic Geology and Petrology of the Mount Longonot,
Central Kenya. Ph. D. Thesis, University of Reading.

SCOTT, S.C., 1980

The geology of Mt. Longonot volcano, central Kenya; a question of volumes. *Philosophical Transactions of the Royal Society, London,* Vol.296, (A.1420), p.437 - 465.

SHACKLETON, R. M., 1951.

A contribution to the geology of the Kavirondo Rift Valley.

Quart. J. Geol. Soc. London, Vol., **106,** 345-389.

SHOTTON, F. W., 1959.

New petrological groups based on axes from the West Midlands.

In Proceedings of the Prehistoric Society, **25,** p. 135-143.

SUTHERLAND, D. S., 1974.

Petrography and Mineralogy of the peralkaline silicic rocks.

Bull. Volcanol, Vol., **38**, 517-547.

THOMPSON, A. O., 1964.

Geology of the Kijabe area.

Rept. Geol. Surv. Kenya. No. **67**.

THOMPSON, A. O. and R. G. Dodson, 1963.

Geology of the Naivasha area.

Rept. Geol. Surv. Kenya. No. **55**.

TIMOTHY, L. G., C. G. David and W. S. Thomas, 1982.

Origin of calc-alkaline series lavas at medicine lake volcano by fractionation assimilation and mixing.

Contr. Mineral. Petrol., **80**: pp.160-182.

WALSH, J. and P. G. Powsys, 1970.

Obsidian flakes from Laikipia District, Kenya.

In Azania, **5**, p. 179-197.

WATSON, E. B. and T. M. Harrison, 1983.

Zircon saturation revisited: temperature and composition effects in a variety of crystal magma types.

Earth. Planet. Sci. Lett., 64, p. 293-304.

WEAVER, S. D., 1976.

The quaternary caldera volcano Emuruangogolak, Kenya Rift, and the petrology of a bimodal ferrobasalt – pantelleritic trachyte association.

Bull. Volcanol. Vol., **404**, p. 1-22.

WENDLANDT, R. F. and P. Morgan, 1982.

Lithosphere thinning associated with rifting in East Africa.

Nature, London, Vol. **298**, 734-736.

WILLIAMS, L. A. J., 1978.

The Volcanological development of the Kenyan Rift.

In Petrology and geochemistry of continental rifts.

N. R. Newman and I. Ramberg (editors). NATO adv. study series.

D. Reidel, Dordretcht, Holland, Wohhletz and Sheridan, 1983.

WINDLEY, B. F., 1984.

The Evolving Continents. (2nd edition). Chichester. Wiley, p.399

YODER, H. S. Jr., 1973.

Contemporaneous Basaltic and Rhyolitic Magmas.

Am. Min., **58**, p. 153-171.

Appendix 1a: Inter-element concentration ratios for Naivasha Quarry sources (normalised against potassium K)

Qry No	Ca	Ti	Mn	Fe*	Cu	Zn	Rb	Y	Zr	Nb	Th	PetGp
HG - 1	0.14	0.03	0.017	1.29	9E-04	0.013	0.022	0.01	0.08	0.017	0.003	II
HG - 2	0.14	0.03	0.017	1.25	0.001	0.014	0.023	0.01	0.08	0.017	0.003	II
HG - 3	0.15	0.03	0.017	1.11	5E-04	0.015	0.022	0.01	0.09	0.016	0.003	II
HG - 4	0.17	0.02	0.015	1.05	4E-04	0.012	0.019	0.01	0.07	0.015	0.003	II
OLB-1	0.16	0.03	0.018	1.38	4E-04	0.016	0.024	0.01	0.1	0.018	0.003	IV
HG - 5	0.14	0.03	0.017	1.15	5E-04	0.016	0.03	0.01	0.11	0.025	0.002	II
OLB-2	0.13	0.03	0.016	1.2	4E-04	0.014	0.022	0.01	0.09	0.016	0.003	IV
OLB-3	0.17	0.03	0.016	1.17	4E-04	0.014	0.002	0.01	0.08	0.015	0.003	IV
KIB-1	0.1	0.03	0.013	0.85	0.001	0.01	0.021	0.01	0.08	0.012	0.002	V
KIB-2	0.16	0.02	0.012	0.99	6E-04	0.013	0.019	0.01	0.09	0.013	0.002	V
KIB-3	0.12	0.02	0.014	1	8E-04	0.014	0.021	0.01	0.1	0.014	0.003	V
KIB-4	0.2	0.03	0.012	1.07	6E-04	0.014	0.02	0.01	0.1	0.014	0.002	V
KIB-5	0.12	0.03	0.013	0.85	6E-04	0.012	0.02	0.01	0.08	0.012	0.002	V
KIB-6	0.14	0.03	0.011	0.9	6E-04	0.013	0.019	0.01	0.08	0.013	0.003	V
OSE-1	0.12	0.02	0.032	1.3	4E-04	0.017	0.027	0.01	0.12	0.018	0.003	V
KN - 1	0.21	0.01	0.055	0.67	-	0.005	0.016	0	0.02	0.009	0.004	VI
OBR-2	0.36	0.15	0.06	1.82	3E-04	0.005	0.002	0	0.01	0.002	3E-04	I
OLF-1	0.17	0.04	0.029	1.19	3E-04	0.009	0.009	0.01	0.06	0.008	7E-04	VIII
OLF-2	0.19	0.07	0.04	1.72	4E-04	0.013	0.011	0.01	0.07	0.012	0.001	VIII
HPF-1	0.2	0.02	0.009	0.75	5E-04	0.005	0.016	0	0.03	0.01	5E-04	IX
GCL-1	0.16	0.01	0.009	0.55	5E-04	0.006	0.012	0	0.02	0.008	0.001	VII
GCL-2	0.18	0.01	0.011	0.55	7E-04	0.009	0.013	0	0	0.008	0.001	VII
NB - 1	0.15	0.02	0.028	0.6	5E-04	0.007	0.017	0	0.02	0.009	0.002	IX
NB - 2	0.2	0.01	0.012	0.61	5E-04	0.005	0.014	0	0.02	0.008	8E-04	IX
LD - 1	0.21	0.06	0.079	2.63	4E-04	0.018	0.012	0.01	0.06	0.013	9E-04	X
LD - 2	0.2	0.05	0.067	2.3	3E-04	0.023	0.02	0.01	0.14	0.018	0.003	X
BX - 1	0.2	0.07	0.079	2.5	5E-04	0.026	0.024	0.02	0.18	0.025	0.003	XI
BX - 2	0.19	0.06	0.065	2.32	3E-04	0.024	0.02	0.02	0.15	0.021	0.003	XI
CH -1	0.26	0.12	0.084	2.83	2E-04	0.015	0.007	0.01	0.04	0.008	5E-04	XIII
CH - 2	0.19	601	0.075	2.47	-	0.017	0.009	0.01	0.07	0.013	7E-04	XIII
EB - 1	0.2	0.05	0.06	2.19	2E-04	0.017	0.011	0.01	0.09	0.016	8E-04	XIII
EB - 2	0.17	0.05	0.058	2.2	4E-04	0.016	0.009	0.01	0.08	0.014	0.001	XIII
HG - 7	0.13	0.02	0.012	0.87	6E-04	0.01	0.011	0.01	0.06	0.012	0.002	II
HG - 8	0.16	0.03	0.02	1.04	5E-04	0.011	0.019	0.01	0.07	0.015	0.003	II
MG - 2	0.19	0.04	0.052	1.87	4E-04	0.018	0.016	0.01	0.12	0.018	0.003	XI
MG - 1	0.18	0.02	0.056	1.83	4E-04	0.019	0.018	0.01	0.14	0.021	0.003	XI
LEB-1	0.26	0.11	0.073	2.44	1E-04	0.013	0.006	0.01	0.05	0.008	4E-04	XII
LEB-2	0.37	0.11	0.082	2.46	4E-04	0.009	0.004	0	0.03	0.005	1E-04	XII
CH - 3	0.21	0.06	0.064	2.05	3E-04	0.015	0.009	0.01	0.07	0.013	4E-04	XIII
EBS-1	0.21	0.06	0.071	2.41	4E-04	0.018	0.01	0.01	0.08	0.015	9E-04	XIII
EBS-2	0.22	0.05	0.082	2.67	4E-04	0.02	0.01	0.01	0.07	0.014	6E-04	XIII
K - 1	0.19	0.05	0.048	1.74	3E-04	0.013	0.01	0.01	0.07	0.01	8E-04	I
HG - 6	0.19	0.03	0.016	1.14	7E-04	0.013	0.019	0.01	0.07	0.014	0.003	II
BX - 3	0.15	0.06	0.059	2.04	5E-04	0.021	0.019	0.02	0.14	0.021	0.003	XI
X - ?	0.15	0.04	0.042	1.42	2E-04	0.011	0.012	0.01	0.04	0.011	8E-04	?
Y - HG	0.14	0.03	0.017	1.16	7E-04	0.016	0.021	0.01	0.09	0.012	0.002	II
HG - 9	0.19	0.04	0.019	1.42	5E-04	0.013	0.021	0.01	0.08	0.016	0.003	II
MD - 1	0.19	0.03	0.012	0.6	3E-04	0.005	0.013	0	0.02	0.008	0.001	IX

Appendix 1b: Inter-element concentration ratios for Naivasha Quarry sources (normalised against calcium Ca)

Qry No	K	Ti	Mn	Fe*	Cu	Zn	Rb	Y	Zr	Nb	Th	PetGp
HG - 1	7.397	0.211	0.126	9.571	0.01	0.1	0.16	0.07	0.57	0.12	0.02	III
HG - 2	66.98	0.227	0.116	8.733	0.01	0.1	0.16	0.06	0.57	0.12	0.02	III
HG - 3	6.852	0.217	0.113	7.605	0	0.1	0.15	0.07	0.61	0.11	0.02	III
HG - 4	6.016	0.135	0.087	6.301	0	0.07	0.12	0.04	0.45	0.09	0.02	III
OLB-1	6.069	0.172	0.112	8.357	0	0.1	0.15	0.07	0.62	0.11	0.02	IV
HG - 5	7.18	0.186	0.119	8.277	0	0	0.22	0.09	0.78	0.18	0.01	III
OLB-2	7.432	0.217	0.118	8.944	0	0.1	0.17	0.07	0.68	0.12	0.02	IV
OLB-3	6.009	0.173	0.095	7.041	0	0.09	0.01	0.05	0.5	0.09	0.02	IV
KIB-1	10.11	0.321	0.129	8.56	0.01	0.1	0.21	0.08	0.81	0.12	0.02	V
KIB-2	6.347	0.148	0.078	6.299	0	0.09	0.12	0.06	0.58	0.08	0.01	V
KIB-3	8.561	0.191	0.121	8.58	0.01	0.12	0.18	0.09	0.81	0.12	0.02	V
KIB-4	5.021	0.154	0.06	5.35	0	0.07	0.1	0.05	0.48	0.07	0.01	V
KIB-5	8.339	0.248	0.104	7.124	0	0.1	0.16	0.07	0.69	0.1	0.02	V
KIB-6	7.043	0.197	0.076	6.313	0	0.09	0.13	0.06	0.57	0.09	0.02	V
OSE-1	8.194	0.147	0.259	10.62	0	0.14	0.22	0.1	0.95	0.15	0.02	V
KN - 1	4.864	0.042	0.267	3.243	-	0.03	0.08	0.02	0.12	0.04	0.02	VI
OBR-2	2.766	0.417	0.166	5.034	0	0.01	0.01	0	0.03	0	0	II
OLF-1	5.859	0.254	0.169	6.966	0	0.05	0.05	0.03	0.32	0.05	0	VIII
OLF-2	5.315	0.358	0.214	9.137	0	0.07	0.06	0.04	0.37	0.06	0.01	VIII
HPF-1	4.994	0.097	0.045	3.725	0	0.02	0.08	0	0.13	0.05	0	IX
GCL-1	6.297	0.081	0.057	3.469	0	0.04	0.07	0.02	0.12	0.05	0.01	VII
GCL-2	5.536	0.066	0.063	3.067	0	0.05	0.07	0.02	0	0.04	0.01	VII
NB - 1	6.657	0.122	0.187	3.981	0	0.04	0.12	0.03	0.16	0.06	0.01	IX
NB - 2	5.041	0.071	0.061	3.052	0	0.02	0.07	0.02	0.11	0.04	0	IX
LD - 1	4.664	0.295	0.368	12.25	0	0.08	0.06	0.04	0.29	0.06	0	X
LD - 2	5.109	0.243	0.343	11.77	0	0.12	0.1	0.07	0.71	0.09	0.01	X
BX - 1	4.961	0.341	0.389	12.38	0	0.13	0.12	0.08	0.87	0.12	0.02	XI
BX - 2	5.381	0.326	0.348	12.49	0	0.13	0.11	0.08	0.82	0.12	0.02	XI
CH -1	3.875	0.474	0.327	10.97	0	0.06	0.03	0.02	0.17	0.03	0	XIII
CH - 2	5.277	0.317	0.397	13.03	-	0.09	0.05	0.05	0.36	0.07	0	XIII
EB - 1	5.054	0.268	0.304	11.04	0	0.09	0.06	0.06	0.47	0.08	0	XIII
EB - 2	5.917	0.289	0.344	10.03	0	0.1	0.06	0.07	0.49	0.08	0.01	XIII
HG - 7	7.456	0.181	0.09	6.457	0	0.07	0.09	0.05	0.45	0.09	0.01	III
HG - 8	6.173	0.185	0.122	6.433	0	0.07	0.12	0.05	0.45	0.09	0.02	III
NG - 2	5.292	0.218	0.273	9.899	0	0.09	0.09	0.06	0.64	0.1	0.01	XI
MG - 1	5.524	0.259	0.308	10.13	0	0.11	0.1	0.08	0.78	0.11	0.02	XI
LEB-1	3.852	0.412	0.251	9.403	0	0.05	0.07	0.03	0.18	0.03	0	XII
LEB-2	2.706	0.304	0.222	6.658	0	0.03	0.01	0.01	0.08	0.01	0	XII
CH - 3	4.813	0.274	0.307	8.843	0	0.07	0.04	0.04	0.34	0.06	0	XIII
FBS-1	4.846	0.21	0.345	11.67	0	0.09	0.05	0.05	0.39	0.07	0	XIII
FBS-2	4.583	0.225	0.374	12.25	0	0.09	0.04	0.05	0.34	0.06	0	XIII
K - 1	5.396	0.265	0.28	9.391	0	0.07	0.06	0.03	0.36	0.05	0	I
HG - 6	5.173	0.152	0.082	5.91	0	0.06	0.1	0.04	0.38	0.07	0.02	III
BX - 3	6.838	0.42	0.405	13.97	0	0.15	0.13	0.1	0.95	0.14	0.02	XI
X - ?	6.616	0.281	0.277	9.41	0	0.07	0.08	0.04	0.27	0.07	0.01	?
T - HG	7.389	0.192	0.123	8.592	0	0.12	0.15	0.06	0.63	0.09	0.02	III
HG - 9	5.19	0.206	0.097	7.351	0	0.07	0.11	0.04	0.4	0.08	0.01	III
MD - 1	5.386	0.153	0.066	3.196	0	0.03	0.07	0.02	0.11	0.04	0.01	IX

Appendix 1c: Inter-element concentration ratios for Naivasha Quarry sources (normalised against titanium (Ti))

Qry No	K	Ca	Mn	Fe*	Cu	Zn	Rb	Y	Zr	Nb	Th	PetGp
HG - 1	35.06	4.741	0.598	45.37	0.031	0.468	0.781	0.332	2.69	0.584	0.112	II
HG - 2	30.83	4.415	0.513	38.56	0.035	0.434	0.71	0.285	2.508	5304	0.083	II
HG - 3	31.51	4.599	0.519	34.98	0.015	0.462	0.681	0.3	2.791	0.514	0.105	II
HG - 4	44.6	7.414	0.647	46.71	0.016	0.544	0.856	0.329	3.337	0.688	0.122	II
OLB-1	35.39	5.831	0.652	48.73	0.013	0.577	0.863	0.391	3.618	0.647	0.115	IV
HG - 5	38.66	5.385	0.643	44.57	0.021	0.605	1.163	0.462	4.208	0.961	0.074	II
OLB-2	34.29	4.613	0.543	41.26	0.014	0.469	0.763	0.339	3.144	0.555	0.11	IV
OLB-3	34.71	5.776	0.547	40.67	0.013	0.494	0.067	0.299	2.87	0.511	0.095	IV
KIB-1	31.47	3.112	0.401	26.64	0.036	0.32	0.65	0.242	2.51	0.385	0.066	V
KIB-2	42.9	6.759	0.529	42.57	0.024	0.575	0.813	0.385	3.9	0.565	0.075	V
KIB-3	44.93	5.248	0.633	45.03	0.034	0.629	0.923	0.462	4.276	0.617	0.127	V
KIB-4	32.71	6.515	0.39	34.85	0.019	0.447	0.647	0.31	3.119	0.468	0.078	V
KIB-5	33.69	4.04	0.421	28.78	0.02	0.4	0.655	0.274	2.768	0.411	0.072	V
KIB-6	35.71	5.07	0.385	32.01	0.023	0.447	0.678	0.304	2.887	0.449	0.089	V
OSE-1	55.89	6.821	1.768	72.45	0.02	0.954	1.49	0.676	6.45	1.013	0.146	V
KN - 1	116.4	23.92	6.378	77.57	-	0.622	1.824	0.527	2.811	1.041	0.46	VI
OBR-2	6.638	2.4	0.397	12.08	0.002	0.032	0.016	0.003	0.069	0.011	0.002	I
OLF-1	23.11	3.944	0.667	27.48	0.007	0.209	0.216	0.13	1.279	0.195	0.017	VIII
OLF-2	14.84	2.793	0.599	25.52	0.005	0.185	0.17	0.101	1.02	0.178	0.02	VIII
HPF-1	51.66	10.34	0.461	38.53	0.024	0.237	0.847	0.003	1.374	0.515	0.027	IX
GCL-1	77.9	12.37	0.702	42.92	0.04	0.48	0.903	0.258	1.499	0.581	0.103	VII
GCL-2	83.31	15.05	0.944	46.15	0.059	0.77	1.066	0.296	0.007	0.638	0.118	VII
NB - 1	54.52	8.19	1.528	32.61	0.025	0.359	0.945	0.221	1.316	0.476	0.083	IX
NB - 2	71.18	14.12	0.867	43.09	0.033	0.332	0.98	0.286	1.555	0.578	0.06	IX
LD - 1	15.84	3.396	1.251	41.58	0.006	0.288	0.19	0.13	0.987	0.197	0.014	X
LD - 2	20.99	4.109	1.409	48.35	0.006	0.48	0.424	0.299	2.909	0.384	0.061	X
BX - 1	14.55	2.932	1.142	36.31	0.007	0.373	0.355	0.249	2.561	0.359	0.049	XI
BX - 2	16.53	3.072	1.069	38.37	0.005	0.391	0.324	0.251	2.528	0.354	0.049	XI
CH -1	8.177	2.11	0.689	23.15	0.002	0.12	0.053	0.048	0.361	0.067	0.004	XIII
CH - 2	16.65	3.156	1.254	41.12	-	0.28	0.146	0.167	1.127	0.217	0.011	XIII
EB - 1	18.88	3.735	1.134	41.24	0.005	0.328	0.211	0.219	1.743	0.296	0.015	XIII
EB - 2	20.45	3.457	1.19	45.06	0.008	0.335	0.192	0.228	1.681	0.28	0.024	XIII
HG - 7	41.17	5.521	0.498	35.65	0.025	0.405	0.457	0.273	2.51	0.509	0.082	II
HG - 8	33.46	5.42	0.663	34.86	0.016	0.379	0.633	0.269	2.455	0.508	0.105	II
MG - 2	24.28	4.588	1.25	45.42	0.011	0.427	0.396	0.289	2.948	0.437	0.061	XI
MG - 1	21.36	3.866	1.19	39.16	0.009	0.406	0.385	0.301	3.026	0.442	0.062	XI
LEB-1	9.333	2.423	0.682	22.78	6E-04	0.117	0.053	0.061	0.429	0.079	0.004	XII
LEB-2	8.911	3.294	0.732	21.93	0.004	0.082	0.034	0.038	0.248	0.048	0.001	XII
CH - 3	17.59	3.655	1.123	35.99	0.006	0.255	0.161	0.157	1.24	0.233	0.008	XIII
EBS-1	16.7	3.447	1.19	40.22	0.007	0.297	0.172	0.185	1.353	0.243	0.015	XIII
EBS-2	20.34	4.437	1.66	54.37	0.008	0.404	0.195	0.213	1.487	0.281	0.011	XIII
K - 1	20.34	3.77	0.981	35.4	0.006	0.262	0.211	0.131	1.356	0.198	0.017	I
HG - 6	34.12	6.596	0.54	38.99	0.025	0.426	0.654	0.271	2.518	0.488	0.11	II
BX - 3	16.27	2.379	0.964	33.24	0.008	0.346	0.306	0.248	2.249	0.336	0.046	XI
X - ?	23.54	3.558	0.986	33.48	0.005	0.256	0.272	0.143	0.957	0.264	0.02	?
Y - HG	38.49	5.208	0.639	44.75	0.026	0.631	0.789	0.338	3.293	0.454	0.09	II
HG - 9	25.25	4.865	0.473	35.76	0.013	0.321	0.517	0.219	1.965	0.392	0.066	II
MD-1	35.09	6.539	0.428	20.9	0.011	0.167	0.461	0.128	0.736	0.263	0.05	[illegible]

Appendix 1d: Inter-element concentration ratios for Naivasha Quarry sources (normalised against manganese Mn)

Qry No	K	Ca	Ti	Fe*	Cu	Zn	Rb	Y	Zr	Nb	Th	PetGp
HG - 1	58.63	7.927	1.672	75.9	0.052	0.783	1.306	0.556	4.499	0.976	0.19	III
HG - 2	60.13	8.609	1.95	75.2	0.069	0.847	1.384	0.556	4.891	1.034	0.16	III
HG - 3	60.74	8.864	1.927	67.4	0.028	0.89	1.312	0.577	5.379	0.991	0.2	III
HG - 4	68.93	11.46	1.546	72.2	0.025	0.84	1.323	0.508	5.157	1.063	0.19	III
OLB-1	54.32	8.95	1.535	74.8	0.02	0.885	1.325	0.601	5.553	0.993	0.18	IV
HG - 5	60.17	8.38	1.556	69.4	0.033	0.941	1.81	0.718	6.549	1.495	0.12	III
OLB-2	63.15	8.497	1.842	76	0.025	0.864	1.405	0.623	5.791	1.022	0.2	IV
OLB-3	63.45	10.56	1.828	74.3	0.023	0.904	0.123	0.547	5.247	0.935	0.17	IV
KIB-1	78.47	7.759	2.493	66.4	0.09	0.797	1.621	0.603	6.259	0.959	0.17	V
KIB-2	81.16	12.79	1.892	80.5	0.046	1.089	1.538	0.728	7.377	1.069	0.14	V
KIB-3	70.99	8.292	1.58	71.1	0.053	0.994	1.458	0.73	6.755	0.975	0.2	V
KIB-4	83.87	16.7	2.564	89.4	0.05	1.145	1.66	0.794	7.997	1.199	0.2	V
KIB-5	80.03	9.597	2.376	68.4	0.047	0.95	1.557	0.651	6.577	0.977	0.17	V
KIB-6	92.88	13.19	2.601	83.2	0.059	1.161	1.762	0.791	7.51	1.169	0.23	V
OSE-1	31.61	3.858	0.566	41	0.011	0.539	0.843	0.382	3.648	0.573	0.08	V
XN - 1	18.24	3.75	0.157	12.2	-	0.098	0.286	0.083	0.441	0.163	0.07	VI
OBR-2	16.71	6.041	2.517	30.4	0.006	0.079	0.041	0.008	0.174	0.028	0	I
OLF-1	34.65	5.914	1.499	41.2	0.01	0.314	0.323	0.194	1.918	0.292	0.03	VIII
OLF-2	24.79	4.665	1.67	42.6	0.009	0.309	0.284	0.169	1.703	0.297	0.03	VIII
HPF-1	112	22.44	2.169	83.6	0.052	0.513	1.838	0.007	2.981	1.117	0.06	IX
GCL-1	111	17.62	1.424	61.1	0.056	0.684	1.286	0.368	2.134	0.827	0.15	VII
GCL-2	88.24	15.94	1.059	48.9	0.063	0.815	1.129	0.314	0.007	0.676	0.13	VII
NB - 1	35.69	5.361	0.655	21.3	0.016	0.235	0.619	0.145	0.861	0.311	0.05	IX
NB - 2	82.09	16.28	1.153	49.7	0.038	0.383	1.13	0.33	1.793	0.667	0.07	IX
LD - 1	12.66	2.715	0.8	33.2	0.005	0.23	0.152	0.104	0.789	0.158	0.01	X
LD - 2	14.9	2.917	0.71	34.3	0.004	0.341	0.301	0.212	2.065	0.272	0.04	X
BX - 1	12.74	2.568	0.876	31.8	0.007	0.327	0.311	0.218	2.243	0.314	0.04	XI
BX - 2	15.47	2.874	0.936	35.9	0.005	0.366	0.303	0.235	2.365	0.331	0.05	XI
CH -1	11.87	3.063	1.452	33.6	0.003	0.174	0.077	0.07	0.524	0.097	0.01	XIII
CH - 2	13.28	2.517	0.798	32.8	-	0.223	0.117	0.133	0.899	0.173	0.01	XIII
EB - 1	16.64	3.293	0.882	36.4	0.004	0.29	0.186	0.193	1.536	0.261	0.01	XIII
EB - 2	17.19	2.906	0.841	37.9	0.007	0.282	0.162	0.192	1.413	0.236	0.02	XIII
HG - 7	82.67	11.09	2.008	71.6	0.05	0.813	0.917	0.548	5.041	1.022	0.17	III
HG - 8	50.48	8.177	1.509	52.6	0.023	0.571	0.955	0.406	3.704	0.766	0.16	III
MG - 2	19.42	3.67	0.8	36.3	0.009	0.342	0.317	0.231	2.358	0.35	0.05	XI
MG - 1	17.95	3.25	0.841	32.9	0.008	0.341	0.324	0.253	2.544	0.371	0.05	XI
LEB-1	13.69	3.554	1.467	33.4	9E-04	0.171	0.078	0.09	0.63	0.115	0.01	XII
LEB-2	12.17	4.499	1.366	30	0.005	0.112	0.047	0.052	0.339	0.065	0	XII
CH - 3	15.67	3.255	0.891	32.1	0.005	0.227	0.143	0.14	1.104	0.207	0.01	XIII
EBS-1	14.04	2.896	0.84	33.8	0.006	0.25	0.145	0.156	1.137	0.205	0.01	XIII
EBS-2	12.25	2.673	6024	32.8	0.005	0.243	0.118	0.128	0.896	0.169	0.01	XIII
K - 1	20.75	3.845	1.02	36.1	0.006	0.267	0.215	0.133	1.383	0.202	0.02	I
HG - 6	63.18	12.21	1.852	72.2	0.047	0.789	1.211	0.503	4.662	0.904	0.2	III
BX - 3	16.88	2.469	1.038	34.5	0.008	0.359	0.317	0.257	2.335	0.349	0.05	XI
X - ?	23.88	3.609	1.015	34	0.005	0.259	0.276	0.145	0.971	0.268	0.02	?
Y - HG	60.19	8.145	1.564	70	0.04	0.988	1.233	0.529	5.15	0.709	0.14	III
HG - 9	53.44	10.3	2.116	75.7	0.027	0.679	1.093	0.462	4.157	0.829	0.14	III
MD - 1	81.95	15.27	2.336	48.8	[illegible]	0.391	1.077	0.299	[illegible]	[illegible]	0.12	IX

Appendix 1e: Inter-element concentration ratios for Naivasha Quarry sources (normalised against iron $Fe_2O_3 + FeO$)

Qry N	K	Ca	Ti	Mn	Cu	Zn	Rb	Y	Zr	Nb	Th	PetGp
HG - 1	0.773	0.105	0.02	0.013	7E-04	0.01	0.02	0.007	0.059	0.01	0.003	II
HG - 2	0.8	0.115	0.03	0.013	9E-04	0.011	0.02	0.007	0.065	0.01	0.002	II
HG - 3	0.901	0.132	0.03	0.015	4E-04	0.013	0.02	0.009	0.08	0.01	0.003	II
HG - 4	0.955	0.159	0.02	0.014	3E-04	0.012	0.02	0.007	0.071	0.01	0.003	II
OLB-1	0.726	0.12	0.02	0.013	3E-04	0.012	0.02	0.008	0.074	0.01	0.002	IV
HG - 5	0.868	0.121	0.02	0.014	5E-04	0.014	0.03	0.01	0.094	0.02	0.002	II
OLB-2	0.831	0.112	0.02	0.013	3E-04	0.011	0.02	0.008	0.076	0.01	0.003	IV
OLB-3	0.853	0.142	0.02	0.014	3E-04	0.012	0	0.007	0.071	0.01	0.002	IV
KIB-1	1.182	0.117	0.04	0.015	0.001	0.012	0.02	0.009	0.094	0.01	0.003	V
KIB-2	1.008	0.159	0.02	0.012	6E-04	0.014	0.02	0.009	0.092	0.01	0.002	V
KIB-3	0.998	0.117	0.02	0.014	7E-04	0.014	0.02	0.01	0.095	0.01	0.003	V
KIB-4	0.939	0.187	0.03	0.011	6E-04	0.013	0.02	0.009	0.09	0.01	0.002	V
KIB-5	1.171	0.14	0.03	0.015	7E-04	0.014	0.02	0.01	0.096	0.01	0.003	V
KIB-6	1.116	0.158	0.03	0.012	7E-04	0.014	0.02	0.01	0.09	0.01	0.003	V
OSE-1	0.772	0.094	0.01	0.024	3E-04	0.013	0.02	0.009	0.089	0.01	0.002	V
XN - 1	1.5	0.308	0.01	0.082	-	0.008	0.02	0.007	0.036	0.01	0.006	VI
OBR-2	0.549	0.199	0.08	0.033	2E-04	0.003	0	2E-04	0.006	0	2E-04	I
OLF-1	0.841	0.144	0.04	0.024	2E-04	0.008	0.01	0.005	0.047	0.01	6E-04	VIII
OLF-2	0.582	0.109	0.04	0.024	2E-04	0.007	0.01	0.004	0.04	0.01	8E-04	VIII
HPF-1	1.341	0.269	0.03	0.012	6E-04	0.006	0.02	1E-04	0.036	0.01	7E-04	IX
GCL-1	1.815	0.288	0.02	0.016	9E-04	0.011	0.02	0.006	0.035	0.01	0.002	VII
GCL-2	1.805	0.326	0.02	0.021	0.001	0.017	0.02	0.006	1E-04	0.01	0.003	VII
NB - 1	1.622	0.251	0.03	0.047	8E-04	0.011	0.03	0.007	0.04	0.01	0.003	IX
NB - 2	1.652	0.326	0.02	0.02	6E-04	0.008	0.02	0.007	0.036	0.01	0.001	IX
LD - 1	0.381	0.082	0.02	0.03	2E-04	0.007	0	0.003	0.024	0	3E-04	X
LD - 2	0.434	0.085	0.02	0.029	1E-04	0.01	0.01	0.006	0.06	0.01	0.001	X
BX - 1	0.401	0.081	0.03	0.031	2E-04	0.01	0.01	0.007	0.071	0.01	0.001	XI
BX - 2	0.431	0.08	0.03	0.028	1E-04	0.01	0.01	0.007	0.066	0.01	0.001	XI
CH - 1	0.353	0.091	0.04	0.03	1E-04	0.005	0	0.002	0.016	0	2E-04	XIII
CH - 2	0.405	0.077	0.02	0.031	-	0.007	0	0.004	0.027	0.01	3E-04	XIII
EB - 1	0.455	0.091	0.02	0.028	5E-04	0.008	0.01	0.005	0.042	0.01	4E-04	XIII
EB - 2	0.454	0.077	0.02	0.028	2E-04	0.007	0	0.005	0.037	0.01	5E-04	XIII
HG - 7	1.155	0.155	0.03	0.014	7E-04	0.011	0.01	0.008	0.07	0.01	0.002	III
HG - 8	0.96	0.156	0.03	0.019	4E-04	0.011	0.02	0.008	0.07	0.01	0.003	III
MG - 2	0.535	0.101	0.02	0.028	2E-04	0.009	0.01	0.006	0.065	0.01	0.001	XI
MG - 1	0.545	0.099	0.03	0.03	2E-04	0.01	0.01	0.008	0.077	0.01	0.002	XI
LEB-1	0.41	0.106	0.04	0.03	-	0.005	0	0.003	0.019	0	2E-04	XII
LEB-2	0.406	0.15	0.05	0.033	2E-04	0.004	0	0.002	0.011	0	-	XII
CH - 3	0.489	0.102	0.03	0.031	2E-04	0.007	0	0.004	0.034	0.01	2E-04	XIII
EBS-1	0.415	0.086	0.02	0.03	2E-04	0.007	0	0.005	0.034	0.01	4E-04	XIV
EBS-2	0.374	0.082	0.02	0.031	1E-04	0.007	0	0.004	0.027	0.01	2E-04	XIV
K - 1	0.575	0.107	0.03	0.028	2E-04	0.007	0.01	0.004	0.038	0.01	5E-04	I
HG - 6	0.875	0.169	0.03	0.014	6E-04	0.011	0.02	0.007	0.065	0.01	0.003	II
BX - 3	0.489	0.072	0.03	0.029	2E-04	0.01	0.01	0.008	0.068	0.01	0.001	XI
X - ?	0.703	0.106	0.03	0.029	2E-04	0.008	0.01	0.004	0.029	0.01	6E-04	?
Y - HG	0.86	0.116	0.02	0.014	6E-04	0.014	0.02	0.008	0.074	0.01	0.002	II
HG - 9	0.706	0.136	0.03	0.013	4E-04	0.009	0.01	0.006	0.055	0.01	0.002	III
MD - 1	1.679	0.313	0.05	0.021	5E-04	0.008	0.02	0.006	0.035	0.01	0.002	IX

Appendix 1f: Inter-element concentration ratios for Naivasha Quarry sources (normalised against copper Cu)

Qry No	K	Ca	Ti	Mn	Fe*	Zn	Rb	Y	Zr	Nb	Th	PetGp
HG - 1	1139	153.9	32.47	19.42	1473	15.21	25.37	10.79	87.37	18.95	3.632	III
HG - 2	874.5	125.2	28.36	14.55	1094	12.32	20.14	8.091	71.14	15.05	2.364	III
HG - 3	2139	312.2	67.89	35.22	2374	31.33	46.22	20.33	189.4	34.89	7.111	III
HG - 4	2749	456.9	61.63	39.88	2879	33.5	52.75	20.25	205.6	42.38	7.5	III
OLB-1	2674	440.6	75.56	49.22	3682	43.56	65.22	29.56	273.3	48.89	8.667	IV
HG - 5	1831	255	47.36	30.43	2111	28.64	55.07	21.86	199.3	45.5	3.5	III
OLB-2	2494	335.6	72.75	39.5	3002	34.13	55.5	24.63	228.8	40.38	8	IV
OLB-3	2707	450.6	78	42.67	3172	38.56	5.233	23.33	223.9	39.89	7.444	IV
KIB-1	875.2	86.54	27.81	11.15	740.8	8.885	18.08	6.731	69.81	10.69	1.846	V
KIB-2	1768	278.6	41.21	21.79	1755	23.71	33.5	15.86	160.7	23.29	3.071	V
KIB-3	1332	155.6	29.65	18.76	1335	18.65	27.35	13.71	126.8	18.29	3.765	V
KIB-4	1689	336.4	51.64	20.14	1800	23.07	33.43	16	161.1	24.14	4	V
KIB-5	1704	204.3	50.57	21.29	1455	20.21	33.14	13.86	140	20.79	3.643	V
KIB-6	1585	225	44.38	17.06	1420	19.81	30.06	13.5	128.1	19.94	3.938	V
OSE-1	2813	243.3	50.33	89	3647	48	75	34	324.7	51	7.333	V
KN - 1	-	-	-	-	-	-	-	-	-	-	-	VI
OBR-2	3029	1095	456.3	181.3	5513	14.38	7.375	1.375	31.5	5	0.875	II
OLF-1	3365	574.4	145.6	97.13	4001	30.5	31.38	18.88	186.3	28.38	2.5	VIII
OLF-2	2820	530.6	190	113.8	4848	35.13	32.25	19.25	193.8	33.75	3.75	VIII
HPF-1	2157	431.9	41.75	19.25	1609	9.875	35.38	0.125	57.38	21.5	1.125	IX
GCL-1	1972	313.1	25.31	17.77	1086	12.15	22.85	6.539	37.92	14.69	2.615	VII
GCL-2	1407	254.2	16.89	15.94	779.4	13	18	5	0.111	10.78	2	VII
NB - 1	2222	333.8	40.75	62.25	1329	14.63	38.5	9	53.63	19.38	3.375	IX
NB - 2	2143	425	30.1	26.1	1297	10	29.5	8.6	46.8	17.4	1.8	IX
LD - 1	2463	528	155.5	194.5	6466	44.7	29.6	20.2	153.5	30.7	2.1	X
LD - 2	3449	675	164.3	231.4	7943	78.86	69.71	49.14	477.9	63	10	X
BX - 1	1957	394.5	134.5	153.6	4885	50.18	47.82	33.45	344.5	48.27	6.636	XI
BX - 2	3151	585.6	190.6	203.8	7314	74.5	61.75	47.88	481.9	67.5	9.25	XI
CH - 1	4075	1052	498.3	343.3	-	59.67	26.5	24	180	33.33	2.167	XIII
CH - 2	-	-	-	-	-	-	-	-	-	-	-	XIII
EB - 1	4216	834.2	223.3	253.3	9211	73.33	47.17	49	389.2	66.17	3.333	XIII
EB - 2	2636	445.6	128.9	153.3	5807	43.22	24.78	29.44	216.7	36.11	3.111	XIII
HG - 7	1667	223.6	40.5	20.17	1444	16.39	18.5	11.06	101.7	20.61	3.333	III
HG - 8	2158	349.6	64.5	42.75	2249	24.42	40.83	17.33	158.3	32.75	6.75	III
MG - 2	2258	426.7	93	116.3	4224	39.75	36.83	26.83	274.2	40.67	5.667	XI
MG - 1	2394	433.3	112.1	133.3	4389	45.5	43.17	33.75	339.2	49.5	6.917	XI
LEB-1	-	3768	1555	1060	-	181.5	82.5	95.5	667.5	122	5.5	XII
LEB-2	2328	860.4	261.3	191.3	5729	21.5	9	9.917	64.75	12.42	0.25	XII
CH - 3	3008	625	171	192	6155	43.6	27.5	26.8	212	39.8	1.3	XIII
EBS-1	2278	470	136.4	162.3	5485	40.55	23.45	25.27	184.5	33.18	2.091	XIII
EBS-2	2530	552	124.4	206.5	6764	50.2	24.3	26.5	185	34.9	1.4	XIII
K - 1	3254	603.1	160	156.9	5664	41.88	33.75	20.88	216.9	31.75	2.75	I
HG - 6	1348	260.6	39.5	21.33	1540	16.83	25.83	10.72	99.44	19.28	4.333	III
BX - 3	2040	298.3	125.4	120.8	4169	43.33	38.33	31.08	282.1	42.17	5.75	XI
X - ?	4585	693	194.8	192	6521	49.8	53	27.8	186.4	51.4	3.8	?
Y - HG	1501	203.1	39	24.94	1745	24.63	30.75	13.19	128.4	17.69	3.5	III
HG - 9	1955	376.7	77.42	36.58	2769	24.83	40	16.92	152.1	30.33	5.083	III
MD - 1	3208	597.9	91.43	39.14	1911	15.29	42.14	11.71	67.29	24	4.571	[illegible]

Appendix 1g: Inter-element concentration ratios for Naivasha Quarry sources (normalised against zinc Zn)

Ory No	K	Ca	Ti	Mn	Fe'	Cu	Rb	Y	Zr	Nb	Th	PetGp
HG - 1	74.86	10.12	2.135	1.277	96.87	0.066	1.668	0.709	5.744	1.246	0.239	III
HG - 2	71	10.17	2.303	1.161	83.78	0.081	1.635	0.657	5.775	1.221	0.192	III
HG - 3	68.28	9.965	2.167	1.124	75.78	0.032	1.475	0.649	6.046	1.114	0.227	III
HG - 4	82.05	13.64	1.84	1.19	85.93	0.03	1.575	0.605	6.138	1.265	0.224	III
OLB-1	61.39	10.11	1.735	1.13	94.53	0.023	1.497	0.679	6.276	1.122	0.199	IV
HG - 5	63.93	8.903	1.653	1.062	73.69	0.035	1.923	0.763	6.958	1.589	0.122	III
OLB-2	73.1	9.835	2.132	1.158	87.97	0.029	1.626	0.722	6.703	1.183	0.234	IV
OLB-3	70.22	11.69	2.023	1.107	82.28	0.026	0.136	0.605	5.807	1.035	0.193	IV
KIB-1	98.51	9.74	3.13	1.255	83.38	0.113	2.035	0.758	7.857	1.204	0.208	V
KIB-2	74.56	11.75	1.738	0.919	73.99	0.042	1.413	0.669	6.777	0.982	0.13	V
KIB-3	71.44	8.344	1.59	1.006	71.59	0.054	1.467	7350	6.798	0.981	0.202	V
KIB-4	73.22	14.58	2.238	0.873	78.02	0.043	1.449	0.694	6.981	1.046	0.173	V
KIB-5	84.28	10.11	2.502	1.053	72	0.05	1.64	0.686	6.926	1.028	0.18	V
KIB-6	79.98	11.36	2.24	0.861	71.69	0.051	1.517	0.681	6.467	1.006	0.199	V
OSE-1	58.61	7.153	1.049	1.854	75.97	0.021	1.563	0.708	6.764	1.063	0.153	V
KN - 1	187.2	38.48	1.609	10.61	124.8	-	2.935	0.848	4.522	1.674	0.739	VI
OBR-2	210.7	76.17	31.74	12.61	383.5	0.07	0.513	0.096	2.191	0.348	0.061	II
OLF-1	110.3	18.83	4.775	3.184	131.2	0.033	1.029	0.619	6.107	0.93	0.082	VIII
OLF-2	80.28	15.11	5.409	3.238	138	0.029	0.918	0.548	5.516	0.961	0.107	VIII
HPF-1	218.4	43.73	4.228	1.949	162.9	0.101	3.582	0.013	5.81	2.177	0.114	IX
GCL-1	162.2	25.76	2.082	1.462	89.37	0.082	1.88	0.538	3.12	1.209	0.215	VII
GCL-2	108.2	19.55	1.299	1.227	89.96	0.077	1.385	0.385	0.009	0.829	0.154	VII
NB - 1	151.9	22.82	2.786	4.256	90.85	0.068	2.633	0.615	3.667	1.325	0.231	IX
NB - 2	214.3	42.5	3.01	2.61	129.7	0.1	2.95	0.86	4.68	1.74	0.18	IX
LD - 1	55.09	11.81	3.479	4.351	144.7	0.022	0.662	0.452	3.434	0.687	0.047	X
LD - 2	43.73	8.56	2.083	2.935	100.7	0.013	0.884	0.623	6.06	0.799	0.127	X
BX - 1	39	7.862	2.681	3.062	97.36	0.02	0.953	0.667	6.866	0.962	0.132	XI
BX - 2	42.3	7.861	2.559	2.735	98.18	0.013	0.829	0.643	6.468	0.906	0.124	XI
CH -1	68.3	17.63	8.352	5.754	193.4	0.017	0.444	0.402	3.017	0.559	0.036	XIII
CH - 2	59.47	11.27	3.571	4.479	146.9	-	0.522	0.596	4.025	0.773	0.041	XIII
EB - 1	57.49	11.38	3.046	3.455	125.6	0.014	0.643	0.668	5.307	0.902	0.046	XIII
EB - 2	60.99	10.31	2.982	3.548	134.4	0.023	0.573	0.681	5.013	0.836	0.072	XIII
HG - 7	101.7	13.64	2.471	1.231	88.1	0.061	1.129	0.675	6.203	1.258	0.203	III
HG - 8	88.38	14.32	2.642	1.751	92.1	0.041	1.672	0.71	6.485	1.341	0.277	III
MG - 2	56.8	10.73	2.34	2.925	106.3	0.025	0.927	0.675	6.897	1.023	0.143	XI
MG - 1	52.61	9.524	2.563	2.93	95.47	0.022	0.949	0.742	7.454	1.088	0.152	XI
LEB-1	79.96	20.76	8.568	5.84	195.2	0.006	0.455	0.526	3.678	0.672	0.03	XII
LEB-2	108.3	40.02	12.15	8.895	266.5	0.047	0.419	0.461	3.012	0.578	0.012	XII
CH - 3	68.99	14.33	3.922	4.404	141.2	0.023	0.631	0.615	4.862	0.913	0.03	XIII
EBS-1	56.18	11.59	3.363	4.002	135.3	0.025	0.579	0.623	4.552	0.818	0.052	XIII
EBS-2	50.4	11	2.478	4.114	134.7	0.02	0.484	0.528	3.685	0.695	0.028	XIII
K - 1	77.72	14.4	3.821	3.746	135.3	0.024	0.806	0.499	5.179	0.758	0.066	I
HG - 6	80.07	15.48	2.347	1.267	91.49	0.059	1.535	0.637	5.908	1.145	0.257	III
BX - 3	47.08	6.885	2.894	2.789	96.2	0.023	0.885	0.717	6.51	0.973	0.133	XI
X - ?	92.07	13.92	3.912	3.855	130.9	0.02	1.064	0.558	3.743	1.032	0.076	?
Y-HG	60.95	8.249	1.584	1.013	70.88	0.041	1.249	0.536	5.216	7183	0.142	III
HG - 9	78.72	15.17	3.117	1.473	111.5	0.04	1.611	0.681	6.124	1.222	0.205	III
MD - 1	209.9	39.11	5.981	2.561	125	0.065	2.757	0.766	4.402	1.57	0.299	IX

Appendix 1h: Inter-element concentration ratios for Naivasha Quarry sources (normalised against rubidium)

Qry No	K	Ca	Ti	Mn	Fe*	Cu	Zn	Y	Zr	Nb	Th	PetGp
HG - 1	44.89	6.069	1.28	0.766	58.08	0.039	0.6	0.425	3.444	0.747	0.143	III
HG - 2	43.43	6.219	1.409	0.722	54.31	0.05	0.612	0.402	3.533	0.747	0.117	III
HG - 3	46.29	6.755	1.469	0.762	51.37	0.022	0.678	4399	4.093	0.755	0.154	III
HG - 4	52.11	8.661	1.168	0.756	54.57	0.019	0.635	3839	3.898	0.803	0.142	III
OLB-1	41	6.755	1.158	0.755	56.45	0.015	0.668	4532	4.191	0.75	0.133	IV
HG - 5	33.25	4.63	0.86	0.553	38.33	0.018	0.52	0.397	3.619	0.826	0.064	III
OLB-2	44.94	6.047	1.311	0.712	54.09	0.018	0.615	0.444	4.122	0.728	0.144	IV
OLB-3	517.3	86.09	14.9	8.153	606.2	0.191	7.615	4.459	42.78	7.728	1.423	IV
KIB-1	48.41	4.787	1.538	0.617	40.98	0.055	0.492	0.372	3.862	0.592	0.102	V
KIB-2	52.78	8.316	1.23	0.65	52.38	0.03	0.708	0.473	4.797	0.695	0.092	V
KIB-3	48.7	5.688	1.084	0.686	48.81	0.037	0.682	0.501	4.634	0.669	0.138	V
KIB-4	50.53	10.06	1.545	0.603	53.85	0.03	0.69	0.479	4.818	0.722	0.12	V
KIB-5	51.4	6.164	1.526	0.642	43.91	0.03	0.61	0.418	4.224	0.627	0.11	V
KIB-6	52.71	7.484	1.476	0.568	47.25	0.033	0.659	0.449	4.262	0.663	0.131	V
OSE-1	37.51	4.578	0.671	1.187	48.62	0.013	0.64	0.453	4.329	0.68	0.098	V
KN - 1	63.78	13.11	0.548	3.496	42.52	-	0.341	0.289	1.541	0.57	0.252	VI
OBR-2	410.7	148.5	61.86	24.58	747.5	0.136	1.949	0.186	4.271	0.678	0.119	II
OLF-1	107.3	18.31	4.641	3.096	127.5	0.032	0.972	0.602	5.936	0.904	0.08	VIII
OLF-2	87.11	16.45	5.892	3.527	150.3	0.031	1.089	0.597	6.008	1.047	0.116	VIII
HPF-1	60.97	12.21	1.18	0.544	45.48	0.028	0.279	0.004	1.622	0.608	0.032	IX
GCL-1	86.3	13.7	1.108	0.778	47.54	0.044	0.532	0.286	1.66	0.643	0.115	VII
GCL-2	78.16	14.12	0.938	0.886	43.3	0.056	0.722	0.278	0.006	0.599	0.111	VII
NB - 1	57.71	8.669	1.058	1.617	34.51	0.026	0.38	0.234	1.393	0.503	0.088	IX
NB - 2	72.63	14.41	1.02	0.885	43.97	0.034	0.339	0.292	1.586	0.59	0.061	IX
LD - 1	83.19	17.84	5.253	6.571	218.4	0.034	1.51	0.682	5.186	1.037	0.071	X
LD - 2	49.47	9.682	2.357	3.32	113.9	0.014	1.131	0.705	6.855	0.904	0.143	X
BX - 1	40.93	8.251	2.844	3.213	102.2	0.021	1.049	0.7	7.205	1.01	0.139	XI
BX - 2	51.03	9.484	3.087	3.3	118.5	0.016	1.207	0.775	7.804	1.093	0.15	XI
CH -1	153.8	39.69	18.81	12.96	435.4	0.038	2.252	0.906	6.793	1.258	0.082	XIII
CH - 2	114	21.61	6.848	8.587	281.6	-	1.917	1.144	7.717	1.483	0.078	XIII
EB - 1	89.38	17.69	4.735	5.371	195.3	0.021	1.555	1.039	8.251	1.403	0.071	XIII
EB - 2	106.4	17.98	5.202	6.188	234.4	0.04	1.744	1.188	8.744	1.457	0.126	XIII
HG - 7	90.12	12.09	2.189	1.09	78.05	0.054	0.886	0.598	5.496	1.114	0.18	III
HG - 8	52.85	8.561	1.58	1.047	55.07	0.025	0.598	0.425	3.878	0.802	0.165	III
MG - 2	61.3	11.58	2.525	3.156	114.7	0.027	1.079	0.729	7.443	1.104	0.154	XI
MG - 1	55.45	10.04	2.597	3.089	101.7	0.023	1.054	0.782	7.857	1.147	0.16	XI
LEB-1	175.9	45.67	18.85	12.25	429.4	0.012	2.2	1.158	8.091	1.479	0.067	XII
LEB-2	258.7	95.6	29.03	21.25	636.5	0.111	2.389	1.102	7.194	1.38	0.028	XII
CH - 3	109.4	22.73	6.218	6.982	223.8	0.036	1.586	9745	7.709	1.447	0.047	XIII
EBS-1	97.11	20.04	5.814	6.919	233.8	0.043	1.729	1.078	7.868	1.415	0.089	XIII
EBS-2	104.1	22.72	25.12	8.498	278.4	0.041	2.066	1.091	7.613	1.436	0.058	XIII
K - 1	96.43	17.87	4.741	4.648	167.8	0.03	1.241	6185	6.426	0.941	0.082	I
HG - 6	52.17	10.09	1.529	0.826	59.61	0.039	0.652	4151	3.85	0.746	0.168	III
BX - 3	53.22	7.783	3.272	3.152	108.8	0.026	1.13	0.811	7.359	1.1	0.15	XI
X - ?	86.51	13.08	3.676	3.623	123	0.019	0.94	0.525	3.517	0.97	0.072	?
Y - HG	48.81	6.606	1.268	0.811	56.76	0.033	0.801	0.429	4.177	0.575	0.114	III
HG - 9	48.88	9.417	1.935	0.915	69.22	0.025	0.621	0.423	3.802	0.758	0.127	III
MD - 1	78.48	14.10	[illegible]	0.929	45.34	0.024	0.363	0.278	1.597	0.57	0.109	IX

Appendix 1i: Inter-element concentration ratios for Naivasha Quarry sources (normalised against ytrrium)

Qry No	K	Ca	Ti	Mn	Fe*	Cu	Zn	Rb	Zr	Nb	Th	PetGp
HG - 1	102.5	14.27	3.01	1.8	136.6	0.093	1.41	2.351	8.098	1.76	0.337	III
HG - 2	108.1	15.48	3.506	1.798	135.2	0.124	1.523	2.489	8.779	1.86	0.292	III
HG - 3	105.2	15.36	3.339	1.732	116.8	0.049	1.541	2.273	9.317	1.72	0.35	III
HG - 4	135.7	22.56	3.043	1.969	142.2	0.049	1.654	2.605	10.15	2.09	0.37	III
OLB-1	90.47	14.91	2.556	1.665	124.6	0.034	1.474	2.207	9.248	1.65	0.293	IV
HG - 5	83.77	11.67	2.167	1.392	96.57	0.026	1.311	2.52	9.118	2.08	0.16	III
OLB-2	101.3	13.63	2.954	1.604	121.9	0.041	1.386	2.254	9.289	1.64	0.325	IV
OLB-3	116	19.31	3.343	1.829	136	0.043	1.652	0.224	9.595	1.71	0.319	IV
KIB-1	130	12.86	4.131	1.657	110.1	0.149	1.32	2.686	10.37	1.59	0.274	V
KIB-2	111.5	17.57	2.599	1.374	110.7	0.063	1.496	2.113	10.14	1.47	0.194	V
KIB-3	97.19	11.35	2.163	1.369	97.4	0.073	1.361	1.996	9.249	1.33	0.275	V
KIB-4	105.6	21.03	3.228	1.259	112.5	0.063	1.442	2.089	10.07	1.51	0.25	V
KIB-5	122.9	14.74	3.65	1.536	105	0.072	1.459	2.392	10.1	1.5	0.263	V
KIB-6	117.4	16.67	3.287	1.264	105.2	0.074	1.468	2.227	9.491	1.48	0.292	V
OSE-1	82.75	10.1	1.48	2.618	107.3	0.029	1.412	2.206	9.549	1.5	0.216	V
XN - 1	220.8	45.38	1.897	12.1	147.2	-	1.18	3.462	5.333	1.97	0.872	VI
OBR-2	2203	796.4	331.8	131.8	4009	0.727	10.45	5.364	22.91	3.64	0.636	II
OLF-1	178.3	30.43	7.715	5.146	212	0.053	1.616	1.662	9.868	1.5	0.133	VIII
OLF-2	146.5	27.56	9.87	5.909	251.9	0.052	1.825	1.675	10.06	1.75	0.195	VIII
HPF-1	-	3E+07	334	154	-	8	79	283	459	172	9	IX
GCL-1	301.5	47.88	3.871	2.718	166.1	0.153	1.859	3.494	5.8	2.25	0.4	VII
GCL-2	281.4	50.83	3.378	3.189	155.9	0.2	2.6	3.6	0.022	2.16	0.4	VII
NB - 1	246.9	37.08	4.528	6.917	147.6	0.111	1.625	4.278	5.958	2.15	0.375	IX
NB - 2	249.1	49.42	3.5	3.035	150.8	0.006	1.163	3.43	5.442	2.02	0.209	IX
LD - 1	121.9	26.14	7.698	9.629	320.1	0.05	2.213	1.465	7.599	1.52	0.104	X
LD - 2	70.17	13.74	3.343	4.709	161.6	0.02	1.605	1.419	9.724	1.28	0.204	X
BX - 1	58.51	11.79	4.022	4.592	146	0.03	1.5	1.429	10.3	1.44	0.198	XI
BX - 2	65.82	12.23	3.982	4.256	152.8	0.021	1.556	1.29	10.07	1.41	0.193	XI
CH -1	169.8	43.82	20.76	14.31	480.8	0.042	2.486	1.104	7.5	1.39	0.09	XIII
CH - 2	99.71	18.9	5.989	7.51	246.3	-	1.677	0.875	6.749	1.3	0.068	XIII
EB - 1	86.04	17.02	4.558	5.17	188	0.02	1.497	0.963	7.942	1.35	0.068	XIII
EB - 2	89.53	15.13	4.377	5.208	197.2	0.034	1.468	0.842	7.359	1.23	0.106	XIII
HG - 7	150.8	20.23	3.663	1.824	130.6	0.091	1.482	1.673	9.196	1.86	0.302	III
HG - 8	124.5	20.17	3.721	2.466	129.7	0.058	1.409	2.356	9.135	1.89	0.389	III
MG - 2	84.15	15.9	3.466	4.332	157.4	0.037	1.481	1.373	10.22	1.52	0.311	XI
MG - 1	70.93	12.84	3.321	3.951	130	0.03	1.348	1.279	10.05	1.47	0.205	XI
LEB-1	152	39.45	16.28	11.1	370.9	0.011	1.901	0.864	6.99	1.28	0.058	XII
LEB-2	234.7	86.76	26.34	19.29	577.7	0.101	2.168	0.908	6.529	1.25	0.025	XII
CH - 3	112.2	23.32	6.381	7.164	229.7	0.037	1.627	1.026	7.91	1.49	0.049	XIII
EBS-1	90.13	18.6	5.396	6.421	217	0.04	1.604	0.928	7.302	1.31	0.083	XIII
EBS-2	95.47	20.83	4.694	7.783	255.2	0.038	1.894	0.917	6.981	1.32	0.053	XIII
K - 1	155.9	28.89	7.665	7.515	271.3	0.048	2.006	1.617	10.39	1.52	0.132	I
HG - 6	125.7	24.3	3.684	1.99	143.6	0.093	1.57	2.409	9.275	1.8	0.404	III
BX - 3	65.63	9.598	4.035	3.887	134.1	0.032	1.394	1.233	9.075	1.36	0.185	XI
X - ?	164.9	24.93	7.007	6.907	234.6	0.036	1.791	1.907	6.705	1.85	0.137	?
Y - HG	113.8	15.4	2.957	1.891	132.3	0.076	1.867	2.332	9.739	1.34	0.265	III
HG - 9	115.6	22.27	4.576	2.163	163.7	0.059	1.468	2.365	8.99	1.79	0.301	III
MD - 1	273.8	51.04	7.805	3.342	163.1	0.085	1.305	3.598	5.744	2.05	0.39	IX

Appendix 1j: Inter-element concentration ratios for Naivasha Quarry sources (normalised against zirconium)

Qry No	K	Ca	Ti	Mn	Fe*	Cu	Zn	Rb	Y	Nb	Th	PetGp
HG - 1	13.03	1.762	0.372	0.222	16.86	0.011	0.174	0.29	0.124	0.217	0.042	II
HG - 2	12.29	1.76	0.399	0.205	15.37	0.014	0.173	0.283	0.114	0.212	0.033	II
HG - 3	11.29	1.648	0.358	0.186	12.53	0.005	0.165	0.244	0.107	0.184	0.038	II
HG - 4	13.37	2.222	0.3	0.194	14	0.005	0.163	0.257	0.099	0.206	0.037	II
OLB-1	9.783	1.612	0.276	0.18	13.47	0.004	0.159	0.239	0.108	0.179	0.032	IV
HG - 5	9.188	1.28	0.238	0.153	10.59	0.005	0.144	0.276	0.11	0.228	0.018	II
OLB-2	10.9	1.467	0.318	0.173	13.12	0.004	0.149	0.243	0.108	0.177	0.035	IV
OLB-3	12.09	2.012	0.348	0.191	14.17	0.005	0.172	0.023	0.104	0.178	0.033	IV
KIB-1	12.54	1.24	0.398	0.16	10.61	0.014	0.127	0.259	0.096	0.153	0.026	V
KIB-2	11	1.733	0.256	0.136	10.92	0.006	0.148	0.208	0.099	0.145	0.019	V
KIB-3	10.51	1.227	0.234	0.148	10.53	0.008	0.147	0.216	0.108	0.144	0.03	V
KIB-4	10.49	2.089	0.321	0.125	11.18	0.006	0.143	0.208	0.099	0.15	0.025	V
KIB-5	12.17	1.459	0.361	0.152	10.4	0.007	0.144	0.237	0.099	0.149	0.026	V
KIB-6	12.37	1.756	0.346	0.133	11.09	0.008	0.155	0.235	0.105	0.156	0.031	V
OSE-1	8.665	1.058	0.155	0.274	11.23	0.003	0.148	0.231	0.105	0.157	0.023	V
KN - 1	41.39	8.51	0.356	2.269	27.6	-	0.221	0.649	0.188	0.37	0.164	VI
OBR-2	96.15	34.76	14.48	5.754	175	0.032	0.456	0.234	0.044	0.159	0.028	I
OLF-1	18.07	3.084	0.782	0.522	21.48	0.005	0.164	0.169	0.101	0.152	0.013	VIII
OLF-2	14.55	2.739	0.981	0.587	25.02	0.005	0.181	0.167	0.099	0.174	0.019	VIII
HPF-1	37.59	7.527	0.728	0.336	28.04	0.017	0.172	0.617	0.002	0.375	0.02	IX
GCL-1	51.99	8.256	0.667	0.469	28.64	0.026	0.321	0.602	0.172	0.387	0.069	VII
GCL-2	-	2288	152	143.5	7015	9	117	162	45	97	18	VII
NB - 1	41.43	6.224	0.76	1.161	24.78	0.019	0.273	0.718	0.168	0.361	0.063	IX
NB - 2	45.78	9.081	0.643	0.558	27.71	0.021	0.214	0.63	0.184	0.372	0.039	IX
LD - 1	16.04	3.44	1.013	1.267	42.12	0.007	0.291	0.193	0.132	0.2	0.014	X
LD - 2	7.217	1.413	0.344	0.484	16.62	0.002	0.165	0.146	0.103	0.132	0.021	X
BX - 1	5.681	1.145	0.391	0.446	14.18	0.003	0.146	0.139	0.097	0.14	0.019	XI
BX - 2	6.54	1.215	0.396	0.423	15.18	0.002	0.155	0.128	0.099	0.14	0.019	XI
CH -1	22.64	5.843	2.769	1.907	64.1	0.006	0.332	0.147	0.133	0.185	0.012	XIII
CH - 2	14.77	2.8	0.887	1.113	36.49	-	0.249	0.13	0.148	0.192	0.01	XIII
EB - 1	10.83	2.144	0.574	0.651	23.67	0.003	0.188	0.121	0.126	0.17	0.009	XIII
EB - 2	12.17	2.056	0.595	0.708	26.8	0.005	0.2	0.114	0.136	0.167	0.014	XIII
HG - 7	16.4	2.2	0.398	0.198	14.2	0.01	0.161	0.182	0.109	0.203	0.033	III
HG - 8	13.63	2.208	0.407	0.27	14.2	0.006	0.154	0.258	0.11	0.207	0.043	III
MG - 2	8.236	1.556	0.339	0.424	15.41	0.004	0.145	0.134	0.098	0.148	0.021	XI
MG - 1	7.058	1.278	0.331	0.393	12.94	0.003	0.134	0.127	0.1	0.146	0.02	XI
LEB-1	21.74	5.644	0.33	1.588	53.07	0.002	0.272	0.124	0.143	0.183	0.008	XII
LEB-2	35.95	13.29	4.035	2.954	88.47	0.015	0.332	0.139	0.153	0.192	0.004	XII
CH - 3	14.19	2.948	0.807	0.906	29.03	0.005	0.206	0.13	0.126	0.188	0.006	XIII
EBS-1	12.34	2.547	0.739	0.879	29.72	0.005	0.22	0.127	0.137	0.18	0.011	XIII
EBS-2	13.68	2.924	0.672	1.116	36.56	0.005	0.271	0.131	0.143	0.189	0.008	XIII
K - 1	15.01	2.781	0.738	0.723	26.12	0.005	0.193	0.156	0.096	0.146	0.013	I
HG - 6	13.55	2.62	0.397	0.215	15.49	0.01	0.169	0.26	0.108	0.194	0.044	III
BX - 3	7.232	1.058	0.445	0.428	14.78	0.004	0.154	0.136	0.11	0.15	0.02	XI
X - ?	24.6	3.718	1.045	1.03	34.98	0.005	0.267	0.284	0.149	0.276	0.02	?
Y - HG	11.69	1.582	0.304	0.194	13.59	0.008	0.192	0.239	0.103	0.138	0.027	III
HG - 9	12.85	2.477	0.509	0.241	18.21	0.007	0.163	0.263	0.111	0.2	0.033	III
MD - 1	47.68	8.885	1.359	0.582	28.4	0.015	0.227	0.626	0.174	0.357	0.068	IX

Appendix 1k: Inter-element concentration ratios for Naivasha Quarry sources (normalised against niobium)

Qry N	K	Ca	Ti	Mn	Fe*	Cu	Zn	Rb	Y	Zr	Th	PetGp
HG - 1	60.1	8.125	1.714	1.025	77.76	0.053	0.803	1.339	0.569	4.611	0.192	II
HG - 2	58.13	8.323	1.885	0.967	72.69	0.067	0.819	1.338	0.538	4.728	0.157	II
HG - 3	61.32	8.949	1.946	1.01	68.06	0.029	0.898	1.325	0.583	5.43	0.204	II
HG - 4	64.87	10.78	1.454	0.941	67.94	0.024	0.791	1.245	0.478	4.853	0.177	II
OLB-1	54.69	9.011	1.546	1.007	75.31	0.021	0.891	1.334	0.605	5.591	0.177	IV
HG - 5	40.24	5.604	1.041	0.669	46.39	0.022	0.63	1.21	0.48	4.38	0.077	III
OLB-2	61.78	8.313	1.802	0.978	74.35	0.025	0.845	1.375	0.61	5.666	0.198	IV
OLB-3	67.87	11.3	1.955	1.07	79.53	0.025	0.967	0.131	0.585	5.613	0.187	IV
KIB-1	81.85	8.094	2.601	1.043	69.28	0.094	0.831	1.691	0.63	6.529	0.173	V
KIB-2	75.94	11.96	1.77	0.936	75.35	0.043	1.018	1.439	0.691	6.902	0.132	V
KIB-3	72.81	8.505	1.621	1.026	72.97	0.055	1.019	1.495	0.749	6.929	0.206	V
KIB-4	69.97	13.93	2.139	0.834	74.56	0.041	0.956	1.385	0.663	6.672	0.166	V
KIB-5	81.96	9.828	2.433	1.024	70.02	0.048	0.973	1.595	0.667	6.735	0.175	V
KIB-6	79.48	11.29	2.226	0.856	71.24	0.05	0.994	1.508	0.677	6.426	0.198	V
OSE-1	55.16	6.732	0.987	1.745	71.5	0.02	0.941	1.471	0.667	6.366	0.144	V
KN - 1	111.8	22.99	0.961	6.13	74.55	-	0.597	1.753	0.507	2.701	0.442	VI
OBR-2	605.8	219	91.25	36.25	1103	0.02	2.875	1.475	0.275	6.3	0.175	I
OLF-1	118.6	20.24	5.132	3.423	141	0.035	1.075	1.106	0.665	6.564	0.088	VIII
OLF-2	83.56	15.72	5.63	3.37	143.6	0.03	1.041	0.956	0.57	5.741	0.111	VIII
HPF-1	100.3	20.09	1.942	0.895	74.83	0.047	0.459	1.645	0.006	2.669	0.052	IX
GCL-1	134.2	21.31	1.723	1.209	73.93	0.068	0.827	1.555	0.445	2.581	0.178	VII
GCL-2	130.5	23.58	1.567	1.479	72.32	0.093	1.206	1.67	0.464	0.01	0.186	VII
NB - 1	114.7	17.23	2.103	3.213	68.58	0.052	0.755	1.987	0.465	2.768	0.174	IX
NB - 2	123.1	24.43	1.73	1.5	74.54	0.058	0.575	1.695	0.494	2.69	0.103	IX
LD - 1	80.21	17.2	5.065	6.336	210.6	0.033	1.456	0.964	0.658	5	0.068	X
LD - 2	54.74	10.71	2.608	3.674	126.1	0.016	1.252	1.107	0.78	7.585	0.159	X
BX - 1	40.55	8.173	2.787	3.183	101.2	0.021	1.04	0.991	0.693	7.138	0.138	XI
BX - 2	46.69	8.676	2.824	3.019	108.4	0.015	1.104	0.915	0.709	7.139	0.137	XI
CH -1	122.3	31.55	14.95	10.3	346.2	0.03	1.79	0.795	0.72	5.4	0.065	XIII
CH - 2	76.91	14.57	4.619	5.792	189.9	-	1.293	0.675	0.771	5.205	0.053	XIII
EB - 1	63.72	12.61	3.375	3.829	139.2	0.015	1.108	0.713	0.741	5.882	0.05	XIII
EB - 2	73	12.34	3.569	4.246	160.8	0.028	1.197	0.686	0.815	6	0.086	XIII
HG - 7	80.89	10.85	1.965	0.978	70.05	0.049	0.795	0.898	0.536	4.933	0.162	III
HG - 8	65.89	10.67	1.97	1.305	68.66	0.031	0.746	1.247	0.529	4.835	0.206	III
MG - 2	55.52	10.49	2.287	2.859	103.9	0.025	0.978	0.906	0.66	6.742	0.139	XI
MG - 1	48.36	8.754	2.264	2.694	88.67	0.02	0.919	0.872	0.682	6.852	0.14	XI
LEB-1	119	30.88	12.75	8.689	290.4	0.008	1.488	0.676	0.783	5.471	0.045	XII
LEB-2	187.5	69.3	21.04	15.4	461.4	0.081	1.732	0.725	0.799	5.215	0.02	XII
CH - 3	75.58	15.7	4.297	4.824	154.6	0.025	1.096	0.691	0.673	5.327	0.033	XIII
EBS-1	68.64	14.16	4.11	4.89	165.3	0.03	1.222	0.707	0.762	5.562	0.063	XIII
EBS-2	72.49	15.82	3.565	5.917	193.8	0.029	1.438	0.696	0.759	5.301	0.04	XIII
K - 1	102.5	19	5.039	4.941	178.4	0.032	1.319	1.063	0.658	6.831	0.087	I
HG - 6	69.91	13.52	2.049	1.107	79.88	0.052	0.873	1.34	0.556	5.159	0.225	III
BX - 3	48.38	7.075	2.974	2.857	98.86	0.024	1.028	0.909	0.737	6.69	0.136	XI
X - ?	89.2	13.48	3.79	3.735	126.9	0.02	0.969	1.031	0.541	3.627	0.074	?
Y - HG	84.86	11.48	2.205	1.41	98.67	0.057	1.392	1.739	0.746	7.262	0.198	III
HG - 9	64.45	12.42	2.552	1.206	91.28	0.033	0.819	1.319	0.558	5.014	0.168	III
MD - 1	133.7	24.91.7	3.81	1.631	79.61	0.042	0.637	1.756	0.488	2.804	0.191	IX

Appendix 11: Inter-element concentration ratios for Naivasha Quarry sources (normalised against thorium)

Qry N	K	Ca	Ti	Mn	Fe*	Cu	Zn	Rb	Y	Zr	Nb	PetGp
HG - 1	313.6	42.39	8.942	5.348	405.7	0.275	4.188	6.986	2.971	24.06	5.217	III
HG - 2	370	52.98	12	6.154	462.7	0.423	5.212	8.519	3.423	30.1	6.365	III
HG - 3	300.9	43.91	9.547	4.953	333.9	0.141	4.406	6.5	2.859	26.64	4.906	III
HG - 4	366.5	60.92	8.217	5.317	383.8	0.133	4.467	7.033	2.7	27.42	5.65	III
OLB-1	308.5	50.83	8.718	5.68	424.8	0.115	5.026	7.526	3.41	31.54	5.641	IV
HG - 5	523.1	72.86	13.53	8.939	603.1	0.286	8.184	15.73	6.245	56.94	13	III
OLB-2	311.8	41.95	9.094	4.938	375.2	0.125	4.266	6.938	3.078	28.59	5.047	IV
OLB-3	363.7	60.52	10.48	5.731	426.1	0.134	5.179	0.703	3.134	30.07	5.358	IV
KIB-1	474.1	46.88	15.06	6.042	401.3	0.542	4.813	9.792	3.646	37.81	5.792	V
KIB-2	575.7	90.7	13.42	7.093	571.3	0.326	7.721	10.91	5.163	52.33	7.581	V
KIB-3	353.8	41.33	7.875	4.984	354.6	0.266	4.953	7.266	3.641	33.67	4.859	V
KIB-4	422.3	84.11	12.91	5.036	450	0.25	5.768	8.357	4	40.27	6.036	V
KIB-5	467.6	56.08	13.88	5.843	399.5	0.275	5.549	9.098	3.804	38.43	5.706	V
KIB-6	402.5	57.14	11.27	4.333	360.7	0.254	5.032	7.635	3.429	32.54	5.064	V
OSE-1	383.6	46.82	6.864	12.14	497.3	0.136	6.546	10.23	4.636	44.27	6.955	V
KN - 1	253.2	54.06	2.177	13.88	168.8	-	1.353	3.971	1.147	6.118	2.265	VI
OBR-2	3461	1251	521.4	207.1	6300	1.143	16.43	8.429	1.571	36	5.714	I
OLF-1	1346	229.8	58.25	38.85	16001	0.4	12.2	12.55	7.55	74.5	11.35	VIII
OLF-2	752	141.5	50.67	30.33	1293	0.267	9.367	8.8	5.133	51.67	9	VIII
HPF-1	1917	383.9	37.11	17.11	1430	0.889	8.778	31.44	0.111	51	19.11	IX
GCL-1	753.8	119.7	9.677	6.794	415.3	0.382	4.647	8.735	2.5	14.5	5.618	VII
GCL-2	703.5	127.1	8.444	7.972	389.7	0.5	6.5	9	2.5	0.056	5.389	VII
NB - 1	658.3	98.89	12.07	18.44	393.7	0.296	4.333	11.41	2.667	15.89	5.741	IX
NB - 2	1190	236.1	16.72	14.5	720.6	0.556	5.556	16.39	4.778	26	9.667	IX
LD - 1	1173	251.4	74.05	92.62	3079	0.476	21.29	14.1	9.619	73.1	14.62	X
LD - 2	344.9	67.5	16.43	23.14	794.3	0.1	7.886	6.971	4.914	47.79	6.3	X
BX - 1	294.9	59.45	20.27	23.15	736.2	0.151	7.562	7.206	5.041	51.92	7.274	XI
BX - 2	340.7	63.31	20.61	22.03	790.7	0.108	8.054	6.676	5.176	52.09	7.297	XI
CH -1	1881	485.4	230	158.5	5325	0.462	27.54	12.23	11.08	83.08	15.38	XIII
CH - 2	1457	276.1	87.5	109.7	3598	-	24.5	12.78	14.61	98.61	18.94	XIII
EB - 1	1265	250.3	67	76	2763	0.3	22	14.15	14.7	116.8	19.85	XIII
EB - 2	847.3	143.2	41.43	49.29	1867	0.321	13.89	7.964	9.464	69.64	11.61	XIII
HG - 7	500.2	67.08	12.15	6.05	433.2	0.3	4.917	5.55	3.317	30.5	6.183	III
HG - 8	319.7	51.79	9.556	6.333	333.1	0.148	3.617	6.049	2.568	23.46	4.852	III
MG - 2	398.5	75.29	16.41	20.51	745.4	0.177	7.015	6.5	4.735	48.38	7.177	XI
MG - 1	346.1	62.65	16.2	19.28	634.6	0.145	6.578	6.241	4.89	49.04	7.157	XI
LEB-1	2639	685	282.7	192.7	6441	0.182	33	15	17.36	121.4	22.18	XII
LEB-2	9312	3442	1045	756	-	4	86	36	39.67	259	49.67	XII
CH - 3	2314	480.8	131.5	147.7	4735	0.769	33.54	21.15	20.62	163.1	30.62	XIII
EBS-1	1089	224.8	65.22	77.61	2623	0.478	19.39	11.22	12.09	88.26	15.87	XIII
EBS-2	1807	394.3	88.86	147.5	4831	0.714	35.86	17.36	18.93	132.1	24.93	XIII
K - 1	1183	219.3	58.18	57.05	2060	0.364	15.23	12.27	7.591	78.86	11.55	I
HG - 6	311	60.13	9.115	4.923	355.4	0.231	3.885	5.915	2.474	22.95	4.449	III
BX - 3	354.8	51.88	21.81	21.01	725	0.174	7.536	6.667	5.406	49.06	7.333	XI
X - ?	1207	182.4	51.26	50.53	1716	0.263	13.11	13.95	7.316	49.05	13.53	?
Y - HG	428.8	58.04	11.14	7.125	498.7	0.276	7.036	8.786	3.768	36.7	5.054	III
HG - 9	384.7	74.1	15.23	7.197	544.7	0.197	4.885	7.869	3.328	29.92	5.967	III
MD - 1	701.7	130.8	20	8.563	418	0.219	3.344	9.219	2.563	14.72	5.25	IX

OBSIDIAN SOURCES IN RELATION TO THE GEOLOGY OF THE NAIVASHA AREA